UNIVERSITÀ DEGLI STUDI DI PARMA

Dottorato di ricerca in Fisica
Ciclo XXV

Mean field models: rigorous results on spin glasses and biological applications to cooperative systems

---

Coordinatore:
Prof. Pier Paolo Lottici

Tutor:
Prof. ssa Raffaella Burioni

Dottorando:
Aldo Di Biasio

Acknowledgements

I wish to express my gratitude to Raffaella Burioni, for her priceless teachings and the patience that she showed during these three years, and to Elena Agliari, for her constant help and incitements.
Adriano Barra, who also I owe much of my little knowledge of Physics, deserves particular thanks for having been always present and helpful, and I am also grateful to Francesco Guerra, who first taught and guided me in the fascinating field of spin glasses. Part of the work of this thesis could have not been realized without the help of Guido Uguzzoni, to whom I offer my gratitude.

Contents

Introduction

This thesis is split in two main parts, having in common the study of mean field models in Statistical Physics and Complex Systems. The first part is dedicated to an application of some of the methods of this science to the analysis of cooperative phenomena in biological systems, while the second part deals with mean field spin glass models, focusing on more formal aspects. Cooperativity is a widespread phenomenon in biochemical reactions: many biological functions involve the interactions of small molecules with specific sites on larger biopolymers, and the formation of some kind on non-covalent bond between the small molecule, called ligand, and the proper binding site; the binding of a ligand to one site can influence the affinity of other sites for the same kind of ligand, and in this case the binding is said to be cooperative. Cooperativity is said to be positive if the affinity of other sites increases after a ligand has bound, viceversa it is said to be negative, functioning a device to sharpen or dampen the responsiveness of a system to the changes in a stimulus. In our approach, the cooperative system is mapped into a spin model, with couplings generated by binary strings associated to each site, similarly to the Hopfield model. The simple non-cooperative systems are mapped into models with zero interactions, while positive and negative cooperativity are described in terms of models with, respectively, ferromagnetic and antiferromagnetic interactions. Thus, many different cooperative behaviors, described by the related binding curves, can be analyzed, in an unified vision, in terms of properties of the free energy for the corresponding spin model, by properly tuning the couplings. We fitted the theoretical curves obtained in this way with some experimental data found in literature, extrapolating the values of the effective interactions between the binding sites, which can be put in direct correspondence with some of the most used coefficients that measure cooperativity. In the first chapter, we give a review of the main concepts from biochemistry involved in the study of cooperative phenomena, focusing in particular in the thermodynamics of solutions and in the applications of the related concepts to biochemical binding reactions. In

the second chapter we briefly introduce the Ising model and the corresponding mean-field version, which is basically the counterpart of our description for magnetic systems. The third chapter, which include the original part of this work, is devoted to the introduction of the proper mean-field model aimed at the study of cooperative phenomena, with a detailed analysis of its properties and extensions, including systems with multiple-interactions among binding sites, heterogeneous couplings and negatively cooperative effects. We also compare the results found with recent experimental findings, taken from a plethora of different contexts.

The second part focuses on mean field spin glass models. The purpose of this part of the work is to show the applications of some techniques recently introduced to give a more rigorous and firm ground to the beautiful heuristic results known in this field for many years, both to prove the validity of such powerful methods and to develop alternative mathematical tools to approach the study of complex systems. The rigorous proof that the Parisi formula for the free energy is correct, in fact, was established only some years ago, split across two works by Guerra [1] and Talagrand [2], and many important rigorous results, such as the existence of the thermodynamic limit for the free energy, or the correctness of the ultrametric hypothesis for low-temperature states, are quite recent. Most of the techniques used for these recent breakthroughs are based on interpolation and coupling the given system with an auxiliary, properly chosen, one. Some of these methods can be formulated through an interesting formal analogy with a mechanical system, governed by a proper Hamilton-Jacobi equation. The analysis of this associated mechanical problem, whose potential is related to the fluctuations of the order parameter, allowed us to reconstruct, in particular, the free energy for the Sherrington-Kirkpatrick model and the p-spin glass model, up to the first step of broken replica symmetry. In chapter five we give an overview of the main properties of these two models, by using the replica method, while the sixth chapter is devoted to the introduction of some interpolation techniques and in particular the ones based on mechanical analogies, constituting the original contribution for this part of the work.

Part I

Mean field approach to cooperativity in biochemical systems

Chapter 1

An overview on cooperativity

1.1 Thermodynamics of reactions in solutions

In this chapter we want to introduce some fundamental concepts and results of solution thermodynamics that will be useful in the rest of our work. In particular, we will focus on the concept of *cooperativity*, a widespread phenomenon in biochemical reactions involving the binding of ligand molecules to larger biopolymers. As we are going to see, positive cooperativity gives to a system more sensitivity over a narrower range of stimulus, whereas negative cooperativiry gives a less sensitive response over a much broader range, and both constitute a fundamental tool that nature developed to modulate the chemical response of biological systems to varying stimuli. We refer to standard textbooks for an extensive account of the topic (see for instance [3] and [4]).

Biochemical reactions and equilibria occurring in biological systems involve small metabolite molecules and proteins, as well as large macromolecules, like nucleic acids, enzymes, and so on. Almost all these reactions occur in solution, mostly aqueous, and the hydrogen-bonded network of water greatly affects the intermolecular and intramolecular reactions. Some molecules, like the proteins found in the phospholipid bilayers of cellular membrane, also exist in non-aqueous environment. A fundamental tool for understanding biochemical reactions is then the thermodynamic study of solutions.

Generally speaking, a solution is a single-phase system with more than one component, thought as an independently variable chemical substance. Note that, whenever chemical equilibria exist in the solution, there are usually more molecular species than the ones defined as components. For instance, let us consider a solution containing water, hemoglobin (Hb), and

dissolved oxygen. Each hemoglobin molecule can bind one to four oxygen molecules, so we could possibly consider the species H_2O, Hb, O_2, HbO_2, $Hb(O_2)_2$, $Hb(O_2)_3$, $Hb(O_2)_4$. Yet If the binding reactions are in equilibrium at a given temperature T and pressure P, it is sufficient to specify three independent components (solvent plus any two of the others), since equilibrium relationships allow us to determine the others.

The appropriate thermodynamic potential to study a chemical solution containing k components is the Gibbs free energy G, which is the quantity that is minimized for a system at equilibrium with constant temperature T and pressure P. It is related to the enthalpy H and the entropy S via the Legendre transform $G = H - TS$. The contribution of the component i of the solution to the total free energy depends on its chemical potential μ_i, also called partial molar Gibbs free energy, defined as the increment of G with respect to the change in the number of moles n_i of the component i:

$$\mu_i = \left(\frac{\partial G}{\partial n_i}\right)_{T,P,n_{j\neq i}}. \tag{1.1}$$

This is an intensive quantity, hence depending on T and P, but not on the size of the system, and its name comes from the fact that differences in its values for different components are the driving potentials for chemical reactions.

The total free energy of the solution can be then expressed in terms of the μ_i's as

$$G = \sum_{i=1}^{k} n_i \mu_i. \tag{1.2}$$

If the state of the system undergoes an infinitesimal change the corresponding change in G is

$$dG = \left(\frac{\partial G}{\partial T}\right)_{P,n_i} dT + \left(\frac{\partial G}{\partial P}\right)_{T,n_i} dP + \sum_i \left(\frac{\partial G}{\partial n_i}\right)_{T,P,n_{j\neq i}} dn_i, \tag{1.3}$$

which becomes, using standard thermodynamic relationships for entropy S, volume V, and chemical potential μ_i

$$dG = -SdT + VdP + \sum_i \mu_i dn_i, \tag{1.4}$$

and, if temperature and pressure are kept constant,

$$dG = \sum_i \mu_i dn_i. \tag{1.5}$$

The chemical potential of a substance A in a mixture depends on its concentration, and this dependence is particularly simple in *ideal* solutions, where

$$\mu_A = \mu_A^0 + RT \log \chi_A. \tag{1.6}$$

Here χ_A is the mole fraction of component A (that is the ratio between the number of molecules of solvent A and the total number of solute molecules), R is the gas constant, and T the absolute temperature. For $\chi_A = 1$ we have $\mu_A = \mu_A^0$, hence the chemical potential μ_A^0, which represents the chemical potential in a *standard state*, equals the molar free energy of pure component A. To be called ideal, a solution should have two properties: first, there should be no difference in interaction energy between solute and solvent molecules, so that the enthalpy change ΔH_m in the solution is zero; second, the entropy change should be the entropy of non-interacting particles mixing, that is,

$$\Delta S_m = -R \sum_{i=k} n_i \log \chi_i. \tag{1.7}$$

In fact, from these two conditions it follows that the free energy for the mixing of a solution is

$$\Delta G_m = \Delta H_m - T\Delta S_m = RT \sum_i n_i \log \chi_i. \tag{1.8}$$

On the other hand, the free energy of n_i moles of a particular pure component is given by $n_i \mu_i^0$, so, using (1.2), we also have

$$\Delta G_m = G(\text{solution}) - \sum_i G_i(\text{pure components}) = \sum_i n_i(\mu_i - \mu_i^0). \tag{1.9}$$

Equating last two equations, and observing that the components n_i are independent variables, we obtain (1.6).

The mole fraction is an inconvenient quantity to deal with, since experiments usually measure concentrations, thus equation (1.6) for component A is often written in terms of the concentration $[A]$. Any proportionality constant between χ_A and $[A]$ can be absorbed by μ_A^0, redefining it in terms of the concentration scale used. Thus, we may equally write, for the solute in dilute ideal solutions,

$$\mu_A = \mu_A^0 + RT \log[A]. \tag{1.10}$$

So far we have considered ideal solutions. To take care of deviations from ideal behavior, one usually starts from Eq. (1.10) and substitutes the

concentration $[A]$ with an effective concentration (or *activity*) $a_A = y_A[A]$, writing a formally analogous equation:

$$\mu_A = \mu_A^0 + RT \log a_A. \tag{1.11}$$

The activity is a unit-less quantity and the coefficient y_A has units of inverse concentration. The latter will be in general a function of T, P, and all the solute concentrations. In practice, to deal with non-ideality, one usually considers virial expansions of the chemical potential, consisting in power series expansions in terms of the termodynamic parameters, around the ideal values. The higher order coefficients give a measure of the non-ideal behavior. We expect that, in general, solutes will approach an ideal behavior ($y_A = 1$) if the solution is very dilute.

1.2 Equilibrium conditions in chemical reactions

Let us consider now a generic chemical reaction

$$aA + bB + ... \rightarrow pP + qQ + ... \tag{1.12}$$

in which a moles of molecule A, b moles of B, and so forth, react and form p moles of P, q moles of Q, and so forth, at molar concentrations $[A], [B], ..., [P], [Q], ...$ We stress that we are not assuming equilibrium here, but we simply take so many moles of the reactants and convert them to the corresponding moles of products, under some given arbitrary conditions (temperature, pressure and concentrations). The driving force of the reaction is the free energy change ΔG, and, if the reaction occurs at constant temperature and pressure, Eq. (1.2) gives

$$\Delta G = p\mu_P + q\mu_Q + ... - a\mu_A - b\mu_B - ... \tag{1.13}$$

whence, using (1.11),

$$\begin{aligned} \Delta G =& (p\mu_P^0 + q\mu_Q^0 + ... - a\mu_A^0 - b\mu_B^0 - ...) \\ &+ RT \log \frac{[P]^p [Q]^q}{[A]^a [B]^b} + RT \log \frac{{y_P}^p {y_Q}^q}{{y_A}^a {y_B}^b}. \end{aligned} \tag{1.14}$$

Here the first term on the r.h.s, involving μ_i^0 values, is called the standard-state free energy change, and it is indicated with ΔG^0. It represents the free energy change that would be observed if a moles of A, and so forth, in the standard state, formed p moles of P, and so forth, also in the standard state.

In the second term, the actual concentrations of reactants and products are taken into account, and the third term, involving only the activities coefficients, can be neglected, assuming that all the components behave ideally. In this case we may write Eq. (1.14) as

$$\Delta G = \Delta G_0 + RT \log \frac{[P]^p [Q]^q}{[A]^a [B]^b}, \tag{1.15}$$

and at equilibrium ($\Delta G = 0$) we find

$$\Delta G_0 = -RT \log \left(\frac{[P]^p [Q]^q}{[A]^a [B]^b} \right)_{\rm eq} = -RT \log K \tag{1.16}$$

where we have defined the equilibrium constant K as

$$K = \left(\frac{[P]^p [Q]^q}{[A]^a [B]^b} \right)_{\rm eq} \tag{1.17}$$

This constant tells us what are the relative concentrations of reactants and products at equilibrium, and will depend on temperature and pressure. The values of ΔG_0 are known for many reactions, and we can also rewrite last equation as

$$K = e^{-\Delta G_0 / RT}. \tag{1.18}$$

Near room temperature we have $RT \simeq 2.5$ kJ/mol, and if we consider as essentially irreversible a reaction with $K > 10^4$, the corresponding free energy change should be about $\Delta G_0 < -23$ kJ/mol, which is a condition satisfied for many biological reactions.

For a reaction beginning at arbitrary concentrations $[A], [B], [P], [Q], ...$, the second term, if there is not a refuelling of components, will gradually change in time until the concentrations are equal to the equilibrium values and $\Delta G = 0$. Note that the concentrations of reactants and products in many biochemical reactions correspond to values out of equilibrium, in physiological conditions. For example, at the concentrations maintained in most cells, the hydrolysis reaction

$$ATP + H_2O \rightarrow ADP + \text{phosphate} \tag{1.19}$$

gives to the cell an energy $-\Delta G \simeq 40$ kJ/mol, while the equilibrium value would be $\Delta G_0 \simeq -31$ kJ/mol.

1.3 Small ligand binding on macromolecules

Many biological functions involve the interactions of small molecules, acting as metabolites, regulators and signals, with specific sites on larger macromolecules, involved in cellular processes. Some typical examples include enzymes, which bind substrates and effector molecules accelerating the kinetics of reactions, transport proteins such as hemoglobin, which binds oxygen molecules, as well as the many proteins that act as buffers by binding hydrogen ions. Such binding mechanisms involve, in most cases, the formation of some kind of non-covalent bond between the small molecule or ion, called the *ligand*, and a specific region, the *binding site* (or *docking site*), on or near the surface of the macromolecule. A single macromolecule can possess binding sites of varying degrees of strength and specificity for different ligands. Enzymes, for instance, usually have a very specific *key-lock* mechanism to bind a molecule. Sometimes, one of the consequences of the act of binding a ligand on a site can be a conformational change in the biopolymer, which may influence the binding on other sites (*allosteric mechanism*), and in general binding affinities can be interdependent, allowing different metabolites, for instance, to interact indirectly.

In principle, except the case of covalent bonds, there is always an appreciable concentration of free ligands $[A]$ in equilibrium with bound ligands $[A_b]$ under physiological conditions. The total ligand concentration $[A_T]$ is obviously the sum

$$[A_T] = [A] + [A_b] \tag{1.20}$$

and the total molar concentration on macromolecules will be designated by $[P_T]$. The equilibrium process is dynamic, and at any instant different macromolecules P will host different numbers of ligands. The measure of the number of moles of A bound per mole of P is then an average

$$\bar{\nu} = \frac{[A_b]}{[P_T]}, \tag{1.21}$$

which increases monotonically with $[A]$ and should approach the limiting value n, equal to the total number of binding sites of P for molecule A, as the concentration $[A]$ increases. The *fraction saturation* is the correspondent normalized quantity

$$\theta = \frac{\bar{\nu}}{n} \tag{1.22}$$

and the curve describing its functional dependence on $[A]$ is called *binding curve*, or *binding isotherm*.

Among the many aspects in the investigation of such phenomena, it is often interesting to try to understand what is the maximum number of moles of ligands that can be bound for mole of the macromolecule, or, in other words, the number of binding sites, and the possible influence of the binding of a ligand on the other binding sites. This question is directly related with the phenomenon of cooperativity, as we are going to explain later.

1.3.1 Experimental measurements

In most cases, experimental measurements do not allow to observe directly the single ligands and binding sites, but they rather focus on the measure of the total fraction of ligand molecules that are bound, or the fraction of occupied binding sites (this is not strictly true, since some single-molecule techniques, such as atomic force microscopy, allow sometimes observation of certain dynamic interactions under physiologic conditions). An example is equilibrium dialysis, a technique based on membrane equilibrium, in which one places the macromolecule solution inside a semipermeable membrane bag, suspended in a solution containing the small ligands. In a nutshell, since the macromolecules cannot pass through the membrane, at equilibrium the excess of ligands in concentration inside the membrane should correspond to the bound molecules. Hence, measuring the concentrations of the smaller molecules inside and outside the bag gives the requested value.

Other methods are based on the change of some physical measurable properties (light-absorption spectra, fluorescence, nuclear magnetic resonance, and so forth) of the macromolecules when a molecule binds. Surface plasmon resonance (SPR), for instance, allows to detect the fraction of occupied sites by measuring the change in refractive index of a dielectric layer of biopolymers attached to a metallic surface, when they bind molecules from a solution. The problem of these methods is that they assume the same linear change in the physical parameter for all the binding sites, which is sometimes inaccurate. Moreover, if the number of sites n is not known a priori, it can be difficult to extrapolate its value from experimental measurements at high concentration of ligands, unless binding is particularly strong. Using a combination of several techniques, however, can give in most cases very accurate measurements.

1.3.2 Single site case

Needless to say, the simplest case to analyze is that of a macromolecule P with a single binding site for a molecule A, and no other species which can

bind on it. The reaction describing the equilibrium process is then

$$[\mathrm{A}] + [\mathrm{P}] \rightleftharpoons [\mathrm{PA}] \tag{1.23}$$

where $[PA]$ denotes the concentration of hosting molecules with an occupied site, and $[P]$ and $[A]$ are the concentration of free ligands and macromolecules, respectively. The equilibrium constant for this reaction is then

$$K = \frac{[PA]}{[A][P]}. \tag{1.24}$$

Since there is only one site per hosting molecule, the measurable parameter $\bar{\nu}$ equals in this case the fraction saturation, and can be written as

$$\theta = \bar{\nu} = \frac{[PA]}{[P] + [PA]}, \tag{1.25}$$

or, using (1.24),

$$\theta = \frac{[A]}{K^{-1} + [A]}. \tag{1.26}$$

This corresponds to a simple hyperbolic dependence, as shown in figure 1.1, where the inverse equilibrium constant K^{-1} gives the concentration $[A]$ at half saturation ($\theta = 1/2$), and so the scale of concentrations involved. Note that $K^{-1} = [P][A]/[PA]$ is the equilibrium constant for the dissociation reaction

$$[\mathrm{PA}] \rightleftharpoons [\mathrm{A}] + [\mathrm{P}]. \tag{1.27}$$

A typical example of a similar behavior is represented by the binding of oxygen molecules on myoglobin, a single-chain globular protein. This protein has a heme (iron-containing porphyrin) prosthetic group, which can bind an oxygen molecule reversibly, and its primary function is to store and carry oxygen in muscle tissue.

In the domain of reactions catalyzed by enzymes, which can bind molecules on different sites on their structure to accelerate some reactions, one is usually interested in determining the rate of product formation, which is a measure of the velocity of such reaction. This quantity can be usually written in the form of a constant times some functions of the concentrations of reactants. For a single-step reaction

$$aA + bB \rightarrow cC + dD$$

the rate assumes the form

$$R = k[A]^a[B]^b$$

but for more complex processes the exponents (called the *order* of the reaction with respect to A and B) are not in general the same as the balancing coefficients a and b. For a substrate A, reacting on a multisite enzyme E to form a product B in the reaction

$$\mathrm{E} + \mathrm{A} \overset{k_1}{\rightleftharpoons} \mathrm{ES} \overset{k_2}{\rightleftharpoons} \mathrm{E} + \mathrm{B} \tag{1.28}$$

with rate constants k_1, k_2, respective inverse rates k_{-1}, k_{-2} and with $k_{-2} \simeq 0$. Eq. (1.26) takes then the name of Michaelis-Menten (MM) equation, and describes the rate of product formation $R = d[B]/dt = k_2[EA]$ as a function of the substrate concentration:

$$R = k_2[EA] = \frac{k_2[E_T][A]}{K_m + k_1[A]}, \tag{1.29}$$

where $[E_T]$ is the total concentration of enzyme $[E]$ and $K_m = (k_{-1}+k_2)(k_1)$ is called Michaelis constant.

There are many cases in which a macromolecule has only a single binding site for a particular ligand, but it is when multiple sites are present that most of the interesting situations, such us cooperative effects, arise. We consider now the case of multiple binding sites.

1.4 Multiple binding sites

When a macromolecule P can bind more than a single ligand ($n > 1$), the expression for $\bar{\nu}$ becomes more complicated, as there can be some molecules binding one ligand, some binding two, and so on, up to n. if we call $[A_b]$ the total concentration of bound ligands on P, we can write

$$[A_b] = [PA] + 2[PA_2] + ...n[PA_n] = \sum_{i=1}^{n} i[PA_i]. \tag{1.30}$$

As for the total molar concentration of the macromolecule P, it is just the sum of its molar concentrations in all forms, from the unliganded one to that with all n sites occupied:

$$[P_T] = \sum_{i=0}^{n} [PA_i] \tag{1.31}$$

So we can write the completely general expression for $\bar{\nu}$

$$\bar{\nu} = \frac{[A_b]}{[P_T]} = \frac{\sum_{i=1}^{n} i[PA_i]}{\sum_{i=0}^{n}[PA_i]} \tag{1.32}$$

This formulation is completely general, and at this point one is led to consider the equilibrium relationships among the $[PA_i]$. This can be done in different but equivalent ways; one is, for instance, to consider the reactions

$$\begin{aligned} \mathrm{P} + \mathrm{A} &\rightleftharpoons \mathrm{PA} \qquad K_1 = \tfrac{[PA]}{[P][A]} \\ \mathrm{P} + 2\,\mathrm{A} &\rightleftharpoons \mathrm{PA_2} \quad K_2 = \tfrac{[PA_2]}{[P][A]^2} \\ &\cdots \\ \mathrm{P} + \mathrm{nA} &\rightleftharpoons \mathrm{PA_n} \quad K_n = \tfrac{[PA_n]}{[P][A]^n} \end{aligned} \tag{1.33}$$

This is just a formal step which says nothing about the mechanism of the reaction, and writing $K_n = [PA_n]/[P][A]$, as in last equation, does not imply that n ligands do actually bind simultaneously to a molecule of P. One could also consider the equilibria in the form

$$\mathrm{A} + \mathrm{PA_{i-1}} \rightleftharpoons \mathrm{PA_i}, \qquad k_i = \frac{[PA_i]}{[A][PA_{i-1}]} \tag{1.34}$$

and note that the coefficients k_i are related to the K_i in (1.33), since $K_i = k_1 k_2 ... k_i$.

We can now use the relations (1.33) above to rewrite Eq. (1.32): defining $K_0 = 1$ and canceling $[P]$, which factors out both in the numerator and denominator, one obtains

$$\bar{\nu} = \frac{\sum_{i=1}^{n} i K_i [A]^i}{\sum_{i=0}^{n} K_i [A]^i}. \tag{1.35}$$

This equation is very general, since nothing has been assumed on the K_i, and it is known as the Adair equation. Thanks to its generality it can describe almost any binding situation, but for large n (even for $n \leq 4$), there are many adjustable parameters, so one should have extensive and precise measurements to determine them. Moreover, simply fitting the data to the equation does not reveal anything about the mechanism involved in binding. Therefore, one is usually led to use more simple models, with fewer parameters.

1.4.1 Independent equivalent sites

Consider a macromolecule whose n binding sites are all equivalent, *i. e.* they have the same affinity for a given ligand. If the affinity of any site is independent of whether or not other sites are occupied, the binding is called

noncooperative, and we are faced with the simplest case of a multiple site binding.

Each concentration $[PA_i]$ is the sum of concentrations of a whole class of $n!/[i!(n-i)!]$ isomers $PA_{i,r}$, with different combinations of the i occupied sites, and with the same average concentrations. However, in the binding of a ligand to a specific site of a particular isomer q,

$$\mathrm{A} + \mathrm{PA_{i-1,q}} \rightleftharpoons \mathrm{PA_{i,r}}, \tag{1.36}$$

the equilibrium constant are identical $(k_i)_{qr} = k$, since a ligand molecule cannot distinguish among binding sites. They bind independently to each site, as if it was a single site macromolecule, so the fraction saturation should simply follow Eq. (1.26), in the form

$$\theta = \frac{\bar{\nu}}{n} = \frac{[A]}{k^{-1} + [A]}. \tag{1.37}$$

With some algebra, we could also have derived this expression from (1.32), by noticing that $K_i = k^i$, and

$$[PA_i] = \frac{n!}{i!(n-i)!} k^i [P][A]^i, \tag{1.38}$$

where we have taken into account the number of different isomers with the same number of bound ligands.

Equation (1.37) can be used to test if the binding sites of a macromolecule are independent and equivalent, by fitting experimental data with appropriate values of the parameters n and k. Usually, it is hard to obtain n as an asymptote, and the evaluation of k depends on knowing this limit. Thus, they are often used together, as adjustable parameters, for nonlinear least-square analysis. A linear analysis can be carried out with a double reciprocal plot

$$\frac{1}{\bar{\nu}} = \frac{1}{n} + \frac{1}{nk[A]}, \tag{1.39}$$

where graphing $\bar{\nu}^{-1}$ vs. $[A]^{-1}$ gives $1/n$ and $1/nk$ as respectively the intercept and the slope of a straight line. In the Scatchard plot, instead, one considers the graph of $\bar{\nu}/[A]$ versus $\bar{\nu}$,

$$\frac{\bar{\nu}}{[A]} = nk - \bar{\nu}k, \tag{1.40}$$

where the slope and the intercept on the horizontal $\bar{\nu}$ axis correspond to $-k$ and n.

An other kind of linear analysis which is frequently used is the *Hill plot*: rewriting Eq. (1.37) in the form

$$\frac{\bar{\nu}}{n-\bar{\nu}} = k[A] \tag{1.41}$$

and taking the logarithm one obtains

$$\log \frac{\bar{\nu}}{n-\bar{\nu}} = \log k + \log[A]. \tag{1.42}$$

For equivalent sites this has a slope of unity, but it is particularly useful in the case of multiple cooperative sites, as we shall see.

Non-equivalent independent sites

In many proteins and biopolymers there are a number of different kinds of independent sites for a given ligand, with different affinities and binding constants. If there are two classes of n_1 and n_2 sites, with equilibrium constants equal to k_1 and k_2 respectively, the binding isotherm reduces to

$$\bar{\nu} = \frac{n_1 k_1[A]}{1+k_1[A]} + \frac{n_2 k_2[A]}{1+k_2[A]}. \tag{1.43}$$

Unless the values of equilibrium constants are very different, it can be difficult to distinguish this situation from the binding by $n_1 + n_2$ independent sites with k intermediate between k_1 and k_2. The situation is obviously more complicated if there are more than two classes of sites. For a sufficiently precise analysis of such situations it is often necessary to use a combination of several graphical techniques (such as Scatchard and Hill plots).

1.5 Cooperative binding

Consider a macromolecule with n binding sites: if the binding of a ligand to one site influences the affinity of other sites for the same kind of ligand, the binding is said to be *cooperative*. If the affinity of other sites increases after a ligand has bound, cooperativity is *positive*; the affinity could be also decreased, and in this case cooperativity is said to be *negative*. In the case of a protein with a number of binding sites, the mechanism causing this affinity change is usually a small change in the tertiary structure, after the binding of a molecule. Such effects are classified as a part of the general phenomenon of *allostery*. Here and in all the first part of this thesis, we will focus exclusively

on *homeoallostery*, which refers to the influence on the binding affinities due to ligand of the same species, but it should be mentioned that many binding phenomena are *heteroallosteric*, that is, the binding of a ligand on a site can influence the binding of other species of ligands on different sites.

The different behaviors of positively and negatively cooperating sites are reflected in different binding curves ($\bar{\nu}$ or θ vs. $[A]$, see figure 1.1). The

Figure 1.1: Binding curves for noncooperative (black), positively (red) and negatively (blue) cooperative binding sites. Note that the case of positive cooperativity corresponds to a sigmoidal curve.

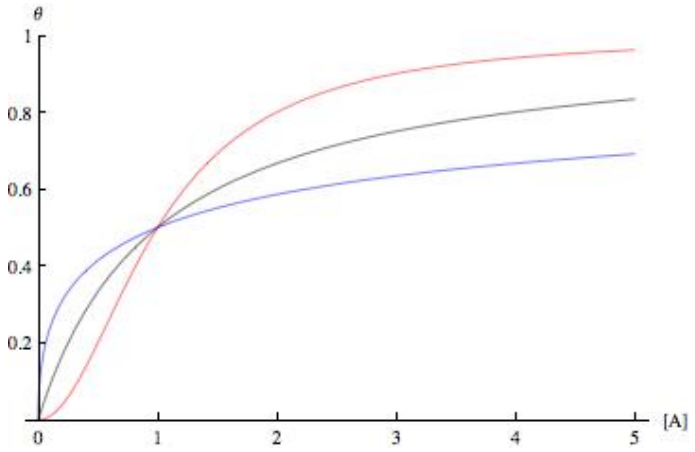

Michaelis-Menten curve (1.26) for noncooperative systems corresponds to a rectangular hyperbola, as we have seen. If there is positive cooperativity the curve has usually a sigmoidal shape (this is not strictly true, since when cooperativity is weak the binding isotherm has a form similar to the Michaelis-Menten curve, see section...). On the contrary, if cooperativity is negative, the remaining non-occupied sites become weaker as the others are filled, and a typical binding curve, compared with the non-cooperative and positively cooperative case, is shown in figure 1.1. The typical example of positive cooperativity is Hemoglobin, which has four binding sites for oxygen molecules. The quaternary structure of this protein consists of four subunits arranged in a roughly tetrahedral form, each containing a heme group (a iron charged atom held in a heterocyclic ring, known as porphyrin), the binding site for oxygen. More precisely, the molecule contains two copies of two kinds of similar subunits (α and β), therefore it can be considered a dimer of α-β copies. Roughly speaking, when oxygen binds to the heme complex, it causes the iron atom to move backward into the heme which holds it, and this in-

duces a series of modifications in the structure, such that binding of oxygen to the other three sites becomes easier. At low concentrations of oxygen the

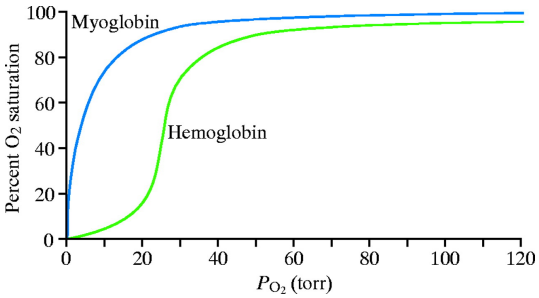

(a) Curves describing the binding of oxygen by myoglobin and hemoglobin. Myoglobin has a single binding site for O_2 molecules, and the resulting curve is hyperbolic. Hemoglobin, on the other hand, has four binding sites to which oxygen binds cooperatively, with a sigmoidal shape for the binding isotherm.

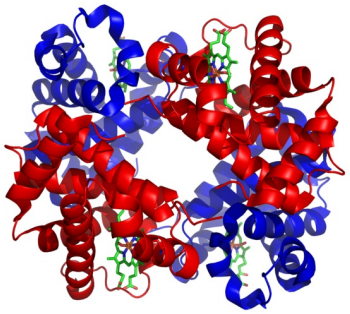

(b) Structure of human hemoglobin. The red and blue subunits represent respectively α and β helices, while the four heme groups, containing the atom charged atoms to which oxygen bind, are in green. From Protein Data Bank.

Figure 1.2: Hemoglobin binding curve confronted with myoglobin, and hemoglobin structure.

binding is very weak, because the molecule is in a weakly binding state, and the first ligands bound tend to bind to different molecules. When the first one or two sites are filled on any molecule, affinity on the remaining sites has increased, so that binding becomes stronger and the curve turns upward, in the typical sigmoidal shape (see Fig. 1.2(a)). This makes the hemoglobin a very efficient carrier for oxygen molecules in the blood, since it easily binds oxygen in the lungs, where the concentration is high, and can release it in the tissues of the body where the concentration is low.

1.5.1 Hill plot

One of the most used methods to see if a macromolecule binds ligands cooperatively is the Hill plot, introduced in the previous section for the single site case. Consider now an ideal system with such strong positive cooperativity that it binds n molecules on its n sites, or none, because when a site is occupied the affinity of the other sites for the ligands increases dramatically. For such a situation the Adair equation (1.35) can be written in the simple

form

$$\bar{\nu} = \frac{nK_n[A]^n}{1 + K_n[A]^n} \tag{1.44}$$

and the Hill equation becomes

$$\log \frac{\bar{\nu}}{n - \bar{\nu}} = \log K_n + n \log[A], \tag{1.45}$$

corresponding to a straight line with slope n and intercept $\log K_n$. Sometimes this is written in terms of the fraction saturation θ, with $\log[\theta/(1-\theta)]$ on the l.h.s. This extreme case represents the maximum possible cooperativity, hence the greatest slope that one can find for a real system is n, the number of cooperative sites on the molecule. The maximum Hill slope n_H that one finds is always less than this, in real cases, and it takes the name of *Hill coefficient* or *Hill number*. We have seen that for a noncooperative system the Hill plot gives a slope equal to one; for a positively cooperative system, the Hill coefficient will range between one and n, and it gives an indication on how strong cooperativity is. On the other hand, if negative cooperativity is at work, we expect a Hill coefficient smaller than one, in some region. In either cases, the curves for Hill plots will approach straight lines with slopes of unity, at both low and high values of $\log[A]$. It is worth noticing that also if a macromolecule has two classes of independent sites with different affinities for the same ligand, the Hill plot contains a region with slope less than one, and often it is almost impossible to distinguish between the two alternatives.

Koshland coefficient and global dissociation quotient

Besides the Hill number, there are other measures of how cooperative a system is. We can mention, among the others, the Koshland coefficient κ [], defined as the ratio between the concentration $\alpha_{0.9}$ corresponding to a fraction saturation of $\theta = 0.9$ and the concentration $\alpha_0.1$, corresponding to $\theta = 0.1$. This value is equal to $\kappa = 81$ in the non-cooperative case, independently on the equilibrium constant K. If $\kappa < 81$ the fraction saturation is expected to grow faster than the Michalis-Menten binding curve, and cooperativity is positive, while for $\kappa > 1$ we have negative cooperativity. This number is easy to measure, but it depends only on two values of concentration, hence ignoring all information that can be derived from the shape of the binding curve.

Another possible approach is to consider a generalized Michaelis-Menten

equation

$$\theta = \frac{[A]}{[A] + K^{-1}([A])}, \tag{1.46}$$

where K^{-1} is considered a function of $[A]$. For a non-cooperative system $K^{-1}([A])$ should be a constant, otherwise one has $K^{-1}([A]) = [A](1-\theta)/\theta$. This can be interpreted as the ratio between free sites and occupied sites, times $[A]$, and it is called *global dissociation quotient*. Thus, if one finds $\gamma = dK^{-1}/d[A] \neq 0$, the binding sites should interact with some form of cooperativity.

1.5.2 Some models for cooperative binding

A large number of models have been proposed in the past, in order to have a quantitative description of cooperative binding on proteins. The most important, introduced for oxygen binding by hemoglobin, are probably the Monod-Wyman-Changeux (MWC) model [5], and the Koshland-Nemethy-Filmer (KNF) model [6], which in a certain sense lay at two extreme descriptions, among the many proposed.

The MWC model is based on the concept of concerted conformational transitions in the subunits of the protein. It is assumed that each subunit contains a binding site: this exists in two states (T and R), with different affinities, but all the subunits undergo the transition in concert. For low concentrations of ligands the T state is favored, while the R form, with a larger affinity for ligands, is more favored at high concentrations. Without going into details, as the concentration of ligands increases from small values, the proportion of unoccupied sites in the R conformation will increase, and they will bind ligands with greater affinity. This model, with all its variants, predicts the behavior observed in homeoallosteric molecules with positive cooperativity, but it cannot describe negative cooperativity.

In the KNC model, on the contrary, it is assumed that the subunits change one at a time from a weak-binding to a strong-binding form, and the interactions between the different pairs of subunit depends on the relative states. This model can describe also negative cooperativity, and can take into account specific topologies for the interactions among binding sites. The model we are going to introduce later has more to do with this approach, as we shall see.

As for the sequential binding of O_2 molecules by hemoglobin, experimental measurements have shown that it has features in common with both the models depicted above, but agrees exactly with neither. In fact, individual α and β subunits can bind O_2 with individual tertiary conformational shifts,

as described by KNC model, and a quaternary T→R change can occur, but only after at least one of the sites on each α-β pair is occupied [7, 8].

Chapter 2

Generalities on the Ising model

In this section we give a short introduction on equilibrium statistical mechanics of Ising-like systems, to illustrate some basic concepts and results that we are going to use for an application to chemical kinetics. Our goal here is not an exhaustive presentation of the Ising model, since there is an huge amount of studies and applications on this topic, and we refer for a review to standard textbooks (see for example [9] or [10]).

In standard equilibrium statistical mechanics we can consider, in general, a system with a fixed number N of particles and in thermal equilibrium with its environment at a temperature T. We are interested in macroscopic observable quantities, which are compatible with a number of different physical states of the single particles (microstates). For instance, if we think about a gas of molecules in a box, there are many different sets of values of positions and velocities which are possible for a given value of the thermodynamic pressure and temperature. Each set of values σ of the internal variables, which fluctuate in time, determines a value $H(\sigma)$ of the energy of the system (and of other macroscopic quantities). In the *ergodic hypothesis* the time averages over these fluctuating microstates (corresponding to the measured macroscopic observables) are equivalent with the averages on an ensemble of copies of the system, distributed in accord with the Boltzmann distribution

$$\rho(\sigma) = \frac{e^{-H(\sigma)/T}}{Z}, \tag{2.1}$$

where the sum over all the possible microstates,

$$Z = \sum_{\sigma} e^{-H(\sigma)/T}, \tag{2.2}$$

is called partition function and ensures the correct normalization. The link with thermodynamics is given by the identification of the Helmholtz free energy F with

$$F = U - TS = -T \log Z. \tag{2.3}$$

Here the equilibrium internal energy U can be identified with the ensemble average of the energy $H(\sigma)$

$$U = \langle H \rangle = \sum_{\sigma} \rho(\sigma) H(\sigma) \tag{2.4}$$

while the associated entropy is given by

$$S = -\sum_{\sigma} \rho(\sigma) \log \rho(\sigma). \tag{2.5}$$

Calling $\beta = 1/T$ the inverse temperature, we can also write the thermodynamic relations

$$U = \frac{\partial}{\partial \beta} \beta F = -\frac{\partial}{\partial \beta} \log Z \tag{2.6}$$

$$S = \beta^2 \frac{\partial F}{\partial \beta}. \tag{2.7}$$

The entropic term, thought as a functional of the distribution ρ, is maximized when the latter is uniform and minimized when the distribution gives nonzero probability only to a single state σ (we refer for simplicity to a discrete space of microscopic states), favoring thus a disordered state. The equilibrium state, identified by the Boltzmann distribution, represents the distribution which minimizes the free energy $F = U - TS$, as it is the best tradeoff between internal energy minimization and entropy maximization at a given temperature T. The most high the temperature, then, the most important the relative role of the disorder, encoded in S.

Generally speaking, the averages on fluctuating variables are obviously more significative if their variance is small, which is what occurs here when the size of the system is large. Moreover, note that the Helmholtz free energy F is an extensive quantity and should be proportional to N, but this does not hold in general for $\log Z$ when N is small. However, when dealing with thermodynamic systems, the number of particles is usually very large (of the order of Avogadro's number $N_A \approx 10^{23}$) and one can go to what the so-called *thermodynamic limit*, replacing the finite size free energy density $f_N = F/N$ with its limit for $N \to \infty$:

$$f = -\lim_{N \to \infty} \frac{1}{\beta N} \log Z. \tag{2.8}$$

From the partition function one can compute all the thermodynamic functions, and it should be able to see, possibly, phase transitions. For a finite system Z is a finite sum of positive analytic functions of the temperature (for $T \neq 0$), and consequently also $f_N = -N^{-1}T \log Z$ is an analytic function of T. Since phase transitions correspond to singularities of thermodynamic functions, it is necessary to go to the thermodynamic limit to see them.

2.1 An overview on the Ising model

The Ising model was born to describe ferromagnetism and other forms of magnetism due to the exchange interaction between unpaired spins. The interacting particles are thought as localized on a hypercubic lattice Λ_N in d dimensions, and with a privileged direction for their magnetization, let's say z, so that the up and down directions for the spin on each site i can be conveniently represented by variables σ_i, assuming the two possible values $\sigma_i = \pm 1$. The set of configurations is thus specified by the vector

$$\sigma = \{\sigma_1, \sigma_2, ..., \sigma_N\}, \tag{2.9}$$

having 2^N possible values, and for a simple ferromagnet the symmetric exchange interaction J_{ij} can be thought as a constant $J > 0$. The configurational energy is given by the hamiltonian

$$H(\sigma) = -J \sum_{<i,j>} \sigma_i \sigma_j, \tag{2.10}$$

where the sum is on nearest neighbor sites. The contribution of a pair (i, j) is $-J$ if $\sigma_i = \sigma_j$ and $+J$ if $\sigma_i \neq \sigma_j$, so that parallel alignment is energetically favorable.

The magnetization associated with a given spin configuration σ is

$$M(\sigma) = \sum_{i=1}^{N} \sigma_i \tag{2.11}$$

and to this extensive quantity we can associate the magnetization density

$$m(\sigma) = M(\sigma)/N. \tag{2.12}$$

A very important property of the energy (2.10) is the invariance under reversal of all spins ($\sigma_i \to -\sigma_i$, for all i), while the magnetization changes sign

under this operation. This symmetry can be *explicitly* broken by adding a new term in the hamiltonian,

$$H(\sigma; h) = -J \sum_{i,j}^{\text{n. n.}} \sigma_i \sigma_j - h \sum_i \sigma_i, \tag{2.13}$$

where the second term represents the interaction of the spins with an external uniform magnetic field h. Note that the average magnetization can be expressed through a derivative with respect to h:

$$\langle m \rangle = \frac{1}{\beta N} \frac{\partial}{\partial h} \log Z = -\frac{\partial f}{\partial h} \tag{2.14}$$

In a real ferromagnetic system the magnetization depends on the external magnetic field, like in a paramagnet, but, unlike this, $\langle m \rangle$ assumes a nonzero value (spontaneous magnetization), also when the external field is put to zero. In the trivial case of Hamiltonian (2.13) with $J = 0$, the partition function factorizes in the sums over the single uncorrelated spins,

$$\sum_\sigma e^{\beta h \sum_i \sigma_i} = \prod_i \left(\sum_{\sigma_i} e^{\beta h \sigma_i} \right) = (2 \cosh(\beta h))^N \tag{2.15}$$

describing a paramagnetic system with magnetization

$$\langle m \rangle = \tanh(\beta h). \tag{2.16}$$

The minimization of the free energy $F = U - TS$ requires the best compromise between minimal energy U (all spins aligned) and maximum entropy S (random spins). For low temperatures it is more efficient to minimize energies in order to minimize F, and consequently the spins can become ordered giving rise to a spontaneous magnetization (ferromagnetic phase). As the temperature increases, entropy plays a major role, so disordered spins are favored (paramagnetic phase) and there is no spontaneous magnetization. A phase transition between these two behaviors is then expected. Despite its simplicity, the partition function Z with the hamiltonian (2.13) can be calculated exactly only for a regular lattice in one dimension and in two dimensions with $h = 0$. In $d = 1$ it comes out, as we will see in the following, that the Ising model do not present any phase transition, since fluctuations destroy any order (in general, there is no phase transition for a one-dimensional system in absence of long-range interactions, as showed by Peierls), but a spontaneous magnetization is present in $d \geq 2$. Note that,

to apply the above energy-entropy argument, it is necessary to explicitly break the spin reversal symmetry by applying, for example, an infinitesimal external field, since the spin reversal symmetry leads immediately to the absence of magnetization in zero external field. The thermodynamic limit of the average magnetization per spin $\langle m \rangle$ should be then computed as

$$\langle m \rangle_0 = \lim_{h \to 0^+} \lim_{N \to \infty} \frac{1}{N} \sum_i \langle \sigma_i \rangle. \tag{2.17}$$

The order of the limits is crucial to obtain the appearance of spontaneous magnetization ($\langle m \rangle_0 \neq 0$), since if we reverse the order we always obtain zero. This situation, in which the low temperature thermodynamic state has a lower degree of symmetry than the Hamiltonian, is called *spontaneous symmetry breaking* and the magnetization m is the *order parameter*.

2.1.1 Ising model in one dimension

In this section we consider the exactly solvable problem of a linear lattice or, in other words, a system of N spins on a line. The Hamiltonian of the model is

$$H = -J \sum_{i=1}^{N-1} \sigma_i \sigma_{i+1} \tag{2.18}$$

and the partition function

$$Z = \sum_\sigma e^{-\beta H} = \sum_\sigma \prod_{i=1}^{N-1} e^{\beta J \sigma_i \sigma_{i+1}} \tag{2.19}$$

can be rewritten, using the identity

$$e^{\beta J \sigma_i \sigma_{i+1}} = \cosh \beta J + \sigma_i \sigma_{i+1} \sinh \beta J,$$

as

$$Z = (\cosh \beta J)^{N-1} \sum_\sigma \prod_{i=1}^{N-1} (1 + \sigma_i \sigma_{i+1} \tanh \beta J). \tag{2.20}$$

Consider a term of the product above, as for example

$$(\tanh \beta J)^3 (\sigma_1 \sigma_2)(\sigma_3 \sigma_4)(\sigma_4 \sigma_5). \tag{2.21}$$

In such a term, every spin appears once with a single bond, like for instance σ_2, or twice, with both its two bonds, like σ_4. In the latter case it does not

matter, since $\sigma_4^2 = 1$. In the former case one can isolate the sum on the two states $\sigma_2 = \pm 1$, and the two corresponding terms sum up to zero. The only surviving term in the product is then 1, and the sum gives the number of configuration 2^N:

$$Z = 2^N \left(\cosh \beta J\right)^{N-1}. \tag{2.22}$$

Sometimes one assumes periodical boundary conditions (spins on a ring), unimportant in the thermodynamic limit. Adding the interaction term $-J\sigma_N\sigma_1$ in the Hamiltonian (2.18) the partition function becomes

$$Z = 2^N \left(\cosh \beta J\right)^{N}. \tag{2.23}$$

Once the partition function is computed, we have access to all the thermodynamic functions, and we can check the existence of a phase transition. In this case, if we assume periodic boundary conditions, the free energy density in the thermodynamic limit is equal to its finite size value $f_N = F/N$, which is independent on N:

$$f = -\frac{1}{\beta} \lim_{N\to\infty} \frac{1}{N} \log Z = -T \log\left(2\cosh(J/T)\right) \tag{2.24}$$

This is an analytic function of the temperature unless $T = 0$, which means that, as we have anticipated, there is no phase transition.

In the more general case of a one dimensional system with a magnetic field h, imposing periodic boundary condition and defining $\sigma_{N+1} = \sigma_i$, we can write the partition function as

$$Z = \sum_{\sigma} \prod_{i=1}^{N} e^{\beta J \sigma_i \sigma_{i+1} + \frac{h}{2}(\sigma_i + \sigma_{i+1})}. \tag{2.25}$$

This can be computed introducing the symmetric transfer matrix [10]

$$V_{ab} = \begin{pmatrix} e^{\beta(J+h)} & e^{-\beta J} \\ e^{-\beta J} & e^{\beta(J-h)} \end{pmatrix},$$

in terms of which Z becomes

$$Z = \sum_{a,b,c,\ldots,r,s} V_{ab}V_{bc}\ldots V_{rs}V_{sa} = \text{Trace}\left(V^N\right) = \lambda_+^N + \lambda_-^N.$$

Here $\lambda_\pm$ are the eigenvalues of the transfer matrix:

$$\lambda_\pm = e^{\beta J}\left[\cosh(\beta h) \pm \sqrt{\sinh^2(\beta h) + e^{-4\beta J}}\right]. \tag{2.26}$$

Since the two eigenvalues are always positive and $\lambda_- < \lambda_+$, we have

$$\log\left(1 + (\lambda_-/\lambda_+)^N\right) < (\lambda_-/\lambda_+)^N \to 0$$

as $N \to \infty$. Hence, in the thermodynamic limit, the free energy density can be expressed as

$$f = -\lim_{N\to\infty} \frac{1}{\beta N} \log Z = -\frac{1}{\beta} \log \lambda_+.$$

2.2 Mean field approximation

The one-dimensional Ising model is easy to deal with, but the exact solution for $d = 2$ can be only computed in absence of external field, and no exact solution is known for $d = 3$, thus it is in general necessary to use some approximation. The most simple and physically intuitive is the mean-field approximation, which is based on the following idea. Consider a particular spin σ_i with z nearest neighbors and assume that every other spin can be replaced by its thermal average $\langle\sigma_j\rangle$: one is lead then to a paramagnetic problem where the external field h on a spin σ_i is replaced by an effective field $h + zJ\langle m\rangle$ depending on the total average magnetization. In this case all the spins are equivalent to the average magnetization, which satisfies the Curie-Weiss equation

$$\langle m\rangle = \tanh\beta\left(zJ\langle m\rangle + h\right). \tag{2.27}$$

This equation can be solved numerically: for $h > 0$ there can be three solutions, but the ones with $\langle m\rangle < 0$ are metastable or instable, the only physically acceptable solution corresponding to the magnetization oriented like the field h; for $h \to 0^+$, the only solution is $\langle m\rangle_0 = 0$ when $T > zJ$, and a spontaneous magnetization $\langle m\rangle_0 > 0$ appears for $T < zJ$ (in this case the solution $\langle m\rangle_0 = 0$ is unstable). The two spins orientations are equivalent, but below the critical (Curie) temperature $T_c = zJ$ the spontaneous magnetization privileges one of these orientations, and it suffices an infinitesimal modification of the magnetic field to pass from one to the other.

2.2.1 Critical behavior

Let us consider now the solutions of equation (2.27) around T_c and for small fields, to analyze the behavior of some thermodynamical observables. Under these conditions $\langle m\rangle$ is small and one can develop the hyperbolic tangent:

$$\langle m\rangle_0 = \beta zJ\langle m\rangle_0 + \frac{1}{3}(\beta zJ)^3\langle m\rangle_0^3 + O(\langle m\rangle_0^5),$$

whence

$$\beta\langle m\rangle_0\,(1-T_c/T) \sim (T_c/T)^3\langle m\rangle_0^3$$

and one finds that for temperatures slightly below T_c the spontaneous magnetization goes as

$$\langle m\rangle_0 \sim (T_c - T)^{1/2}. \tag{2.28}$$

The magnetic susceptibility χ

$$\chi = \left.\frac{\partial\langle m\rangle}{\partial h}\right|_{h=0}, \tag{2.29}$$

which measures the response of the system under a small magnetic field, can be computed from (2.27) as

$$\chi = \frac{1-\langle m\rangle_0^2}{T - T_c(1-\langle m\rangle_0^2)}. \tag{2.30}$$

For $T > T_c$ we have $\langle m\rangle_0 = 0$, so that

$$\chi = (T - T_c)^{-1} \tag{2.31}$$

For $T < T_c$ one can assume $\langle m\rangle \sim \langle m\rangle_0 + \epsilon$, with $\epsilon \sim h$, and substituting in

$$\beta(\langle m\rangle_0 + \epsilon)\,(1-T_c/T) \sim (T_c/T)^3(\langle m\rangle_0 + \epsilon)^3$$

one finds again

$$\chi \sim (T_c - T)^{-1}. \tag{2.32}$$

At $T = T_c$ we have

$$\langle m\rangle_0 = \langle m\rangle_0 + \frac{1}{3}\langle m\rangle_0^3 + \frac{h}{T_c}$$

so that on the critical isotherm the magnetization as a function of the field goes as

$$\langle m\rangle_0 \sim h^{1/3}. \tag{2.33}$$

In the mean field approximation, having replaced each spin with its average value $\langle m\rangle_0$, the internal energy U_N for a zero magnetic field is simply

$$\begin{aligned} U_N &= -\frac{1}{2}zJN\langle m\rangle_0^2 \quad T < T_c \\ U_N &= 0 \qquad\qquad\qquad\quad T > T_c. \end{aligned}$$

The specific heat C at zero field is given by the derivative of the internal energy with respect to the temperature, so for $T < T_c$

$$C = \left.\frac{\partial U}{\partial T}\right|_{h=0} = \frac{3}{2}N. \tag{2.34}$$

Since C is obviously zero for $T > T_c$ it has a discontinuity equal to $3N/2$ at the transition temperature.

Experimental data show that the spontaneous magnetization, the susceptibility, the critical isotherm and the specific heat obey power laws near $T = T_c$, with *critical exponents* $\alpha, \beta, \gamma, \delta$

$$C \sim |T - T_c|^{-\alpha} \tag{2.35}$$

$$\langle m \rangle_0 \sim (T - T_c)^{\beta} \qquad (T < T_c) \tag{2.36}$$

$$\chi \sim |T - T_c|^{-\gamma} \tag{2.37}$$

$$h \sim \langle m \rangle_0{}^{\delta} \qquad (T = T_c) \tag{2.38}$$

Other scaling laws with suitable critical indexes can be found for the Fourier transform of the spin correlation function and the correlation length.

The mean field approximation, as we have shown, predicts $\alpha = 0$; $\beta = 1/2$; $\gamma = 1$; $\delta = 3$; so they do not depend on the dimension d. Having replaced each spins with its mean value, we have totally neglected spin fluctuations. However these values can be confronted with the exact values for $d = 1, 2$ and the numerical values for $d = 3$.

For $d = 1$, the mean field approximation does not work at all, since it predicts a phase transition for $T_c = 2J$. For $d = 2$ we know that the phase transition exists and the approximation is more accurate, also if the predicted critical temperature $T_c = 4J$ is larger than the real T_c. The critical exponents are still different from the exact values, but the improvement is apparent, and the situation gets better for $d = 3$. The point is that the neglected fluctuations contrast the appearing of a transition (and they increase when the transition is near, as an analysis of the correlation length shows), and this approximation should work better when the number of nearest neighbors is large. Actually, it is the space dimension that matters: it can be proved that the mean field approach is exact for $d \to \infty$ and the critical exponents are correct for $d > 4$, or when the interactions are long-range.

In particular, if each spin interacts with the same coupling strength J/N with all the others, the exact solution is the same as the one predicted by the mean field approximation. As the number of spins interacting with each spin is very large, in this case it is legitimate to replace σ_i with its average $\langle m \rangle$.

2.2.2 Curie-Weiss model

We focus now on the solution of the Curie-Weiss model, corresponding to the infinite-range Ising model in which the interaction J/N, with $J > 0$, is independent on distance and each spin interact with all the others. This is equivalent to a mean field approximation for the Ising model, and will lead us to the Curie-Weiss equation (2.27) for the magnetization.

The Hamiltonian is given by

$$H(\sigma; h) = -\frac{J}{N} \sum_{1 \le i < j \le N} \sigma_i \sigma_j - h \sum_i \sigma_i \tag{2.39}$$

or, in terms of the magnetization $m(\sigma) = \sum_i \sigma_i / N$,

$$\tilde{H}_N(m(\sigma), h) = -\frac{1}{2} N J m^2(\sigma) + \frac{J}{2} - N h m(\sigma). \tag{2.40}$$

The second term is a constant of $O(1)$ and will be neglected, while the other two terms are $O(N)$, making H extensive, as it should be. The Hamiltonian, thus, depends on the configurations only through $m(\sigma)$. We can introduce the density of states $D(m)$ with a given magnetization $m(\sigma)$,

$$D(m) = \sum_\sigma \delta(m - m(\sigma)) \tag{2.41}$$

and the partition function can be written as

$$Z = \int_{-\infty}^{+\infty} dm \; D(m) e^{-\beta \tilde{H}(m,h)} \tag{2.42}$$

$$= \int_{-\infty}^{+\infty} dm \; e^{-N \beta \phi(m,h)} \tag{2.43}$$

where the effective free energy $\phi(m, h)$, which we may call constrained free energy, since it is constrained to the values of magnetization m, is given by

$$\phi(m, h) = \frac{1}{2} J m^2 + h m - \frac{1}{\beta N} \log D(m) \tag{2.44}$$

$$= -\frac{\tilde{H}_N(m, h)}{N} - \frac{1}{\beta} s(m). \tag{2.45}$$

Note that we are using the same symbol for the observable $m(\sigma)$ and its values m. However, this should not cause confusion, since which one is meant is clear from wether the argument σ is given or not. The second term,

$$s(m) = \frac{1}{N} \log D(m) \tag{2.46}$$

can be thought as the constrained entropy associated with the density $D(m)$, the most the configurations associated with a given magnetization m, the largest $s(m)$.

Saddle-point integration

For large N, the only values of m that matter in the integral in (2.43) are the ones minimizing $\phi(m,h)$. In the thermodynamic limit, in particular, the free energy can be evaluated via a saddle-point integration as

$$f(\beta,h) = -\lim_{N\to\infty} \frac{1}{\beta N} \log \int dm\, e^{-N\beta\phi(m,h)} = \min_m \phi(m,h). \tag{2.47}$$

This requires the explicit computation of $D(m)$. A magnetization $m(\sigma)$ can be obtained with $N_+ = N(1+m(\sigma))/2$ spins up, and the remaining, pointing down, are $N_- = N(1-m(\sigma))/2$. The number of configurations compatible with this scenario is then

$$\frac{N!}{\left[\frac{N(1+m(\sigma))}{2}\right]!\left[\frac{N(1-m(\sigma))}{2}\right]!}$$

and $s(m)$ can be evaluated via the Stirling approximation for $N \to \infty$.

An other way to compute D is based on the integral representation of the delta, whence the density of states (2.41) can be expressed as

$$\begin{aligned} D(m) &= \sum_\sigma \frac{N}{2\pi} \int dx\, e^{iNxm - ix\sum_i \sigma_i} \\ &= \frac{N}{2\pi} \int dx\, e^{iNxm} \sum_\sigma e^{-ix\sum_i \sigma_i}. \end{aligned} \tag{2.48}$$

The sum over configurations factorizes in the sums over the single spins

$$\sum_\sigma e^{-ix\sum_i \sigma_i} = \prod_i \left(\sum_{\sigma_i} e^{-ix\sigma_i} \right) = (2\cos(x))^N \tag{2.49}$$

and one finds

$$D(m) = \frac{N}{2\pi} \int dx\, e^{N(ixm + \log 2 + \log\cos(x))}. \tag{2.50}$$

The exponent is minimized by

$$x = \arctan(im) = i\,\mathrm{artanh}(m) = \frac{i}{2}\log\frac{1+m}{1-m}. \tag{2.51}$$

Substituting in $\log\cos(x)$ we have

$$\log\cos(x) = \log\cosh(\operatorname{artanh}(m))$$

and, using $\cosh\alpha = (1-\tanh^2\alpha)^{-1/2}$, we find

$$\log\cos(x) = -\frac{1}{2}\log(1+m) - \frac{1}{2}\log(1-m).$$

Thus, saddle-point evaluation of the integral in (2.49) gives

$$s(m) = -\frac{1+m}{2}\log\left(\frac{1+m}{2}\right) - -\frac{1-m}{2}\log\left(\frac{1-m}{2}\right). \tag{2.52}$$

The terms $(1\pm m)/2$ can be interpreted as the probability for a spin to point up or down, and $s(m)$ is the entropy of a distribution over the two states with these probabilities. Its maximum is obtained when the two states are equiprobable and $m=0$ (in fact this is the value of magnetization with the maximum number of compatible configurations).

On the other hand, the energetic term $\tilde{H}(m,h)$ favors large values of $|m|$ and the minimization of $\phi(m,h)$ is a tradeoff between the two. The derivative of entropy is

$$s'(m) = -\frac{1}{2}\log\left(\frac{1+m}{1-m}\right) = -\operatorname{artanh}(m)$$

so that the extremal condition

$$0 = \partial_m\phi(m,h) = Jm + h - \frac{1}{\beta}\operatorname{artanh}(m) \tag{2.53}$$

gives us the Curie-Weiss equation

$$m = \tanh(\beta J m + \beta h). \tag{2.54}$$

Fluctuations

The macroscopic observables, as the magnetization, describe the overall behaviour of the system, and we may consider their fluctuations around their average equilibrium values, for N large but finite. The probability of $m(\sigma)$ taking a certain value m can be evaluated as

$$P(m) = \frac{1}{Z}\sum_{\sigma} e^{-\beta H(\sigma)}\delta(m-m(\sigma)) \tag{2.55}$$

$$= \exp\left(-N\beta\phi(m,h) - \beta F\right). \tag{2.56}$$

Now, for N large, suppose that $\phi(m,h)$ has a global minimum in $\bar{m}$: the free energy F, apart from negligible terms, can be approximated as $F = N\phi(\bar{m},h)$, with $\phi(\bar{m},h)$ computed in the thermodynamic limit, and the probability is

$$P(m) = \exp\left(-N\beta[\phi(m,h) - \phi(\bar{m},h)]\right) \tag{2.57}$$

$$\approx \exp\left(-N\beta\frac{1}{2}\left.\frac{\partial^2}{\partial m^2}\phi(m,h)\right|_{m=\bar{m}}(m-\bar{m})^2\right), \tag{2.58}$$

that is a Gaussian distribution centered on $\bar{m}$, and of width $O(1/\sqrt{N})$. Only values of m for which $m - \bar{m} = O(1/\sqrt{N})$ have a significant probability of occurring. For $N \to \infty$ the fluctuations vanish and m takes the value $\bar{m}$ with probability one.

Chapter 3

Mean-field model for cooperativity

In this chapter, in analogy with the Curie-Weiss model described before, we introduce a mean-field model for cooperative systems. We will see how different behaviors, in the binding of small molecules to homeoallosteric biopolymers with multiple docking sites, can be reconstructed and described in this way. In particular, different cooperative phenomena, such as positive and negative cooperativity, can be interpreted in terms of an effective interaction between sites, and the observables commonly used to describe such phenomena, like the Hill coefficient (see section 1.5.1), are easily related to these interactions. This constitutes the original contribution of this work to the study of cooperative phenomena, and the results have been published in [11, 12].

We will focus exclusively on homeoallosteric binding, that is binding of the same ligand molecules on sites with the same affinities. Consider a macromolecule, like for instance an enzyme, which can bind to its N sites some smaller ligand molecules. The state of occupation of a single site i can be described then by an Ising variable, assuming the two values $\sigma_i = \pm 1$, respectively when the site is occupied or empty, and the global configuration of the molecule is thus specified by the vector

$$\sigma = \{\sigma_1, \sigma_2, ..., \sigma_N\}.$$

The interesting macroscopic quantity is the fraction saturation, introduced in section 1.3, that can be expressed as

$$\theta(\sigma) = \frac{1}{N} \sum_i \frac{1 + \sigma_i}{2}. \tag{3.1}$$

In terms of $m(\sigma) = \sum_i \sigma_i/N$ this becomes

$$\theta(\sigma) = \frac{1 + m(\sigma)}{2}. \tag{3.2}$$

The probability of a configuration $P(\sigma)$ at a given temperature will be influenced, in general, by the total concentration of ligands α and by the possible cooperative effects among sites. The distribution $P(\sigma)$ determines the average fraction of occupied sites

$$\langle\theta(\sigma)\rangle = \sum_\sigma P(\sigma)\theta(\sigma) \tag{3.3}$$

which is the quantity measured by experiments.

3.1 Independent binding sites

Let us suppose that binding sites are independent, and there is no cooperativity. In this simple case we know that the binding curve obeys the Michaelis-Menten law (1.26), and the total probability factorizes in the single probabilities for the occupation of a site: $P(\sigma) = \prod_i p(\sigma_i)$. Now, since $\sigma_i^2 = 1$, the most general function of σ_i is a linear function, but, without losing generality, we can also express it as an exponential

$$p(\sigma_i) = \frac{1}{Z} e^{h\sigma_i} \tag{3.4}$$

where Z is a normalization factor, which for the constraint $p(+1)+p(-1) = 1$ is equal to $Z = 2\cosh h$, and h is a parameter that will depend on the total concentration of ligands, here designated by α. This probability also correspond to the distribution of a paramagnetic spin in an external field h, at unitary temperature. The average fraction of occupied sites is particularly easy to compute in the case of independent sites:

$$\begin{aligned}
\langle\theta\rangle &= \sum_\sigma P(\sigma) \frac{1}{N} \sum_i \frac{1+\sigma_i}{2} \\
&= \frac{1}{2} + \frac{1}{2N} \sum_i \left(\sum_{\sigma_i = \pm 1} p(\sigma_i)\sigma_i \right) \\
&= \frac{1}{2} + \frac{1}{2}\tanh(h)
\end{aligned} \tag{3.5}$$

where we can note the analogy between the second term in last equation and the magnetization of a paramagnetic system (2.16).

The most natural choice to link the concentration of ligands and the probabilities is to assume that the ratio between the probability of having the site occupied to the probability for an empty site is equal to the total concentration, that is,

$$\frac{p(+1)}{p(-1)} = e^{2h} = \alpha, \tag{3.6}$$

With this simple assumption the average fraction of occupied sites (3.5) as a function of the concentration α is given by

$$\langle\theta\rangle = \frac{\alpha}{1+\alpha}, \tag{3.7}$$

which describes, as expected, a Michaelis-Menten behavior, with an equilibrium constant K for binding equal to unity, so that assuming (3.6) makes perfectly sense (see sec. 1.4.1).

The term $\frac{1}{2}\log(\alpha)$ can be interpreted as the energy (chemical potential) necessary for the release of a molecule from a binding site. In fact, if the concentration is not too large, it is known that the chemical potential of a given species in a solution can be expressed as the logarithm of its concentration (see sec. 1.1). To be more accurate, we could write it as

$$\frac{1}{2}\log\left(\frac{\alpha}{\alpha_0}\right), \tag{3.8}$$

where α_0 gives the scale of concentration. When $\alpha > \alpha_0$ this energetic term is positive and tend to favor binding of molecules on sites. On the contrary, if $\alpha < \alpha_0$ the logarithm is negative so that empty sites ($\sigma_i = -1$) are energetically favorable. So $(1/2)\log\alpha_0$ corresponds to a sort of standard-state chemical potential. Substituting α with α/α_0 in Eq. (3.7), one finds

$$\langle\theta\rangle = \frac{\alpha}{\alpha_0+\alpha}, \tag{3.9}$$

hence, confronting this equation with (1.26), we may note that the equilibrium constant K is also tuned by α_0, having $K^{-1} = \alpha_0$.

3.2 Cooperative sites

So far we have been considering non-cooperative system, where the probability to bind a molecule on a site is independent on the occupations of other sites. The model above can be easily extended to cooperative systems, by

assuming an Ising-like form for the probability of a given configuration, that is

$$P(\sigma) = \frac{1}{Z}\exp\left(\sum_{i,j} J_{ij}\sigma_i\sigma_j + \frac{1}{2}\log(\alpha)\sum_i \sigma_i\right), \tag{3.10}$$

$$Z = \sum_{\sigma}\exp\left(\sum_{i,j} J_{ij}\sigma_i\sigma_j + \frac{1}{2}\log(\alpha)\sum_i \sigma_i\right). \tag{3.11}$$

The first term in the exponential represent an interaction energy between couples of sites: the couplings J_{ij} are assumed positive in the case of a cooperative system and the structure of these couplings will depend on the particular macromolecule considered. In any case, one obviously expects that the stronger the couplings, the stronger the cooperative effects.

For instance, we can consider the paradigmatic example of hemoglobin [10]. This molecule has four binding sites (heme groups) for oxygen molecules, laying at the vertices of a tetrahedral structure, formed by two α-subunits and two β-subunits (Fig. 1.2(b)). As a first approximation, one can consider cooperative effects only between α-β subunits, and with the same degree of cooperativity J. Hence, the protein can be represented by a ring of four sites with nearest-neighbor interactions, and the average fraction saturation is given by

$$\begin{aligned}\langle\theta\rangle &= \frac{1}{2} + \frac{1}{2}\sum_{\sigma} P(\sigma) \\ &= \frac{1}{2} + \frac{1}{2}\frac{\partial}{\partial h}\log Z\end{aligned} \tag{3.12}$$

with $h = (1/2)\log\alpha$. As we have seen in sec. 2.1.1, the partition function for this model is

$$Z = \lambda_+^N + \lambda_-^N, \qquad N = 4 \tag{3.13}$$

$$\lambda_\pm = e^J\left[\cosh(h) \pm \sqrt{\sinh^2(h) + e^{-4J}}\right]. \tag{3.14}$$

Then, with a tedious but straightforward computation, one is led to the following expression for the fraction saturation

$$\langle\theta\rangle = \frac{\alpha\left[K + (2K + K^2)\alpha + 3K\alpha^2 + \alpha^3\right]}{1 + 4K\alpha + (4K + 2K^2)\alpha^2 + 4K\alpha^3 + \alpha^4} \tag{3.15}$$

with $K = \exp(-4J)$. Note that this particular form of Adair equation reduces to the Hill equation

$$\langle\theta\rangle = \frac{\alpha^4}{1+\alpha^4} \tag{3.16}$$

in the limit of an infinite interaction strength J between sites. This theoretical binding curve, which has only K as adjustable parameter, can be confronted with experimental measurements, and a good agreement is found, apart from systematic deviation appearing at high oxygen concentrations. As we have mentioned in sec. 1.5, the molecule undergoes a quaternary conformational change if at least one of the two sites on each $\alpha\beta$ pair is occupied, and interactions are more important across the interface between the two $\alpha\beta$ dimers. To take into account such an effect, one should add into (3.10), adapted for the hemoglobin as in the model above, some interaction terms for three and four sites together, besides considering possibly interactions also between the sites that were previously considered decoupled. This should make the predictions more accurate, but at the price of more complicated computations, and with a larger number of adjustable parameters.

In general, we could adapt this model to different proteins and enzymes, using a suitable interaction topology, possibly considering interactions among more than two sites at time, to take into account quaternary structural change. However, we are going to consider a more simple mean-field approach, with an unique parameter for the interactions among couples of sites. This simple model is able to capture, in a semi-quantitative way, several behaviors occurring in the binding of small ligands to macromolecules.

3.3 Mean-field model

In the previous section, we have seen how the oxygen-binding curve of hemoglobin can be modeled through a simple one-dimensional Ising model. A natural extension, that should be adaptable to a large class of homeoallosteric proteins and, in general, positively cooperative macromolecules, is a Curie-Weiss like model, where the probability of a configuration is

$$P(\sigma) = \frac{1}{Z}\exp\left(\frac{J}{N}\sum_{1\le i<j\le N}\sigma_i\sigma_j + \frac{1}{2}\log(\alpha)\sum_i\sigma_i\right), \tag{3.17}$$

$$Z = \sum_\sigma \exp\left(\frac{J}{N}\sum_{1\le i<j\le N}\sigma_i\sigma_j + \frac{1}{2}\log(\alpha)\sum_i\sigma_i\right). \tag{3.18}$$

Here, the interaction is again between couples of sites, but there is no topology, and every site interacts in the same way with all the others. In the previous section, we considered the interactions between sites on a single macromolecule, which is the common approach. Now we would like to extend somehow this approach, by considering N as the total number of binding sites, localized on different macromolecules, for a ligand. The binding of a ligand on a given site of a macromolecule has cooperative effects on the sites of the same molecule. However, if the concentration of macromolecules is large, we may expect that binding on less filled molecules will be more likely, since there is a large number of free sites. For instance, consider the oxygen binding curves for different concentration of hemoglobin, shown in figure 3.1. For low Hb concentration the binding affinity is higher, but the cooperative effects are more strong when the concentration is higher. The exponent in

Figure 3.1: Oxygen-binding curves for hemoglobin at different concentrations (decreasing from right to left). For diluted solutions the equilibrium between $\alpha\beta$ dimers and $(\alpha\beta)_2$ tetramers is shifted toward dimers, and this is the prevailing form. The leftmost solid curve is for dissociated $\alpha^1\beta^1$ dimers (D), with $n_H = 1.0$, while the rightmost curve pertains to tetramers (T), with $n_H = 3.3$. The concentration of hemoglobin for intermediate curves ranges form $4 \times 10^{-8}M$ to $1 \times 10^{-4}M$. Note the different cooperative effects (and affinities). Figure from [7].

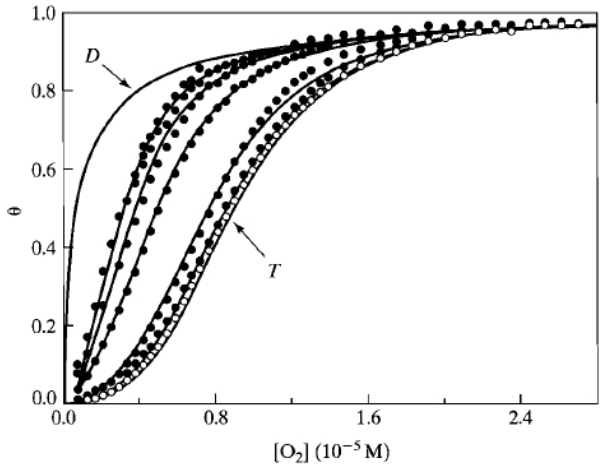

(3.17), then, can be considered as an effective microscopic interaction energy, and the coupling J, as we will see, can be directly related to the Hill number, giving an effective number for the interacting sites.

The main point in our analysis is the effective microscopic description, typical of statistical mechanics and allowing for a clear interpretation of dif-

ferent macroscopic cooperative behaviors. The general interaction parameter we introduce is certainly not sufficient to reproduce correctly the complex mechanisms acting at the elementary level, but its effective value encodes some of the most relevant features observed in binding curves. That is to say, from different observed shapes in binding isotherms we can infer the effective microscopic structure of interactions between active sites. In our framework, Hill coefficients and cooperativity measures can be given an elementary interpretation and the comparison between systems associated to different cooperativity values can be translated in a relation between their structural properties.

In analogy with the Curie-Weiss model, in the limit of large N the average value $\langle\theta\rangle$ can be obtained by minimizing, with respect to the parameter $\theta \in (0,1)$, an effective free energy

$$F(\theta,\alpha) = \inf_{|\theta|} \Big(-\frac{J}{2}(2\theta-1)^2 - \frac{1}{2}(1-\theta)\log(\alpha) - s(\theta)\Big). \tag{3.19}$$

The first two terms at the r.h.s. stand for the internal energy, which corresponds to the Boltzmann average of the Hamiltonian $H(\{\sigma\}, J, h)$ expressed as a function of θ and α, while

$$s(\theta) = -\theta\log(\theta) - (1-\theta)\log(1-\theta) \tag{3.20}$$

is the entropic term, whose weight is ruled by the temperature T, which is taken equal to one in this analogy. This effective free energy can be seen as a generating function, whose derivative with respect to the chemical potential $(1/2)\log\alpha$ yields to the fraction saturation at a given concentration. We are going to see what happens for different values of the coupling J, since this is the parameter regulating the behavior of the system. Valid descriptions of binding phenomena in terms of this mean-field model are dependent on there being a very large number of solute particles in the sample observed, so that macroscopic fluctuations in properties will be very unlikely. As for biopolymers, we can consider an extreme example: in a solution containing 0.01 mg/ml of a virus of molecular weight 100 million, we still find approximately 1010 particles per milliliter. This is a number that is large enough that we need not worry about fluctuations in macroscopic volumes. It is only when we begin considering volumes comparable to that of a single cell that some problems can arise.

For large values of J, the most likely configurations are those associated to small values of the effective internal energy, while for smaller values the

most likely configurations are those corresponding to higher values of entropy[1]. Therefore, the minimum of F is the optimal compromise between the minimization of the effective internal energy and the maximization of entropy. We expect that for large interactions J (or chemical potentials) the energetic term in (3.19) is the leading contribution, and the optimal fraction is ruled by this term, so that the sites tend to be in the same state and the binding isotherm displays a sigmoidal shape, while for small values of the interaction strength the leading term will be the entropic one, which at a fixed value of the chemical potential prefers disordered states, i.e. states obtained by a large number of configurations, and pushes the binding curve towards a MM form:

The minimum condition for (3.19) with respect to the order parameter θ corresponds to the analogous of the CW self-consistence equation (2.54)

$$\theta(\alpha, J) - \frac{1}{2} = \frac{1}{2} \tanh\left(J(2\theta - 1) + \frac{1}{2}\log(\alpha)\right) \tag{3.21}$$

and gives the average fraction saturation corresponding to the equilibrium state for the system at a given concentration of binding ligands α.

As we have seen, equation (3.21) describes a second order phase transition for $J = J_c = 1$ and $\alpha = 1$. When $J > J_c$ and $\alpha = \alpha_c = 1$, the transition is first order and the average fraction θ has a discontinuity. Equation (3.21) holds rigorously just in the thermodynamic limit ($N \to \infty$); for finite systems, beyond $\mathcal{O}(1/N)$ corrections, we recall that the discontinuous functions are mildly smoother, accordingly with the experimental counterparts.

We consider separately the two cases $0 \leq J < 1$ and $J > 1$ for the interactions between sites, because, as stated, while in the former case θ is everywhere continuous in α, in the latter it has a discontinuity in $\alpha = 1$, taking a value smaller than $1/2$ when $\alpha \to 1^-$ and greater than $1/2$ when $\alpha \to 1^+$. In both cases, however, it is easy to check that $\theta(\alpha, J) \to 0$ for $\alpha \to 0$ (which corresponds to the $h \to -\infty$ limit) and $\theta(\alpha, J) \to 1$ for $\alpha \to \infty$ ($h \to +\infty$). This means that the fraction saturation vanishes when the substrate concentration vanishes and it saturates to one when the substrate concentration is large, as expected. It should be clear that $\theta(\alpha, J)$ is the value corresponding to the average value $\langle\theta\rangle$ with respect to the distribution (3.17). In the following, we will often drop the dependence on α and J (and

[1] We notice that the entropic term is connected to the logarithm of the number of configurations associated to a given fraction θ of occupied sites: It is maximized for fractions around $1/2$, which have a larger number of configurations associated, and minimized for $\theta = 0,\ \theta = 1$, corresponding to just one configuration and a vanishing entropy.

the brackets) but it should be clear, from the context, that we are talking about this average value.

Figure 3.2: Different binding curves obtained by varying the coupling J. For $J = 0$ (blue line) the hyperbolic Michaelis-Menten law represents the curve for a non-interacting system; for $J = 0.2$ (green) the system has a weakly cooperative behavior; for $J = 0.6$ (red) strong cooperativity manifests itself with the typical sigmoidal shape; $J = 1$(light green) is the critical regime: the derivative in the inflection point which gives the Hill coefficient is infinite; $J = 1.8$ (purple) represents the discontinuous case, with an extremely strong cooperativity.

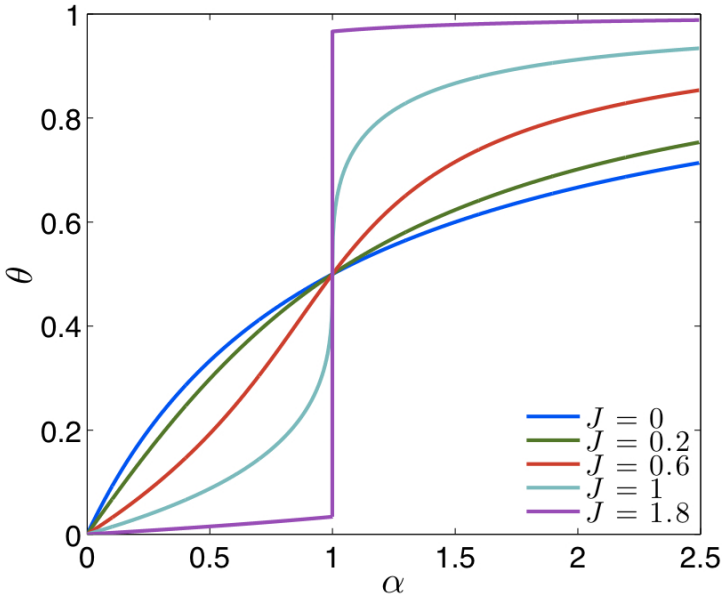

When $J \to 0$, no cooperativity is expected (as the model reduces to a one-body theory) and, coherently, we recover the MM binding curve. In fact, Eq. (3.21) can be equivalently expressed as

$$\theta(\alpha, J) = \frac{\alpha \exp\left[2J(2\theta(\alpha, J) - 1)\right]}{1 + \alpha \exp\left[2J(2\theta(\alpha, J) - 1)\right]} \tag{3.22}$$

which properly gives, for $J = 0$

$$\theta(\alpha, J)|_{J=0} = \frac{\alpha}{1 + \alpha}. \tag{3.23}$$

From Eq. (3.22), we see that when $J > 0$ the fraction saturation for a given concentration is smaller than the corresponding value for a non interacting system when $\alpha < 1$, and becomes greater when $\alpha > 1$. In fact, the

greater the interaction and the steeper the sigmoidal shape of the curve. The fraction saturation curves resulting from Eq. 3.22 are plotted in Figure 3.2 versus α, for several values of J. Interestingly, a global change in the system considered, e.g. concerning ph or temperature, may lead to variations in the affinity between binding sites and ligands as well as in the coupling strength between binding sites themselves, giving rise to a curve $\theta(\alpha)$ displaying a different steepness.

Now, the derivative[2] of θ with respect to α, which is strictly related to the Hill coefficient and, consequently, to the cooperativity of the system, can be computed from (3.21):

$$\frac{\partial\theta}{\partial\alpha} = \frac{1}{4\alpha}\frac{1-(2\theta-1)^2}{1-J\left[1-(2\theta-1)^2\right]}. \tag{3.24}$$

This is always positive and finite for $J < 1$, meaning that θ is an increasing function of α, as we expected. In the limit of low concentration of ligands we obtain

$$\left.\frac{\partial\theta}{\partial\alpha}\right|_{\alpha=0} = \exp(-2J) \tag{3.25}$$

so the binding at very low concentration is governed by the two-bodies interaction J: the greater J and the flatter the fraction saturation curve. When $J = 0$, $\partial_\alpha\theta|_{\alpha=0} = 1$ and one properly recovers the same trend as that of the MM curve, which has a first order behavior with the same coefficient for small concentrations.

Finally, to recognize the sigmoidal shape typical of cooperative systems, we have to study the second derivative, which can be easily computed and expressed in terms of the first one:

$$\frac{\partial^2\theta}{\partial\alpha^2} = -\frac{1}{\alpha}\frac{\partial\theta}{\partial\alpha}\left[1+\frac{2\theta-1}{\left(1-J\left[1-(2\theta-1)^2\right]\right)^2}\right]. \tag{3.26}$$

When α ranges in $(1,\infty)$, this is always negative, so that θ is a concave function of α in that range, for any value of J. For $\alpha = 1$ we have $\partial^2_{\alpha^2}\theta =$

[2]Note that in the frame of the Curie-Weiss model this is strictly related to the generalized susceptibility

$$\chi = \frac{\partial m(h)}{\partial h}$$

which measures the response of the system to a change in the field h. In fact, we have

$$\frac{\partial\theta}{\partial\alpha} = \frac{1}{2}\frac{\partial m(h(\alpha))}{\partial\alpha} = \frac{1}{2}\frac{\partial h}{\partial\alpha}\chi(h(\alpha)) = \frac{1}{4\alpha}\chi(h(\alpha))$$

$-(1/4)/(1-J)$, so that θ is still concave there. For $\alpha \in (0,1)$ we can compute numerically the second derivative: it comes out, not surprisingly, that it is not sufficient to have a positive coupling J between binding sites to see a sigmoidal curve. In fact, if this interaction is small, the second derivative is negative for all concentration, and the hyperbolic form will resemble the MM curve.

J<1/4: Weak cooperativity

The values of the coupling for which the curve is hyperbolic are the ones below the value $J \leq 1/4$. In fact, expanding θ to the first order in α one finds

$$\left.\frac{\partial^2\theta}{\partial\alpha^2}\right|_{\alpha=0} = -2(1-4J)\exp(-4J) \tag{3.27}$$

so for this values of the interaction the binding curve θ is everywhere concave, tending, for $J \to 0$, to the hyperbolic MM form (whose second derivative $-2(1+\alpha)^{-3}$ is always negative). Note that when $J = 0$ the expression (3.27) gives, correctly, the MM value -2. The absence of an inflection point in the region $J \in [0, 1/4]$ allows us to define it as a weak cooperativity region: the shape of the binding isotherm is practically indistinguishable from that of a non-cooperative system.

1/4 < J < 1: Strong cooperativity

From the analysis of Eq. 3.26 it comes out that when $1/4 < J < 1$, there is a unique inflection point α^* (whose value increases with J), which separates the region where θ is convex (small concentration), to the one where it is concave. For $J = 1/4$ this point corresponds to $\alpha^* = 0$, while it is shifted towards unitary concentrations ($\alpha = 1$) when J is close to 1. As a sigmoidal curve has necessarily an inflection point, we may talk about strong cooperativity in this interval, in contrast to the weak cooperativity previously introduced. These very simple definitions have the advantage of being directly related to an effective microscopic interaction J, so that the experimental behavior of a system could allow one to reconstruct this interaction strength and interpret the binding curve in terms of the mean-field model.

J>1: Discontinuous binding curve

We have seen that when $J < 1$ we can consider two regions, a weak cooperative one, where the binding curve is hyperbolic, and a strong cooperative one, with an inflection point growing gradually with the interaction strength.

When $J > 1$ (corresponding in the original Ising model to the "ferromagnetic" phase) the binding curve is still increasing with α, and the expressions (3.25-3.27) remain valid for $\alpha \neq 1$. In this point the curve is discontinuous and the jump is given by $\theta_+(J) - \theta_-(J)$, where

$$\theta_\pm(J) = \lim_{\alpha \to 1^\pm} \theta(\alpha, J).$$

These two limits depend on J: they are both equal to $1/2$ for $J = 1$, when the curve is still continuous, and their difference increases smoothly with the square root of $J - 1$ when $J > 1$ (see Figure 3.2). This means that, starting from vanishing concentration, the system has less sites occupied, for a given α, than the corresponding non interacting one, until the concentration reaches the reference value. Here, it is sufficient to increase infinitesimally the number of free molecules to obtain a large filling (depending on J). After that value, the number of occupied sites is always greater than the corresponding value for MM. Note that, in principle, if the concentration varies slowly one could observe metastability, with a curve which continues growing continuously up to values of $\alpha > 1$. The entire out of equilibrium features of the model are ruled out in this treatment as we deal with equilibrium statistical mechanics, however -as a second step- the bridge could be extended in that direction. If $J \to \infty$ this discontinuity increases, while its derivative in zero vanishes, so that in the large volume limit we obtain a step function. This corresponds to an ideal situation where no binding site is occupied until the concentration has reached the critical value $\alpha = 1$, and when this value has been reached all sites are occupied. This kind of discontinuous behavior can be observed, for example, in the binding isotherms of small surfactants onto a polymer gel [13]

When $J \to 1$ a second order phase transition appears. This indicates that the correlation between binding sites becomes stronger and the typical trend of thermodynamical observables is a power law. Let us consider a little more in detail the behavior of the curve for $J \to 1$. The discontinuity for $J > 1$ is given by $\theta_+(J) - \theta_-(J)$, whose dependence from J near the critical point $(\alpha = 1, J = 1)$ can be expressed as

$$\theta_+(J) - \theta_-(J) \approx (J - 1)^{1/2}$$

while on the critical isotherm (i.e. for $J = 1$) around the critical concentration $\alpha = 1$, mean-field theory predicts

$$\theta(\alpha, 1) - \frac{1}{2} \approx (\alpha - 1)^{1/3}\,.$$

In this regime one can also predict the behavior of the α dependence of the Hill coefficient defined in section 1.5.1, which, when $\alpha \to 1$, diverges as

$$n_H(\alpha) \approx (\alpha - 1)^{-2/3} .$$

Moreover, we know that when $J \to 1^{\pm}$ the susceptibility, and so the derivative of θ respect to α, diverges as

$$\chi|_{\alpha=1} \approx |1 - J|^{-1} .$$

As hinted previously, the exponents of these power laws are only valid in the limiting case of a very large number of interacting site, while for finite-size systems corrections depending on the real dimension of the space in which they are embedded are expected. However these scalings, in particular those related to the reaction rate around the discontinuity as a function of α, suggests some new measures for almost discontinuous reaction curves.

Cooperativity through the Hill coefficient

As explained in Sec. 1.5.1, an usual way to define in a quantitative manner the cooperativity of a system is by the Hill coefficient n_H, obtained from the maximum slope of $\log[\theta/(1-\theta)]$ vs. $\log \alpha$. If binding on different sites is an independent process, one simply finds $n_H = 1$, while in the extremum case in which sites are either all empty or all occupied $n_H = N$. We call a system cooperative (non cooperative) if $n_H > 1$ ($n_H = 1$), while the cooperativity is said to be negative, meaning that binding is reduced if there are occupied sites, for $n_H < 1$. This number gives then a lower bound for the number of interacting sites, and it is possible to see that it is related to the variance of the mean number of occupied sites, in our model.

The Hill coefficient for our general model depends, as expected, on the interaction J; in particular for $J < 1$ we find

$$n_H \equiv \frac{\partial \log [\theta/(1-\theta)]}{\partial \log \alpha} = 4 \left. \frac{\partial \theta}{\partial \alpha} \right|_{\alpha=1} = 1/(1-J). \tag{3.28}$$

Being the derivative of θ for $\alpha = 1$, the Hill coefficient is finite (and greater than one) for $J < 1$ and it diverges for $J \to 1^-$ when the discontinuity appears. An infinite Hill coefficient may seem unrealistic, however it is not an unavoidable feature of our modeling: in fact h scales with the connectivity of the underlying network of interactions and, while the latter diverges in this minimal fully connected representation, diluted mean fields can still work finely. The equation above gives a new interpretation of the Hill number

n_H, in terms of microscopic effective interactions among sites. On the other hand, the coupling J can be related in this way to the effective number of interacting sites.

Cooperativity through the global dissociation quotient measure

Among the useful tools to describe cooperativity, we introduced in section 1.5.1 the global dissociation quotient $K(\alpha)$, whose derivative γ is expected to be different from zero when some form of cooperation occurs; in particular, γ should be negative when there is a positive cooperation. Figure 3.3(a) shows some plots of $\gamma(\alpha)$ for different values of J: consistently with the definition of $K(\alpha)$, in the region of $\alpha < 1$, we find that the stronger the interaction, the smaller γ, properly indicating the deviation from the K-constant MM curve. Since the derivative of θ with respect to α appears in the definition of γ, in correspondence of the critical value $J = 1$, $\gamma(\alpha)$ diverges for $\alpha = 1$. In fact this is the (critical) region where the correlations between sites, and so the cooperativity, are expected to diverge. Observe that the curve corresponding to $J = 1$ stays above with respect to the others, corresponding to smaller values of J. For $J > 1$ this is even more accentuated (but for clarity it is not shown in the figure). as the binding curve tends to saturate before and it is more flat at high concentrations. On the other hand, the larger is the coupling the larger is the value of gamma, in absolute value, for values of concentration smaller than $\alpha_0 = 1$.

Cooperativity through the Koshland measure

Lastly, we want to recover also the measure of cooperativity introduced by Koshland (see sec. 1.5.1): To this aim, we plotted the previously defined Koshland coefficient as a function of the two-bodies interaction coupling J, as the latter is the only relevant tunable parameter to explore cooperativity at work. In our model, the coefficient can only be defined for $J < 1.5$; in fact, for $J > 1$, $\theta(\alpha)$ is a discontinuous function and when $J \geq 1.5$ the fraction saturation assumes only values smaller than 0.1, for $\alpha < 1$, and larger than 0.9, for $\alpha > 1$. As shown in Figure 3.3(b), we find that it is a decreasing function of J, which takes the value $\kappa = 81$ for non-interacting systems ($J = 0$), and $\kappa = 1$ when $J = 1.5$. This coefficient is essentially a measure of the average increasing between two points, and we can note the similarity of this measure with the Hill number expressed in terms of J, which goes as $1/(1 - J)$. However, since the Koshland coefficient measures an average increasing, it does not take into account the fact the curve is discontinuous

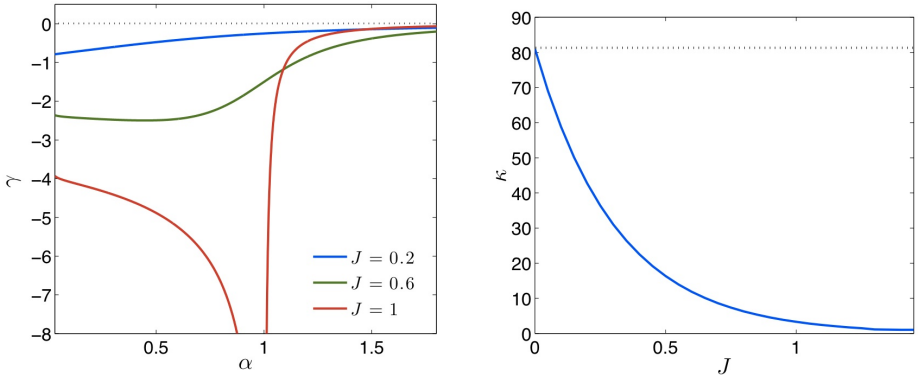

(a) The figure shows different regimes for the derivative of the global dissociation quotient $\gamma(\alpha) = dK/d\alpha$ obtained by varying the interaction strength J. For $J = 0.2$ (green) γ remains quite close to zero, indicating that K is nearly constant in α, as one expects for a non-cooperative system; for $J = 0.6$ (red) the global dissociation quotient has a stronger dependence on α: we know that in this case the binding isotherm has a sigmoidal shape and strong cooperativity appears; when $J = 1$(cyan) we are in the critical regime, where the derivative of θ, and so γ, diverges at $\alpha = 1$. For the sake of clarity the function γ is not plotted for values of $J > 1$.

(b) The Koshland coefficient $\kappa = \alpha_{0.9}/\alpha_{0.1}$ obtained measured in our model as a function of the two-sites interaction J. It is a decreasing hyperbolic function, defined for values of J below $J = 1.5$, which tends to be lower when cooperatively is larger and the binding isotherm takes a steeper sigmoidal form. The dotted lines represent in both figures the reference values corresponding to a non-cooperative system, i.e., with $J = 0$.

Figure 3.3: Global dissociation quotient and Koshland coefficient

for $J > 1$.

3.3.1 Fit with experimental data

To conclude this section, we show as an example the fit of some experimental data found in literature with our model. Data come from two different experiments. In the first case, the cooperativity in the binding of Ca^{2+}-calmodulin (CaM) molecules to an enzyme (calcium-calmodulin-dependent protein kinase II, CaMKII) is analyzed. CaMKII is a henzyme involved in many important signaling cascades which has, around a central ring-shaped scaffold, 12 (kinase) subunits where the molecules can bind. Experiments show that binding is cooperative, with a measured Hill coefficient of $n_H = 3.0 \pm 0.3$. We fitted experimental data (from Fig. 2b in [14], properly

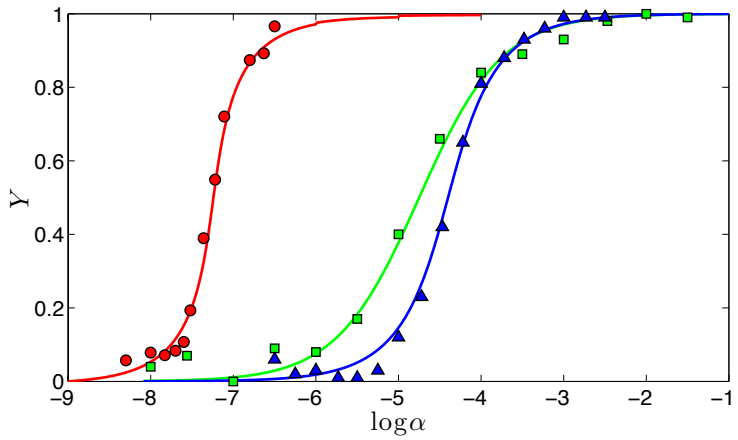

Figure 3.4: The plots show data from recent experiments (symbols) concerning non cooperative and cooperative binding and fits through our model (Eq. 3.21). Here Y stands for the fraction saturation θ and the horizontal axis is logarithmic to the scale 10, with concentrations of ligands α expressed in mol. Red circles represent fraction saturation measurements of CaM binding on CaMKII, for which an original Hill fit revealed a coefficient $n_H = 3.0$ (hence positive cooperativity) [14]. Red continuous line is the best fit with our model, predicting $n_H = 2.94 \pm 0.06$, in complete agreement with the literature. The green and blues experimental data (squares and triangles) represent the binding of glycine molecules by the VC I-II RNA (blue triangles, cooperative) and the VCII RNA (green squares, non-cooperative) [15]. The line for the VC II is a Michaelis-Menten curve with $\alpha_0 = 7.5 \times 10^{-5}$ mol ($J \equiv 0$ in our theory) while, the line for the VC I-II is the best fit within our cooperative model, giving $n_H = 1.66 \pm 0.03$. This value is in agreement with the one found in [15] with a Hill fit, which is $n_H = 1.64$. Note that the MM curve has a sigmoidal form, due to the log scale.

rescaled) with Eq. 3.21, and using J and α_0 as fit parameters. Our optimal values $Log_{10}(\alpha_0) = -7.2 \pm 0.2$ and $J = 0.70 \pm 0.04$, corresponding to a Hill number $n_H = 3.3 \pm 0.4$ are in good agreement with the values in literature. In the second case we consider glycine binding to a riboswitch (an RNA filament) that uses cooperative binding to control gene expression: the VC I-II RNA, which has two binding sites for glycine, and the VC II, with only one site. The latter case is clearly non-cooperative, while for the former a Hill fit gives $n = 1.64$. The fit with our model gives $Log_{10}(\alpha_0) = -4.4 \pm 0.06$ and $J = 0.40 \pm 0.03$, and consequently $n_H = 1.66 \pm 0.08$, again in good agreement with the coefficient found in literature (Fig. 3 in [15]).

3.4 Multiple interacting systems

In the previous section we analyzed the case of effective interactions between couples of sites. However, there are cases in which the cooperative effects in biopolymers involve large structural changes, as a certain number of sites has been filled, like in hemoglobin. Thus, in the following, we want to analyze the effects of multiple interactions, involving more than two elements together, in particular three and four bodies interactions. Strictly speaking, this effect should be considered directly in the effective interaction energy, adding the proper terms in the Hamiltonian representing the effective interaction energy. In general, the simplest p-body interaction among N sites which can be either occupied or empty ($\sigma_i = +1$ or -1 respectively) can be expressed by a Hamiltonian (3.29)

$$H_N(\{\sigma\}, J, h) = -\sum_{p=2}^{\infty} \frac{p!}{2N^{p-1}} J_p \sum_{1 \le i_1 < \ldots < i_p \le N} \sigma_{i_1} \ldots \sigma_{i_N} - \frac{1}{2}\log(\alpha) \sum_{i=1}^{N} \sigma_i. \tag{3.29}$$

The interaction strength J_p will be assumed positive (for $J = 0$ we recover the standard MM curve again) and the combinatorial factor before the summation makes the energy extensive. For simplicity, we will consider the separate contributions of different terms, to isolate the different weight in the global behavior of the independent binding capability represented by each independent p-term in the effective energy. However, we stress that the binding curve cannot be simply seen as a sum of the binding curves resulting from the different terms. It is easy to see that the energy (the mean value of the Hamiltonian) scales as

$$\langle H_N \rangle \propto N \langle m\Phi(m) \rangle, \ \Phi(m) = \sum_{k=1}^{p-1} c_k m^k + \frac{1}{2}\log(\alpha), \tag{3.30}$$

where c_k is the coefficient of the Taylor series implicitly defined by eq. (3.30), and $m = 2\theta - 1$. Notice that the σ's acting on a single site could tend to keep it in the state -1 or $+1$ according to their product. For example, for $p = 4$ one could have three sites, acting on the i-th site, in a configuration, say (+1, +1, -1), which favors the state $\sigma_i = -1$, even if in the whole there are more sites in the state $\sigma = +1$. The same local field is obtained when the configuration is (-1,-1,-1), i.e. if all the three sites are empty. The energetic behavior of this extension is then deeply different from the previous case: Usually one deals with linear forces, which are generated by quadratic

potentials (i.e. $p = 2$) such that the Maxwell-Boltzmann probability distribution is Gaussian accordingly with what naively expected by a simple Central Limit Theorem argument and critical behavior, at $\alpha = 0$, arises to confirm this picture [16]. If a more complex scenario appears then a violation of this linear framework is expected: for instance for $p = 3$ it is straightforward to check that even a positive J may have subtle anti-cooperation features: in fact it is immediate to check that the energy would prefer the orientation of the spins $+1, +1, +1$ but also $+1, -1, -1$; this can be thought of as a competitive feature of the multi-attachment that naturally introduce negative cooperativity in the process under investigation. To be more precise, one could consider, for instance to model hemoglobin behavior, different values of J_3 (and J_4), according to the sites considered.

This extension still shares with the simplest $p = 2$ case the same entropy: In fact, as in the two-body case, for this long range interacting system the energy can be easily expressed as a function of the parameter θ describing the fraction of occupied sites, and of the concentration α

$$N^{-1}H_p(\theta, \alpha) = -\frac{J}{2}(2\theta - 1)^p - \frac{1}{2}\log(\alpha)(2\theta - 1), \tag{3.31}$$

while the entropy per site is exactly the same as in the $p = 2$ case. Given the effective free energy

$$F(\theta, J, \alpha) = -\frac{J}{2}(2\theta - 1)^p - \frac{1}{2}\log(\alpha)(2\theta - 1) - s(\theta) \tag{3.32}$$

the minimum condition with respect to the order parameter θ, which gives the fraction saturation at a given concentration, reads off as

$$\theta(J, \alpha) - \frac{1}{2} = \frac{1}{2}\tanh\left(\frac{1}{2}pJ(2\theta - 1)^{p-1} + \frac{1}{2}\log(\alpha)\right). \tag{3.33}$$

This corresponds to the equilibrium state for the system, and the average fraction of occupied sites will be given by the solution of this equation. Once again, this equation, as in the $p = 2$ case, is strictly valid when the number of sites is large.

Again, we expect that for large interactions J (or chemical potentials) the energy term in (3.32) is the leading one, and the sites tend to be in the same state (this corresponds to a large magnetization), while for small values of the interaction strength the leading term is the entropic one, which prefers disordered states, i.e. states where the sites do not see each other. Let us consider now the cases of interactions among three and four sites together, respectively.

3.4.1 Case $p = 3$

Figure 3.5: Binding curves e line of discontinuity for $p = 3$.

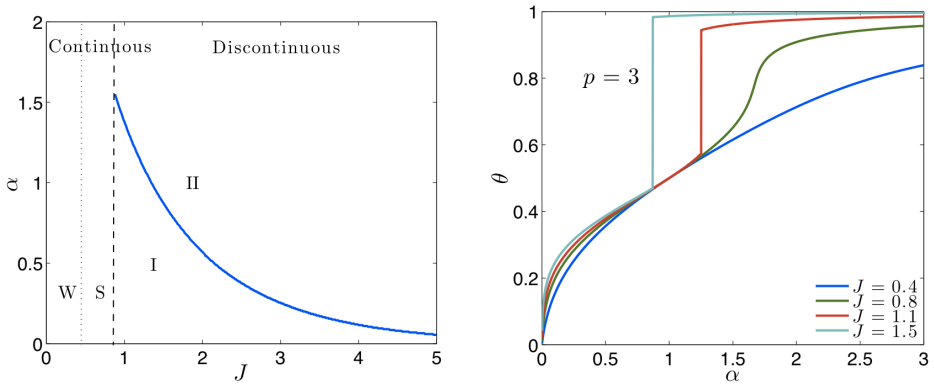

(a) The figure shows, in blue, the line of discontinuity of the binding isotherm, occurring for $J_3 = 0.86$. For $J_3 < 0.50$ the system is weakly (W) cooperative, with no inflections; for $0.50 < J_3 < 0.86 = J_{3c}$ it is strongly (S) cooperative, having at least one inflection point. The line signaling the discontinuity goes exponentially towards vanishing concentrations as the interaction increases

(b) Binding isotherms $\theta(\alpha)$ for different values of J_3. For $J_3 = 0.4$ (blue line) the system is weakly cooperative, with a hyperbolic form; for $J_3 = 0.8$ (green) it has two inflections, the first for $\alpha = 1/2$ and the second for a larger α; for $J_3 = 1.1$ (red) the isotherm has a strong inflection for $\alpha < 1$ and a discontinuity for a value of the concentration between 1 and 1.5, corresponding to a transition to a more ordered state; for larger J_3, as the curve for $J_3 = 1.5$ shows, the discontinuity is shifted towards $\alpha < 1$.

In this case the energy (3.31) is an odd function of $m = 2\theta - 1$ at fixed α

$$N^{-1}H_3(\theta, \alpha) = -J_3(2\theta - 1)^3/2 - \frac{1}{2}\log(\alpha)(2\theta - 1). \tag{3.34}$$

Its global minimum corresponds to a fraction of occupied sites θ satisfying the equation

$$\theta = \frac{1}{2} + \frac{1}{2}\tanh\left(\frac{3}{2}J_3(2\theta - 1)^2 + \frac{1}{2}\log(\alpha)\right). \tag{3.35}$$

Note that, as shown in figure 3.6(b), whatever the value of the interaction, for unitary concentrations the sites are half filled. For J_3 less than $J_{3c} = 0.86$, one can see numerically that the effective free energy has only one minimum, and the binding curve is continuous, while a discontinuity appears

for $J_3 > J_{3c}$. In the range for which the curve is continuous, we can perform a numerical study of its second derivative with respect to α, to understand when an inflection point, and consequently a sigmoidal shape, appears. As before, we can denote as weakly cooperative a system whose curve has no changes in its concavity, and in this case this occurs for interactions below the threshold of $J_3 = 0.5$. In correspondence of this value there is just one inflection point, for a concentration $\alpha = 1.5$, and two inflection points for interactions in the range $0.5 < J_3 < 0.86$, which will then correspond to the strongly cooperative counterpart. This is related to the fact that the effective free energy 3.32 has in the former case only one minimum, while in the latter, when the chemical potential $(1/2)\log\alpha$ is not too large in absolute value, we can identify two minima for $\theta = \theta_1^*$ and $\theta = \theta_2^*$; of these two minima one is only local and the other is global, according to the value of α. At lower concentrations the global minimum is found in correspondence of the smaller fraction saturation θ_1^*; then, increasing α, the values of the energy in the two minima coincide at some concentration, and at some α the global minimum shifts to θ_2^*, corresponding to the larger value of θ (see figure 3.6). For $0.5 < J_3 < 0.86$ the two minima coincide at $\theta_1^* = \theta_2^*$, and the resulting binding isotherm is continuous. On the contrary, for $J_3 > 0.86$ they assume the same value for some $\theta_1^* \neq \theta_2^*$, so that $\theta(\alpha)$ has a discontinuity.

Figure 3.6: Some plots of $F(\theta, J, \alpha)$ vs. θ for $J = 1.5$, showing the positions of the minima.

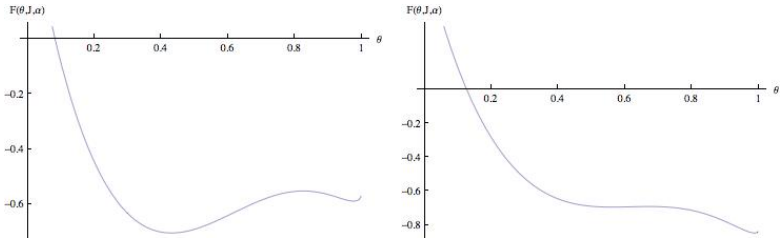

(a) $\alpha = 0.7$: in this case the minimum is located at the lower value of the fraction saturation

(b) $\alpha = 1.2$: increasing the concentration the minimum of F shifts abruptly to larger values of the fraction saturation

Thus, when the interaction among sites is weak, we have obviously a binding curve similar to the MM curve. Unlike the case $p = 2$, a stronger value of the interaction here makes easier to fill sites at low concentration, since if most sites are empty the effect on each of these site without ligands will be an increase of the probability to bind a ligand. However, as the frac-

tion saturation increases with growing concentration the cooperative effect gets more complicated. A regime of strong cooperativity can be identified, as in the case $p = 2$, for the curves with some change in the concavity, but in this case there are two inflection points, with a more visible change of concavity at larger values of the fraction saturation. Notice that, in the discontinuous binding isotherms, the concentration at which the discontinuity appears depends on the value of the coupling J, and this is due to the fact that the effective Hamiltonian in this case is no longer symmetric under the transformation $\sigma_i \to \sigma_i$ for all i. On the other hand, this symmetry is present in the case $p = 4$, which we are going to analyze.

3.4.2 Case $p = 4$

As for $p = 2$, in this case the interaction energy 3.31 is symmetric with respect to the exchange $\theta - 1/2 \to 1/2 - \theta$ when the concentration is equal to the unitary value, thus also the free energy features this symmetry

$$F(\theta, \alpha, J) = -\frac{J_4}{2}(2\theta - 1)^4 - \frac{1}{2}\log(\alpha)(2\theta - 1) - s(\theta). \tag{3.36}$$

To find the value of the fraction saturation for a system with a given coupling J at concentration α requires its minimization (w.r.t. θ), thus the binding curve can be reconstructed from the equation

$$\theta = \frac{1}{2} + \frac{1}{2}\tanh\left(2J_4(2\theta - 1)^3 + \frac{1}{2}\log(\alpha)\right). \tag{3.37}$$

Let us analyze this, starting from small values of the coupling: if the interaction among sites is small, again, we have a fraction saturation ruled by the concentration of free ligands and vanishing as the latter goes to zero. If J_4 is larger or equal than $J_4 = J_{c1} = 0.69$, the binding curve two discontinuities: coming from small concentrations, there is a value $\alpha_c(J_4) < 1$ for which θ changes abruptly to a larger value, which is smaller than $1/2$. Then $\theta(\alpha)$ varies continuously in the interval $\alpha_c(J_4) < \alpha < \alpha_c(J_4)'$, passing through the point $(1, 1/2)$, and there is a new transition with a discontinuity at an inverse value of $\alpha_c(J_4)$, $\alpha_c(J_4)' = \alpha_c(J_4)^{-1}$. In fact for this range of interaction strengths J_4, and for concentrations around $\alpha_c(J_4)$, the free energy has two local minima coming from the well matched competition between the energetic and the entropic terms, the former preferring small, "ordered" θ, while the latter has always its maximum at $\theta = 1/2$, corresponding to the largest number of configurations of bound molecules. The concentration tells us which is the global minimum and the two minima are equal at α_c.

The same happens around the symmetrical value $\alpha_c(J_4)'$. In the language of magnetic models, there are two first order symmetric transition, with corresponding discontinuities in the magnetization as a function of the magnetic field.

Figure 3.7: Binding curves for $p = 4$ and lines of discontinuity on the (J_4, α) plane.

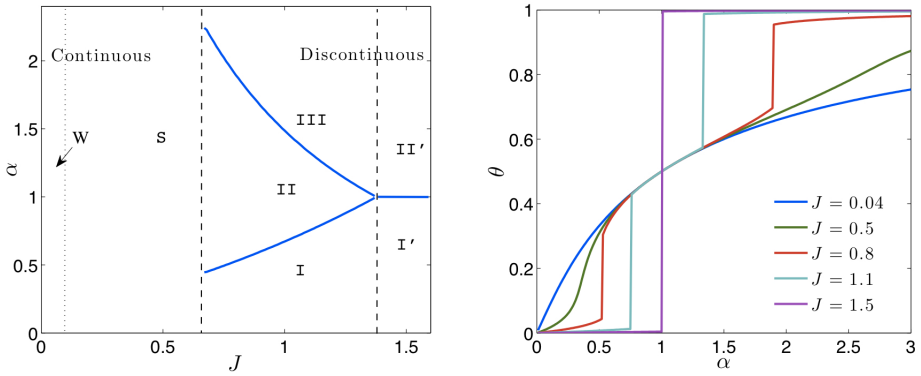

(a) The blue lines identify the concentration for which, at a given J_4, the binding curve θ is discontinuous. For $J_4 < J_{c1} = 0.69$ it is continuous, and it passes from a weak (W) to a strong (S) - both continuous - regime at $J_4 = 1/24$; for $J_{c1} < J_4 < J_{c2} = 1.37$ isotherms have two discontinuities, one for a critical $\alpha_c < 1$ and the other one for $\alpha_c' = 1/\alpha_c > 1$.

(b) Binding isotherms $\theta(\alpha)$ of a 4-bodies interacting system, for different values of the interaction J_4. The binding isotherm for $J_4 = 0.04$ (the blue line) has no inflections and represents a practically non cooperative system (weak cooperativity); when $J_4 = 0.5$ (green) the curve has an inflection point for a small concentration; for $J_4 > J_{c1}$ two inflection points appear and the isotherms develop two discontinuities corresponding respectively to the concentrations α_1 and α_2 such that $\alpha_1\alpha_2 = 1$ (see the curves for $J_4 = 0.8$ and $J_4 = 1.1$); for interactions larger than J_{c2}, the system has just one discontinuity for $\alpha = 1$ and the binding isotherm tends to a step function, as for the purple line corresponding to $J_4 = 1.5$.

The critical concentration α_c, at which the discontinuity of the binding curve occurs, increases and tends to one with the coupling J_4 growing, and from the value $J_4 = J_{c2} = 1.37$ on the curve has only one discontinuity. In this case the mutual interaction is the overwhelming force driving the system, and, similarly to the case $p = 2$, the binding isotherm has a discontinuity when passing from $\alpha < 1$ to $\alpha > 1$, changing abruptly from a large negative value (depending on J_4) to a positive, opposite value (see Figure 3.7). It

is interesting to note that the values of α_c and α'_c depend on J_4 and even for $p = 3$ we find a critical concentration depending on J_4: because this dependence is absent in the $p = 2$ case, an experimental J_4-dependent critical concentration may indicate that a multiple interaction effect is acting (this can be seen for example in [13]).

Analogously to the previous cases $p = 2, 3$, we can determine exactly the value $J_4 = 1/24$ as the one for which a first inflection point appears, so that the binding isotherm passes from a weak to a strong cooperativity curve. In fact, as for the $p = 2$ case (see eq. 3.27) by gaining the second derivative of the binding isotherm for small α one can see that the leading term is proportional to $(1 - 24J_4)$. Again, starting from small J_4, the curve has a unique inflection point until $J_4 = 0.45$; then, from this value on, a second point appears first at $\alpha = 2.4$, and for larger J_4 it splits in two points, thus for $0.45 < J_4 < J_{c1}$ we have three inflections. The ones corresponding to the smaller and to the larger values of α disappear when J_{c1} is reached and, instead of these inflections, the binding curve has two discontinuities.

A discontinuous behavior which could be explained in term of two and multisite interactions between hosting sites has been observed, for instance, in the binding isotherm of long chain alkyl sulphates and sulphonates to the protein bovin serum albumin, and in the adsorption isotherm of alkylammonium chlorides chains on the biotite surface [17]. Typically, if there are multi-site interactions (with $p > 2$) it is very likely that also two-bodies effects are present, and, as said before, one should consider the several possible interactions with different strengths J_p in the energy term.

As we have shown, the phenomenology pertaining to systems with p-body interactions depends sensitively on p and this allows to infer information about the properties of the system under study, starting from the behavior of the binding curve. On the other hand, we also notice that, when looking at the most likely configuration, that is the most likely value of θ for a given parameter set (p, J, α), we find that it exists and it is unique: if we, for the sake of simplicity, focus just on even $p > 2$ values, we can see that the amount of solutions is constant, namely, independent by the amount and complexity of the cooperating/anti-cooperating binding sites. More precisely, the self-consistent relation in Eq. 3.33 may allow for one or two distinct solutions, but only one is a global minimum for the free energy: the minima of the free energy do not scale, but simply shift, with p, while the global minimum is always unique. This argument may be applied to the problem concerning the folding of (long) proteins, whose secondary and tertiary structure is essentially always the same, despite a large number of multi-attachment is in principle possible [18].

Moreover, the analysis of multiple interactions can give an interesting insight when looking at complex binding curves, since we have seen that positively cooperative behavior rising from two-body interactions is essentially represented by a sigmoid (apart from the cases of weak cooperativity or the ultracooperative case of discontinuous binding isotherms). A binding curve departing from this simple form, and with a measured Hill coefficient larger than one, may be due to the interplay among many sites together causing large conformational changes.

Up to now, we have considered the case of positively cooperative systems, and with the same interaction for all the couples of sites. In the following, we generalize the approach used before to negatively cooperative systems, and we consider the possibility of different values for the couplings between sites, to take into account heterogeneity effects.

3.5 Extension to heterogeneous interactions

In this section we extend the mean-field model described before to account for more general interactions and for heterogeneous systems. The first extension we implement concerns the topology where the system is embedded in: the fully-connected graph is replaced by its simplest generalization, namely a complete bipartite graph, where nodes are divided in two groups: A and B. Each node in A (B) is linked to all node in B (A), but no link within the same group is present. While this generalization essentially plays no role for the case $J > 0$ (but we will introduce it anyway, to preserve the symmetry of the model) [19, 20], it will be crucial for the case $J < 0$.

Parties are made of by $N_A = N_B = N/2$ elements respectively, such that $N = N_A + N_B$ and their relative densities are $\rho_A = N_A/N = \rho_B = N_B/N = 1/2$. The elements in A and in B, labeled $i \in N_A$ and $j \in N_B$, respectively, represent, for instance, the two binding sites of a dimer. Note that, for the sake of simplicity, we introduced the simplest bipartite structure, which naturally maps dimers, but one can straightforwardly generalize to the case of an n-mer by an n-partite system. The second extension we implement concerns chemical heterogeneity, which recent experimental findings [21, 22] have highlighted to play a crucial role in determining cooperative effects. To include this feature in our theory we associate to each element $i \in N_A$ or $j \in N_B$ a string ξ_i (or ξ_j) encoding in same way its chemical structure, and we introduce a functional, which associates to any couple of strings (ξ_i, ξ_j) a proper measure of their coupling strength J_{ij}. We assume binary strings, i.e. for any entry $\mu = 1, ..., P$, $\xi_i^\mu \in \{0, +1\}$ (See figure 3.8). To

Figure 3.8: Couplings between elements in different parties.

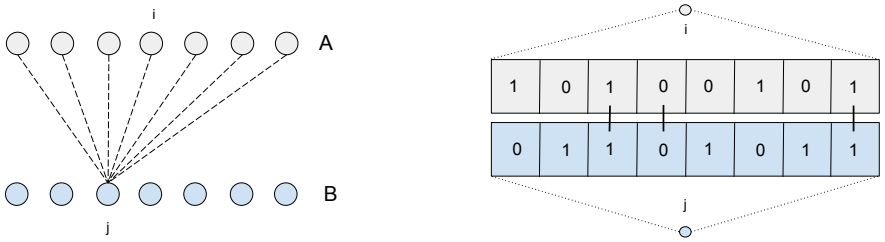

(a) Bipartite couplings: every element of A interacts with elements in B, and viceversa.

(b) The coupling is determined by the number of overlapping bits between two strings.

simulate heterogeneous couplings, the entries in the strings are supposed to be random, and the probability distribution is chosen, seeking for simplicity, as

$$P(\xi_i^\mu = 0) = \frac{1-a}{2}, \qquad P(\xi_i^\mu = 1) = \frac{1+a}{2}, \tag{3.38}$$

where the parameter $a \in [-1, +1]$ tunes the similarity between strings: for $a = \pm 1$ all the strings coincide and inhomogeneity in couplings is lost, and the coupling assumes its maximum value; for $a = 0$ strings are purely random and the inhomogeneity is maximum. As for couplings, here we focus on a similarity-based interaction which enhances the interaction between similar strings, such that

$$J_{ij} = J_0 \frac{1}{P} \sum_{\mu=1}^{P} (\xi_i^\mu \xi_j^\mu + \bar{\xi}_i^\mu \bar{\xi}_j^\mu), \tag{3.39}$$

where we defined $\bar{\xi} = 1 - \xi$ and J_0 is a tuning parameter that regulates the importance of the couplings (Fig. 3.9(b)). The string entries ξ_i^μ are all independent and "quenched[3]" and we denote with $\mathbb{E}$ the expectation with respect to their random values. The resulting average interaction strength is given by $\mathbb{E}J_{ij} = J_0(1 + a^2)/2$ with variance $\sigma_J^2 = J_0^2(1 - a^4)/4P$, so that for a large number of bits P, the coupling distribution approaches to a delta peaked at $\bar{J}$[4]. As a consequence of the coupling rule of Eq. 3.39, the larger

[3] See also part II for a detailed analysis of the meaning of this assumption.

[4] We stress that, whatever the possible scaling between P and N, e.g. $P \sim N^\gamma$, $\gamma > 0$, due to CLT convergence, the distribution of the couplings, hence of the inhomogeneity among ligands, becomes a Gaussian, according with [21].

the similarity shared by the two strings ξ_i and ξ_j, the stronger the interaction between sites i and j. In particular, for the positively cooperative system, i.e. $J_0 > 0$, the higher the magnitude J_{ij} and the higher the probability of finding sites i and j both occupied; viceversa, for the negatively cooperative system, i.e. $J_0 < 0$, the higher the magnitude J_{ij} and the higher the probability of finding one site occupied and the other empty. Finally, the particular choice $J_0 = 0$ recovers again Michaelis-Menten behavior.

As we have seen before, it is possible to associate an effective energy to a system whose sites interact with such couplings, and with a concentration of ligands α:

$$H(\sigma, \alpha; \xi) = -\frac{J_0}{N} \sum_{i \in A} \sum_{j \in B} \left(\frac{1}{P} \sum_{\mu=1}^{P} (\xi_i^\mu \xi_j^\mu + \bar{\xi}_i^\mu \bar{\xi}_j^\mu) \right) \sigma_i \sigma_j - \frac{1}{2} \log(\alpha) \sum_i^N \sigma_i. \tag{3.40}$$

We remind here that the concentration (and consequently the chemical potential) can be rescaled by taking $\alpha \to \alpha/\alpha_0$, with suitable α_0. The probability in this case depends also on the random strings, and is given by

$$P(\sigma; \xi) = \frac{1}{Z} \sum_\sigma \exp\left(-H(\sigma, \alpha; \xi)\right), \quad Z = \sum_\sigma P(\sigma; \xi). \tag{3.41}$$

One can associate to this a free energy $F = -\frac{1}{N} \log Z$ and compute, for instance, the fraction saturation of a given system in presence of the 'disorder" due to the random bits, by properly deriving F with respect to $\log(\alpha)$(see also appendix A). This would be a value depending on the particular choice of the strings, and one should then take its average $\mathbb{E}$ with respect to ξ, which will be denoted by the brackets $\langle . \rangle$. Note that in this case there is a double process of averaging.

We are going to study separately the two cases of positive ($J_0 > 0$) and negative ($J_0 < 0$) cooperativity. Suppose that we are not able to distinguish, in our measurements, the fraction saturations $\langle \theta_A \rangle$ and $\langle \theta_B \rangle$ relative to the two parties, and that the affinities for ligands are the same. Then we just measure the total fraction saturation as the arithmetic mean, $\langle \theta \rangle = (\langle \theta_1 \rangle + \langle \theta_2 \rangle)/2$. The qualitative different behaviors expected for θ as a function of the concentration of ligands α are shown in Fig. 3.8. Let us analyze now in detail the cases of positive and negative cooperativity.

3.5.1 Positive cooperativity

In the cooperative case $J_0 > 0$ one can show that the bipartite topology does not induce any qualitative effects: results are the same (apart proper

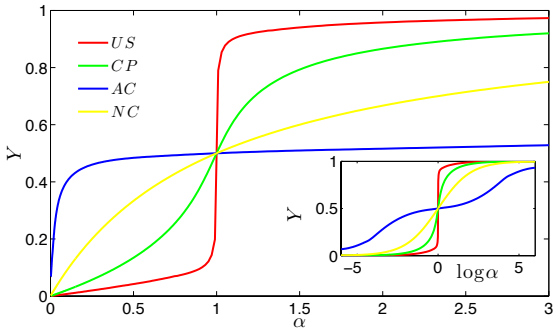

Figure 3.9: Theoretical predictions of typical binding isotherms obtained from SM models. Different colors refer to different behaviors, as explained by the legend. In particular, as the interaction strength J is varied, qualitative different outlines emerge: ultra-sensitive (US) for $J = 6$, cooperative for $J = 2$ (CP), anti-cooperative for $J = 0.5$ (AC), non-cooperative for $J = 1$ (NC).

rescaling) as for the CW model; indeed, in this case one can think bipartition as a particular dilution on the fully-connected model [19, 20]. The order parameters in the spin model counterpart are two, one for each party, namely

$$m_A(\sigma_A) = \frac{1}{N_A}\sum_{i=1}^{N_A}\sigma_i, \quad m_B(\sigma_B) = \frac{1}{N_B}\sum_{j=1}^{N_B}\sigma_j \tag{3.42}$$

and the the fraction saturations for a given configuration of occupied sites are expressed as

$$\theta_A(\sigma_A) = \frac{1}{N_A}\sum_{i}^{N_A}\frac{1}{2}(1+\sigma_i^A) = \frac{1+m_A(\sigma_A)}{2}, \tag{3.43}$$

$$\theta_B(\sigma_B) = \frac{1}{N_B}\sum_{j}^{N_B}\frac{1}{2}(1+\sigma_j^B) = \frac{1+m_B(\sigma_B)}{2}. \tag{3.44}$$

If we simply take the average value of the interaction energy (3.40) with respect to the random couplings, we find

$$\mathbb{E}H(\sigma,\alpha;\xi) = -N\left[J_0\left(\frac{1+a^2}{2}\right)m_A m_B + \frac{1}{4}\log(\alpha)(m_A+m_B)\right]. \tag{3.45}$$

Here we stress again that, differentely from low-dimensional systems such as the linear Ising-chains, this model admits sharp (eventually discontinuous in

the thermodynamic limit) transitions from an empty ($\langle m_A\rangle = \langle m_B\rangle = 0$) to a completely filled ($\langle m_A\rangle = \langle m_B\rangle = 1$) panorama as the concentration α is tuned; a discontinuous behavior has been experimentally well established as it is at the basis of the ultra-sensitive chemical switches [23]. The solution of the statistical mechanics problem trivially generalizes results from previous sections and reads as

$$\langle m_A\rangle = \tanh\left[J_0\rho_B\frac{(1+a^2)}{2}\langle m_B\rangle + \frac{1}{2}\log\alpha\right], \tag{3.46}$$

$$\langle m_B\rangle = \tanh\left[J_0\rho_A\frac{(1+a^2)}{2}\langle m_A\rangle + \frac{1}{2}\log\alpha\right], \tag{3.47}$$

However, having assumed an equal number of elements in the two sets ($\rho_A = \rho_B$=1/2), one has obviously $\langle m_A\rangle = \langle m_B\rangle$, whence

$$\langle m_A\rangle = \tanh\left[\frac{J_0}{2}\frac{(1+a^2)}{2}\langle m_A\rangle + \frac{1}{2}\log\alpha\right] \tag{3.48}$$

and the overall binding curve

$$\langle\theta\rangle = \frac{1}{2}(\langle\theta_A\rangle + \langle\theta_B\rangle) \tag{3.49}$$

$$= \frac{1}{2}\left(1 + \frac{\langle m_A\rangle + \langle m_B}{2}\right) \tag{3.50}$$

$$= \frac{1}{2}\left(1 + \langle m_A\rangle\right) \tag{3.51}$$

fulfills the following self-consistence equation (here we drop the brackets to have a more readable expression):

$$\theta(\alpha; J_0, a) = \frac{1}{2} + \frac{1}{2}\tanh\left[\frac{J_0}{2}\left(\frac{1+a^2}{2}\right)(2\theta - 1) + \frac{1}{2}\log\alpha\right] \tag{3.52}$$

This expression, which returns the average fraction of occupied sites corresponding to the equilibrium state for the system, is analogous to Eq. (3.21), discussed in section 3.3. The only difference is in the coupling term in the argument of the hyperbolic tangent, which is replaced here with the average coupling divided by two, since in this case each site interacts with only $N/2$ sites. The resulting fraction saturation is continuous for $J < J_c = J_0(1+a^2)/4$, while for $J = J_c$ we have the scenario, previously depicted, corresponding to a second order phase transition. Conversely, when $J > J_c$ and $\alpha = \alpha_c = 1$, transition is first order, that is the fraction saturation θ has a discontinuity and the model becomes ultra-sensitive. The

parameter a, introduced for the distribution of bits in the strings that regulate the couplings, acts as a heterogeneity parameter for the interactions: as we have seen, inhomogeneity in the strings is maximum for $a = 0$ and the couplings assume their minimum value in this case, vice versa for increasing $|a|$ the interactions increase, and $|a| = 1$ corresponds to the less homogeneous situation, with maximum coupling. Moreover, the distribution of couplings assumes a Gaussian form for a large number of bits codified in the strings, and the width of this distribution (as well as the average value) depends on the heterogeneity parameter a: the more its absolute value is near to one, the less is the width (but the larger is the average interaction strength), while for small $|a|$ the width of the distribution, and so heterogeneity, is maximum (with the minimum value of the average interaction).

Modern single-molecule methods show that heterogeneity exists in many instances: the affinities for a ligand, for example, can also vary in a ensemble of macromolecules which have the same binding cooperativity [21]. One of the consequences of this property is that summing up the individual binding curves, to obtain the overall curve for the ensemble, can lead to a measure of cooperativity (Hill number, for instance) which is less than the cooperativity parameter of single macromolecules (see Fig. 3.10).

Figure 3.10: (a) Simulated distribution of ligand-binding chemical potentials ΔG^0, with a heterogeneity parameter H. (b) Theoretical Hill binding isotherms (blue lines) with Hill coefficient $n = 3$. The resulting bulk cooperativity parameter for the best Hill fit to the bulk binding curve (red line) is $n_{bulk} = 1.6$ for this example. (c) Reduction of the bulk Hill coefficient as a function of the heterogeneity parameter. From [21]

.

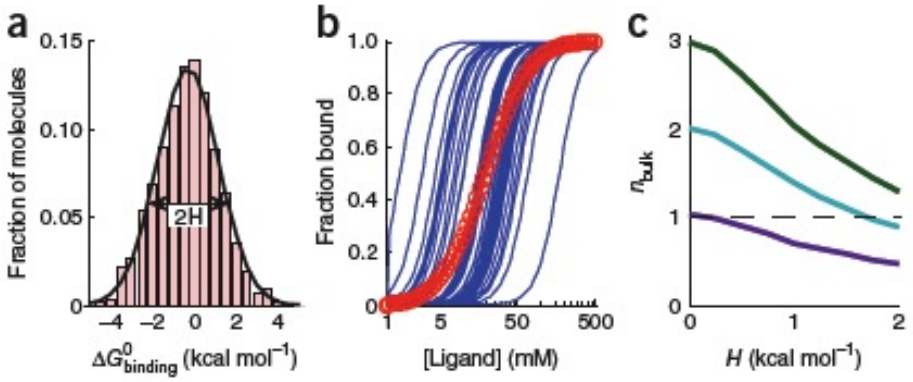

3.5.2 Negative cooperativity

A fascinating aspect of the model under investigation is its natural ability to extend the previous scheme for the description of a negatively cooperative system, simply applying parity $J_0 \to -J_0$, with $J_0 > 0$, over the energy in Eq. 3.40, namely by choosing a negative interaction among sites:

$$H(\sigma, \alpha; \xi) = \frac{J_0}{N} \sum_{i \in A} \sum_{j \in B} \left(\frac{1}{P} \sum_{\mu=1}^{P} (\xi_i^\mu \xi_j^\mu + \bar{\xi}_i^\mu \bar{\xi}_j^\mu) \right) \sigma_i \sigma_j - \frac{1}{2} \log(\alpha) \sum_i^N \sigma_i. \tag{3.53}$$

The first term in this expression tends to privilege opposed configurations for the two site subsets: if a site in A has bound a ligand, its effect on the other sites in B is to reduce the probability that they bind a molecule, and vice versa, which is just a negatively cooperative effect. The parameter a, introduced in (3.38), has again the function of tuning the heterogeneity of couplings.

Taking apart the strings for a moment, this is the analogous of an antiferromagnetic mean field model, in which the long range ordering at low temperatures is quite different from that in the ferromagnet, and the correct order parameter for the study of the system is the staggered magnetization $m_A - m_B$. For large values of temperature and field the stable state is paramagnetic ($m_A = m_B$), but lowering these parameters the system goes through a second-order phase transition in an antiferromagnetic state, with a staggered magnetization different from zero (see for instance [24] for a detailed analysis). In this state there is an asymmetry between the two subsets, as one of the two is more magnetized.

As for our original problem, we can solve it and find the average total fraction saturation of sites by using a method analogous to the one of sec. 2.2.2. The detailed computation can be found in appendix A, and here we just report the self-consistence equations giving the two average partial fraction saturations versus the concentration of ligand molecules α:

$$\langle \theta_A \rangle = \frac{1}{2} \tanh \left(-\frac{J_0}{2} \frac{(1+a^2)}{2} (2\langle \theta_B \rangle - 1) + \frac{1}{2} \log \alpha \right), \tag{3.54}$$

$$\langle \theta_B \rangle = \frac{1}{2} \tanh \left(-\frac{J_0}{2} \frac{(1+a^2)}{2} (2\langle \theta_A \rangle - 1) + \frac{1}{2} \log \alpha \right). \tag{3.55}$$

Not surprisingly, these expressions strongly resemble the previous self-consistence equations (3.46, 3.47), but now, with the minus sign in front of the couplings J_0 at the r.h.s.. The binding energy $\log \alpha$, as usual, acts on the

same way on the two subsets, as it tends to keep both kind of sites empty when α is small, and filled when α is large. Just like for the antiferromagnetic counterpart, it is possible to check (see the appendix for details) that there are two possible behaviors for the system, depending on the interaction strength J, and on the concentration of ligands α: if J is below a critical value $J_c = J_0(1 + a^2)/4$, the two partial fractions are always equal, for any concentration of external ligands (Fig. 3.12(a)); however, when the interaction is larger than this value, the two partial fractions are different, in a region of chemical potential $\log(\alpha)$ around zero, as shown in Fig. 3.12(b). In this region, because of the strong interaction and the small chemical potential, it is more convenient for the system to fill sites on one of the subsystems and keep less molecules of ligands on the other subsystem. In this case, starting from low concentrations, there is a critical value $\alpha_c < 1$ (and, consequently, of the chemical potential $\log \alpha$), above which $\langle\theta_A\rangle - \langle\theta_B\rangle$ start increasing with the concentration, reaches a maximum in $\alpha = 1$ and then start decreasing, until, from $\alpha = \alpha_c^{-1}$ on, it is again always equal to zero. This value of α_c, and the corresponding interval width $(\alpha_c, \alpha_c^{-1})$ where $\langle\theta_A\rangle \neq \langle\theta_B\rangle$, depends on the interaction strength J_0 (and on a, of course); when the average interaction equals J_c, we are in the limiting condition $\alpha_c = 1$ and, increasing the coupling, this interval of concentrations becomes wider. This region where the two fractions are different corresponds, in the magnetic models, to the anti-ferromagnetic phase, where the staggered magnetization, measuring the long range order of the system, assumes a non-zero value.

If measurements do not discriminate the subsystem to which a site belongs, we have seen that the total fraction saturation is simply given by $\langle\theta\rangle = (\langle\theta_A\rangle + \langle\theta_B\rangle)/2$. Thus, if the interaction is such that $\langle\theta\rangle_A \neq \langle\theta\rangle_B$ for a given range of concentrations, the total fraction of occupied sites will assume an intermediate value between the two. In all cases, the binding curves stay above the value of the corresponding non-cooperative curve for a concentration below the scale α_0 (which we have assumed to be equal to one for simplicity), and below the non-cooperative curve for larger concentrations (Fig. 3.12). This is typical of negatively cooperative systems, which can thus respond to concentrations on a broader range with respect to non-cooperative macromolecules, which can be a useful mechanism in biological systems. On the contrary, we have seen that the effect of positive cooperativity is to trigger a response in the system with small variations of concentrations [25]. Note that we can express the extent of negative cooperativity in terms of a Hill coefficient by generalizing Eq. (3.28) for negative J, as in this case the resulting number satisfies $n_H = 1/(1 - J) < 1$, which is a common feature of negatively cooperative systems.

Figure 3.11: Theoretical binding curves (fraction saturations) predicted by the model. (a) Theoretical curve for $J_0 = 1.5$ and $a = 0.8$ (blue line) confronted with the non-cooperative case (in black). In this case the fraction saturations of the two parties coincide for any value of the concentration of ligands, and the total fraction saturation coincide with them. (b) Fraction saturations of the two subsystems (red and blue lines) for $J_0 = 2.5$ and $a = 0.8$; note that in this case there is a difference in the two values for a given range of concentrations, and in this range the total fraction saturation is the average of the two (dashed line). The black line represents the non-cooperative case.

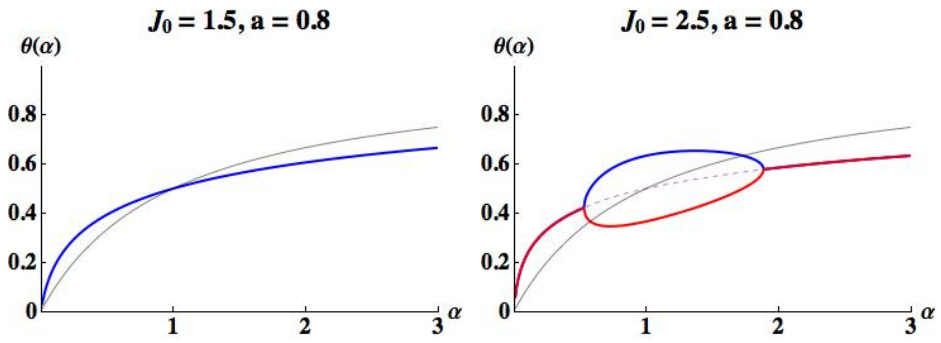

(a) (b)

Binding isotherms are often plotted taking a logarithmic scale for the concentration of ligands, and in Fig. 3.12 we show some theoretical binding curves with the total fraction saturation plotted as a function of the logarithm of ligands concentration. Fig. 3.13(a) shows the binding curve predicted for a system with interaction strength $J_0 = 2$ and heterogeneity parameter $a = 0.8$ (blue line). Here the partial fraction saturations coincide over all concentrations, with negative cooperativity manifesting itself in the reduced steepness of the curve with respect to the non-cooperative counterpart (black line). In Fig. 3.13(b) we show an analogous plot with $J_0 = 3.3$ and $a = 0.8$ (in blue). In this case the trend of the curve is more complicated, as in the central region, where the interaction among sites manifests mostly, privileging the occupation of a subsystem with respect to the other ($\langle\theta_A\rangle \neq \langle\theta_B\rangle$), the steepness of the curve decreases coming from low concentrations and then starts increasing for a while for $\alpha > 1$, until it start decreasing again for larger concentrations. Interestingly, this effect can only be seen on a logarithmic scale of concentrations (confront with Fig. 3.12(b)). For low concentrations, the sites of the two subsystems are equally filled with ligands, but then, if the negative interaction strength among sites is suffi-

Figure 3.12: Theoretical binding curves (blue lines) for the total fraction saturation versus the concentration in log scale, confronted with the non-cooperative case (in black). (a) Binding curve for a negatively cooperative system with $J_0 = 2$ and $a = 0.8$. (b) Curve for a negatively cooperative system with $J_0 = 3.3$ and $a = 0.8$. Note that here, unlike the other case, there is a range of concentrations around $\alpha = 1$ for which the steepness of the curve, coming from lower concentrations, decreases and then start increasing again for a while.

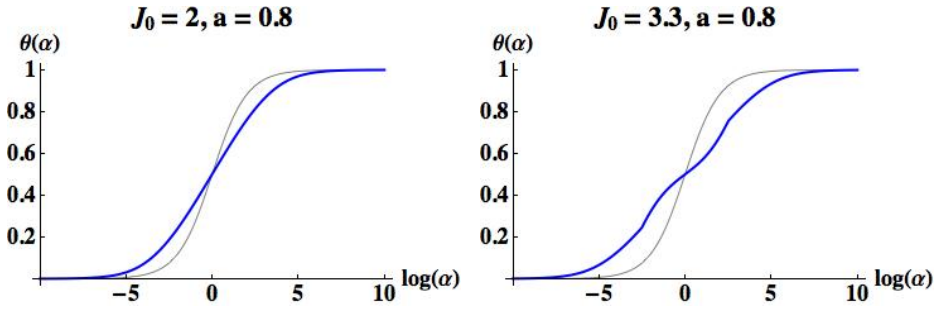

(a) (b)

ciently strong, at a certain concentration one of the two subsystems begins binding more ligands than the other. The strong effect of mutual negative cooperativity (with respect to the smaller effect of the chemical potential $\log \alpha$ in that range) decreases the steepness of the global fraction saturation in a range of concentrations around unity, but, when the concentration start increasing over that values, its effect becomes more important, and the steepness of the binding curve starts increasing again, until the partial fraction saturations are re-equilibrated at high concentrations, where it becomes decreasing towards the total saturation of sites.

As a concrete example, we can consider the binding of some molecules to the homodimeric hemoglobin of bacteria *Vitreoscilla*[5]. Experimental measurements show that cyanide (CN^-), azide(N_3^-), thiocyanate ($[SCN]^-$) and imidazole (an aromatic heterocyclic compound) bind each anticooperatively, in solution, to the two Ferric *Vitreoscilla Hb* binding sites. In particular ligand-linked conformational changes in the monoligated species lead to an observed 300-fold decrease in the affinity of these species for the monoligated ferric *Vitreoscilla* Hb with respect to that of the fully unligated homodimer [27]. Binding a molecule on a site A, thus, has a strong negative effect to

[5] *Vitreoscilla* species are areobes bacteria found in oxygen poor environments, and *Vitreoscilla Hb* has many interesting properties which are exploited in biotechnology to improve the efficiency of cell and plant growth processes on the industrial scale [26].

the second binding site (which we can imagine to belong to an other class of sites B) and we can expect a behavior like the one previously described and exemplified by Fig. 3.13(b). In fact, we fitted some data from [27], relative to the binding of cyanide, azide, thiocyanate and imidazole to *Vitreoscilla Hb* with our model, finding a good qualitative agreement (Fig. 3.13). This

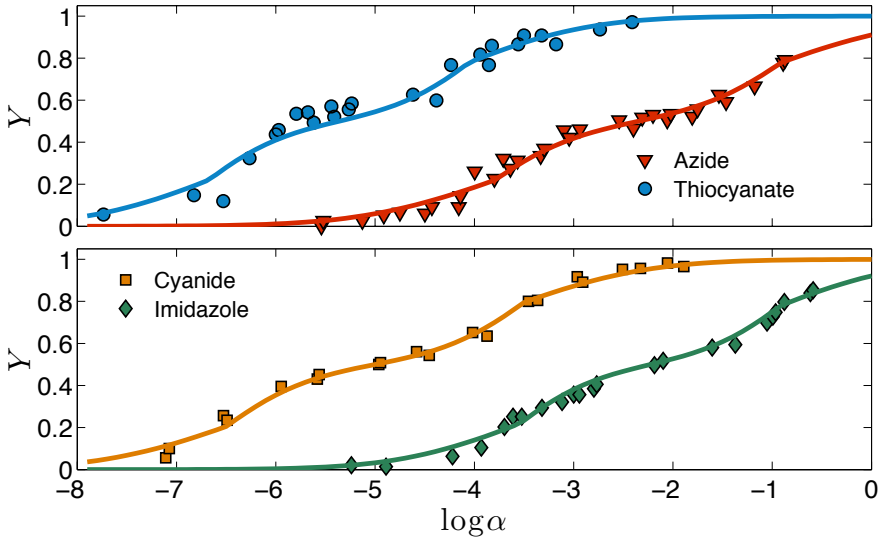

Figure 3.13: Anti-cooperative behavior, experimental data taken from Figure 1 *in [27] for the binding of different ligands to the recombinant homodimeric ferric Vitreoscilla Hemoglobin in solution at pH* 7.0 *and temperature* 293 *Kelvin(Y stands for the fraction saturation). Comparisons among the fitted solutions of our theory (solid line) and the experimental data (symbols) are shown for the ligand binding isotherms for cyanide (■), azide(▼), thiocyanate (●) and imidazole (♦). The fitting values of the parameters are (with* $a = 1$*): (a) cyanide* $J_0 = 3.05 \pm 0.05$, $\alpha_0 = 3.6\ 10^4 \pm 10^2$, *(b) azide* $J_0 = 2.9 \pm 0.05$, $\alpha_0 = 1.0\ 10^2 \pm 1$, *(c)thiocyanate* $J_0 = 2.9 \pm 0.05$, $\alpha_0 = 5.9\ 10^5 \pm 10^3$ *and (d) imidazole* $J_0 = 2.9 \pm 0.05$, $\alpha_0 = 5.8\ 10^2 \pm 1$.

kind of qualitative behavior is typical of strong negative cooperative effects in dimers. In fact, as one of the binding site has bound a molecule, the affinity of the other sites for ligands decreases in such a way the the fraction saturation curve tends to flatten a bit, as we have seen also in our model.

As another example, we can skip to a very different situation, that is the formation of protein monolayers on colloidal nanoparticles [28]. In this case anti-cooperative effects may arise from steric hindrance, which imposes an energetic penalty on proteins binding to a partially coated nanoparticle. The hydrodynamic radius of the particle, which can be extracted from diffusion

time measurements, can be also expressed in terms of the average number of protein molecules bound to the nanoparticles. We fitted our model with data from [29], where the binding of human serum albumin onto small (10 - 20 nm) polymer-coated FePt and CdSe/ZnS nanoparticles is analyzed by using fluorescence correlation spectroscopy, and the resultin curve is plotted in Fig. 3.14. There is, again, a good qualitative agreement: one can figure that each

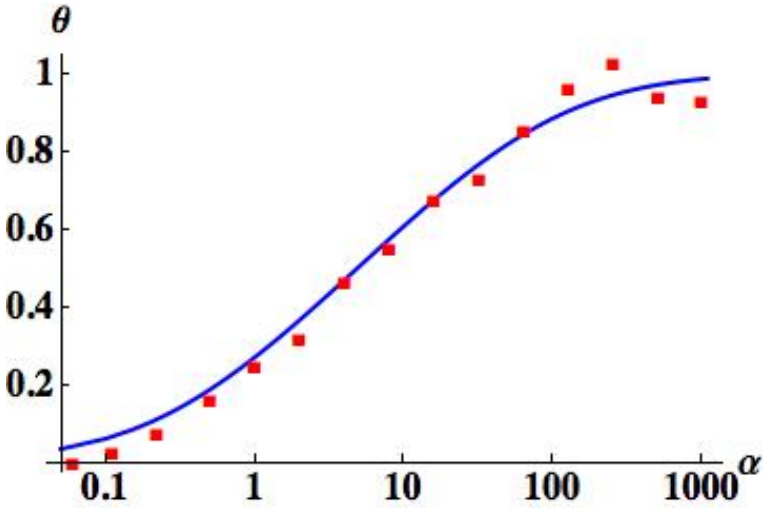

Figure 3.14: Experimental data (■) taken from Figure 3 in [29] for the anti-cooperative binding of human serum albumin onto small (10 - 20 nm) polymer-coated FePt and CdSe/ZnS nanoparticles. The blue line is the best fit within our model (for $a = 1$), with $J_0 = 1.29 \pm 0.05$ and $\alpha_0 = 5.0 \pm 0.3$ mol.

protein "feels" the negative effect of a certain number of proteins adsorbed onto the surface of the macromolecule, which prevent it to find a free binding site, coherently with the description of the model. The advantage of such a model, thus, is its generality and capacity to adapt to a large number of situations where negative cooperativity occurs.

3.6 Conclusions

We have seen how a simple mapping of cooperative phenomena into spin-models allows a semi-quantitative description of a large class of cooperative phenomena, giving a unifying picture where the leading role is played by the interaction strength among sites. We get an analytical expression for

the saturation function which is successfully compared with recent experimental findings, taken from a plethora of different contexts to check robustness. Varying the interaction, many different behaviors for the binding of molecules to larger biopolymers (or nanoparticles) are reconstructed, ranging from slightly cooperative cases, to the stronger effects where the binding isotherm assumes a sigmoidal form. Classical measures of cooperativity can be easily put in correspondence with the interaction strength of our model. We also suggested an analys of the cooperative effects due to large conformational changes, resulting from the interplay of several binding sites together, in terms of models with multiple-spins interactions, which can describe more complex binding behaviors. The interaction among sites has a corresponding effective energy term in the spin-model counterpart, with a juxtaposed binding energy, depending on the concentration of ligand molecules, interpretable as the chemical potential for binding. Negative cooperativity can be modeled in this unified framework by simply considering negative interactions between couples of sites, in a direct correspondence with anti-ferromagnetic models. Moreover, we codified possible heterogenous couplings through similarity among random strings of bits; the parameter entering in the distribution of the bits can be interpreted as a measure of heterogeneity, tuning the width of the resulting distribution of interactions. Finally, we tested the predictions of the model by fitting data found in literature for some very different systems with several cooperative behaviors, ranging from positive cooperativity to weak and strong anticooperative effects, and finding a good agreement with the data. The advantage of the description introduced lays in its generality and in the unifying framework, where many different behaviors for different kind of system can be integrated. Moreover, an analysis of the qualitative behavior of fraction saturation versus the concentrations of ligands in terms of the model can give an idea of the kind of interactions among sites which are involved.

Possible future developments include the study of a chemical inverse problem, to determine for instance a heterogeneity parameter without resorting to single molecules experiments. It could be interesting, in this sense, to introduce in the model an heterogeneity in the affinities of sites for the ligands, which may be modeled by a random parameter tuning the binding energy (this corresponds to a random field in the magnetic model counterpart). The introduction of a topology in the interaction could also be an useful refinement to address specific problems.

Part II

Spin Glasses

Chapter 4

General framework

4.1 Introduction

Spin glasses, with their puzzling and still not well understood physics, are among the paradigmatic models in complex systems theory, besides constituting "a challenge for mathematicians" [30]. Their fields of applications include optimization theory, computer science, biology, economics etc. [31, 32, 33, 34, 35].

The expression *spin glass* was originally born to designate some magnetic alloys with a very peculiar behavior, characterized by lack of long range order and very long scale dynamics at low temperatures. Experimentally one can observe in such alloys, for example, a non periodic arrangement of magnetic moments below a critical temperature, and memory effects in susceptibility and residual magnetization. To understand some of these phenomena, Edwards and Anderson (EA) proposed in 1975 an extension of the Ising model in which the interactions between couple of spins are represented by random variables with positive and negative values [36].

The next step was the introduction of a simpler model by Sherrington and Kirkpatrick (SK), i.e., the mean field version [37] of the EA model. Curiously, the title of the paper was "Solvable Model of a Spin-Glass", but also if the authors - using the famous replica-trick in the replica symmetric approximation - found an explicit form for the free energy, they realized that their solution was only valid above a certain temperature, and it took some years to understand which was the valid solution, with the seminal works of Parisi [38, 39, 40], where he proposed a formula for the free energy per site in the thermodynamic limit and a description of the pure states of the system.

The rigorous proof that the Parisi formula is in fact correct was estab-

lished only some years ago, split across two works by Guerra [1] and Talagrand [2], and apart from a few exceptions [41, 42], most important rigorous results are quite recent. The existence of the thermodynamic limit for the free energy, for example, was proven in 2002 [43], just after the rigorous analysis of the high temperature region, and the validity of the de Almeida-Thouless (AT) line [44] only in 2007 [45]. The techniques used for these recent breakthroughs, which are mainly based on interpolation, found fruitful applications also in neighboring fields, such as for example optimization problems and diluted spin glasses [46], finite-range spin glasses [47], or neural networks [48].

The purpose of this work is to show some applications of these techniques, based in particular on analogies with mechanical systems, both to prove the validity of such powerful methods and to develop alternative mathematical tools to approach the study of complex systems. We will show how it is possible to study some general features of the mean field spin glass models, such as the existence of the thermodynamic limit, by coupling the given system with an auxiliary, suitably chosen, one. Then we will use an approach based on similar methods, and in particular on the introduction of an auxiliary partition function containing external random fields, to compute the free energy of the Sherrington-Kirkpatrick and the p-spin glass models using a formal analogy with a mechanical system. The results of the original part of this work have been published in [49] and [50].

4.2 Generalities

Spin glasses can be simply defined as magnetic systems with a non-periodic freezing of the spins at low temperatures. The first experiments which drew some attention to these characteristics were performed on dilute solutions of magnetic transition metal impurities in noble metal hosts. In these systems, the impurity moments produce a magnetic polarization of the host metal conduction electrons, which is positive at some distances and negative at others. Beneath a characteristic temperature, a Mössbauer line-splitting in zero applied field was observed, indicating a local hyperfine field due to local freezing of the magnetic moments. Moreover, the absence of any corresponding magnetic Bragg peak in neutron diffraction demonstrated that the freezing was not periodic. An other sign of non-ferromagnetic freezing came from earlier measurements of the susceptibility, which had shown a peak at a similar temperature, highlighting the presence of a phase transition. Other remarkable features, such as preparation-dependence effects and a consider-

able slowing-down of response to external perturbations, demonstrated the presence of many metastable states in this new low-temperature phase, with significant free energy barriers separating these states. We refer to [51] for a complete experimental review about the topic.

The first historical attempt to produce a theory of the described transition is due to Edwards and Anderson [36], which proposeded a Ising-like Hamiltonian, with the magnetic moments placed on the N sites of a hypercubic lattice, and keeping only a single spin component $\sigma_i = (\vec{\sigma}_i)_z = \pm 1$:

$$H_N(\sigma; J) = -\sum_{\langle i,j \rangle} J_{ij}\sigma_i\sigma_j, \tag{4.1}$$

where the nearest neighbors interactions J_{ij} are random independent and identically distributed variables (gaussian, for example), with random signs.

It is then clear that a key ingredient is *disorder*: the Hamiltonian depends not only on the configuration of the system, which we denote by σ, and possibly on the strength of the external applied fields, like the magnetic field, but also on some random parameters (usually, the couplings among the elementary degrees of freedom), whose probability distribution is supposed to be known. The random parameters are collectively denoted as "quenched" or "frozen" disorder. From a physical point of view, the word "frozen" means that we are modeling a disordered system whose impurities have a dynamics which is many orders of magnitude slower than the dynamics of the spin degrees of freedom. Therefore, the disorder does not reach thermal equilibrium on the time scales of the spin relaxation and can be considered as fixed. This fact has deep consequences on the way we have to perform the averages over the couplings, compared to the configurations σ. The second key ingredient, following from disorder, is *frustration*, i.e., competition between different terms in the Hamiltonian, so that they can not all be satisfied simultaneously. More precisely, a system is said frustrated if there exist a loop on which the product of the couplings is negative (see Fig. 4.1). We have seen (see sec. 2.2.2) how in the Curie-Weiss model each spin-spin interaction is minimized when the two spin are parallel, i. e., $\sigma_i\sigma_j = +1$ for all couples (i, j). There are only two such configurations, one with all the spins equal to $+1$, the other with spins -1, and they are connected by the global spin-flip symmetry $\sigma_i \to -\sigma_i \ \forall\, i$. If the couplings J_{ij} are random sign (and possibly modulus), the ground state has a high degeneracy and different ground states are not connected to one another by elementary symmetry transformations[1].

[1]Notice that frustration disappears when considering a lattice without loops, for example a tree.

Figure 4.1: A very simple example of a frustrated system: the spins tend to be parallel when there's a positive interaction and anti-parallel when the interaction is negative. Obviously not all the conditions can be met simultaneously, so there is frustration.

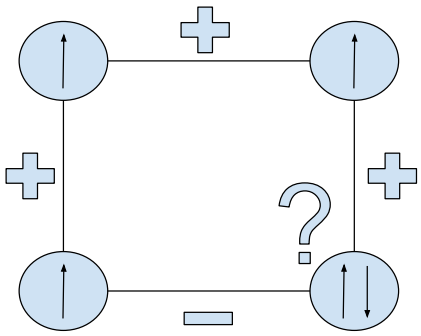

4.3 The mean-field spin glass model

The Edwards-Anderson (EA) model is already somewhat simplified with respect to the actual physical situation: a more realistic model could consider, for instance, interactions $J = \{J_{ij}\}$ decaying with distance, instead of nearest-neighbors couplings, or Heisenberg spins $\vec{\sigma}_i$, with more than one component attached on each site. However, despite its level of abstraction, it was too difficult to be attacked analytically, and suitable approximation schemes were developed. In particular the most important one and the richest in surprises was the mean-field approximation. In this case, while maintaining the fundamental features of disorder and frustration, as we have seen in the Curie-Weiss model the geometrical structure of the lattice is disregarded, so that every magnetic moment interacts with all the others, irrespective of the distance. The first model of this kind was introduced by Sherrington and Kirkpatrick (SK) [37], and it is defined by the Hamiltonian

$$H_N(\sigma, h; J) = -\frac{1}{\sqrt{N}} \sum_{1 \le i < j \le N} J_{ij}\sigma_i\sigma_j - h \sum_{1 \le i \le N} \sigma_i. \tag{4.2}$$

The first term is a long range random two body interaction, while the second one represents the interaction of the spins with an homogeneous magnetic field h. In the following, we will often consider a zero field model, denoting the Hamiltonian with $H_N(\sigma; J)$.

The $N(N-1)/2$ couplings J_{ij} are assumed to be centered unit Gaussians, so that, denoting with $\mathbb{E}$ the average on disorder, we have

$$\mathbb{E}J_{ij} = 0 \quad \text{and} \quad \mathbb{E}J_{ij}^2 = 1.$$

This choice is a matter of convenience. In fact, as already noticed in [52], any other symmetric probability distribution with finite moments could be chosen for J_{ij}, without modifying the free energy of the system, apart from error terms vanishing in the thermodynamic limit. The case $J_{ij} = \pm 1$ with equal probability $1/2$, for instance, is often considered in the literature.

The normalization factor $1/\sqrt{N}$ guarantees that $H_N(\sigma; J)/N$ and the free energy density are of order unity in the thermodynamic limit. In the Curie-Weiss model the correct factor is $1/N$, but in this case the random signs of the couplings J_{ij} produce cancellations among the many terms of the Hamiltonian H_N. The correctness of this choice can be easily understood by considering a duplicated system with configurations σ^1 and σ^2, but with the same disorder, and computing the quantity

$$\begin{aligned}
\mathbb{E}(H_N(\sigma^{(1)}; J)H_N(\sigma^{(2)}; J)) &= \frac{1}{N}\sum_{i<j}^{1,N}\sum_{k<l}^{1,N}\mathbb{E}(J_{ij}J_{kl})\sigma_i^{(1)}\sigma_j^{(1)}\sigma_k^{(2)}\sigma_l^{(2)} \\
&= \frac{1}{N}\sum_{1\le i<j\le N}\sigma_i^{(1)}\sigma_j^{(1)}\sigma_i^{(2)}\sigma_j^{(2)} \\
&= \frac{N}{2}\left(\frac{1}{N}\sum_{i=1}^{N}\sigma_i^{(1)}\sigma_i^{(2)}\right)^2 - \frac{1}{2}. \qquad (4.3)
\end{aligned}$$

The term

$$q_{12} = q(\sigma^{(1)}, \sigma^{(2)}) = \frac{1}{N}\sum_{i=1}^{N}\sigma_i^{(1)}\sigma_i^{(2)}, \qquad (4.4)$$

which occurs in the previous equation, is a fundamental one, as we will see in the following, and it is called *overlap*. In fact, it measures the resemblance between the configurations of the two copies $\sigma^{(1)}$ and $\sigma^{(2)}$, going from -1, when each spin of a system is opposed to the corresponding one of the other copy, to $+1$, when they are perfectly aligned. It is related with the Hamming distance $d(\sigma^{(1)}, \sigma^{(2)})$, which counts the number of non-aligned spins:

$$d(\sigma^{(1)}, \sigma^{(2)}) = \frac{1}{2}(1 - q_{12}).$$

So, taking two identical copies $\sigma^{(1)} = \sigma^{(2)}$, we note that

$$\mathbb{E}\left(H_N(\sigma; J)\right)^2 = \frac{N}{2} - \frac{1}{2}, \qquad (4.5)$$

showing that the normalization factor is correct.

4.3.1 Quenched and annealed free energies

For a given inverse temperature $\beta = 1/T$, we introduce the disorder dependent partition function $Z_N(\beta, h; J)$, the *quenched* average of the free energy per site $f_N(\beta, h)$, and the disorder dependent Boltzmann-Gibbs state ω_J:

$$f_N(\beta, h) = -\frac{1}{\beta N}\mathbb{E}\log Z_N(\beta, h; J) \tag{4.6}$$

$$\omega_J(A) = Z_N(\beta, h)^{-1}\sum_{\sigma} A(\sigma)\exp(-\beta H_N(\sigma, h; J)), \tag{4.7}$$

where $A = A(\sigma)$ is a generic observable (for example the energy H_N), depending on σ. Note that, for compactness, we omitted in the partition function and in the Boltzmann state the dependence on the disorder, as well as for the Hamiltonian. In some cases it will be more practical to deal, rather than with $f_N(\beta, h)$, with the average normalized log-partition function

$$\alpha_N(\beta, h) = \frac{1}{N}\mathbb{E}\log Z_N(\beta, h; J) = -\beta f_N(\beta, h), \tag{4.8}$$

often referred to as the pressure. As for the Hamiltonian, in the following we will shorten the notation in $Z_N(\beta; J), f_N(\beta), \alpha_N(\beta)$ etc. when considering the case of zero external field ($h = 0$).

The quenched free energy is the correct average if one looks for the free energy of a system where the disorder is frozen and its dynamics is many orders of magnitude slower than the dynamics of the spin degrees of freedom, like in real spin glasses. Moreover, the free energy per spin for a given realization of disorder

$$-\frac{1}{\beta N}\log Z_N$$

has the *self-averaging* property, meaning that its deviations from the quenched value vanish in the thermodynamic limit with probability one. In general it is easier to handle with the quenched value, which has no explicit dependence on J even for finite-size systems.

One can also consider the so-called *annealed* free energy

$$f_N^a(\beta, h) = -\frac{1}{\beta N}\log \mathbb{E}Z_N(\beta, h; J), \tag{4.9}$$

where one averages on disorder directly in the partition function. From a physical point of view this corresponds, somehow, to treat the disorder

degrees of freedom on the same level of the spins, and let them participate in the thermal equilibrium. This terminology comes from metallurgy and the thermal processing of materials: a "quench" corresponds in this jargon to preparing a sample by suddenly bridging it from high to low temperatures, so that atoms do not change their position apart from small vibrations. In an "annealing" process, on the contrary, the cooling down is slower and gradual, and atoms can move and find favorable positions.

The computation of the annealed free energy is trivial, since the Boltzmann factor in this case can be written as the product of $N(N-1)/2$ statistically independent terms, one for each pair of sites,

$$Z_N(\beta, h; J) = \sum_{\sigma} \prod_{1 \le i < j \le N} \exp\left(\frac{\beta}{\sqrt{N}} J_{ij}\sigma_i\sigma_j\right) \times \exp\left(\beta h \sum_{1 \le k \le N} \sigma_k\right),$$

and the disorder average factorizes:

$$\begin{aligned} \mathbb{E}Z_N(\beta, h; J) &= \sum_{\sigma} \exp\left(\frac{\beta^2}{2N}\frac{N(N-1)}{2}\right) \times \exp\left(\beta h \sum_{1 \le k \le N} \sigma_k\right) \\ &= 2^N \cosh^N(\beta h) \exp\left(\frac{\beta^2}{4}(N-1)\right), \end{aligned}$$

so that:

$$f_N^a(\beta, h) = -\frac{1}{\beta}\log 2\cosh(\beta h) - \frac{\beta}{4}\frac{N-1}{N} \tag{4.10}$$

and in the thermodynamic limit we have:

$$f^a(\beta, h) = \lim_{N\to\infty} f_N^a(\beta, h) = -\frac{1}{\beta}\log 2\cosh(\beta h) - \frac{\beta}{4} \tag{4.11}$$

Since the function $x \to \log x$ is a concave one, from the Jensen inequality we can immediately say that the quenched free energy is always greater or equal than the annealed one

$$-\frac{1}{\beta N}\mathbb{E}\log Z_N(\beta, h; J) \ge -\frac{1}{\beta N}\log \mathbb{E}Z_N(\beta, h; J).$$

It is also immediate to see that the annealed free energy cannot be the correct one, at least at low temperatures, if we look at the corresponding annealed entropy. In the zero-field case, in fact, this is given by

$$s^a(\beta) = \beta^2 \partial_\beta f^a(\beta) = \log 2 - \frac{\beta^2}{4} \tag{4.12}$$

and it becomes negative for $\beta < \beta^* = 2\sqrt{\log 2}$. But entropy is by definition the logarithm of the number of configurations, and it cannot be negative for a discrete system.

However it is interesting to observe that at zero magnetic field and $\beta < 1$ the quenched free energy coincides with the annealed one in the infinite volume limit [41]. The general case with $h \neq 0$ is much more complicate to study from a mathematical point of view [30].

4.3.2 Replicas and overlap

Previously, we introduced the concept of overlap, as defined in Eq. 4.4, by considering two copies of the system. In general, we can consider a generic number n of independent copies of the system, characterized by the spin configurations $\sigma^{(1)}, ..., \sigma^{(n)}$, distributed according to the product state

$$\Omega_J = \omega_J^{(1)} \times \omega_J^{(2)} \times ... \times \omega_J^{(n)}$$

where each $\omega_J^{(a)}$ acts on the corresponding $\sigma_i^{(a)}$ variables, and we stress that they are all subject to the same sample $J = \{J_{ij}\}$ of the external disorder. These copies of the system are usually called *real replicas*, to distinguish them from those appearing in the *replica trick*, where one takes a limit $n \to 0$ at some stage [31]. When considering such a replicated system the Boltzmann factor is given by the product of the Boltzmann factor for the single n replicas

$$\exp\left(-\beta\left(H_N(\sigma^{(1)}, h; J) + H_N(\sigma^{(2)}, h; J) + ... + H_N(\sigma^{(n)}, h; J)\right)\right). \quad (4.13)$$

Given a generic observable, which is a smooth function $A = A(\sigma)$ of the configuration of the n replicas, we define the $\langle\rangle$ averages as

$$\langle A(\sigma^{(1)}, \sigma^{(2)}, ..., \sigma^{(n)})\rangle = \mathbb{E}\Omega_J(A(\sigma^{(1)}, \sigma^{(2)}, ..., \sigma^{(n)})). \quad (4.14)$$

Replica overlaps are the quantities that one usually measures in numerical experiments. It is important to note that if we consider Boltzmann averages Ω_J over different groups of replicas they factorize:

$$\Omega_J(q_{12}q_{34}) = \Omega_J(q_{12})\Omega_J(q_{34}).$$

It is the average over disorder which introduces correlations between them, as in general

$$\langle q_{12}q_{34}\rangle \neq \langle q_{12}\rangle\langle q_{34}\rangle,$$

but, on the other hand, they are invariant under permutation of replica indices, for instance

$$\langle q_{12}q_{23}\rangle = \langle q_{24}q_{45}\rangle.$$

The whole physical content of the theory is in the distribution of overlap [31], and the averages of many physical quantities can be expressed as $\langle\rangle$ averages over overlap polynomials. Let us consider, for example, the disorder average of the internal energy per spin $N^{-1}\omega_J(H_N)$ for $h = 0$. Using the integration by parts formula

$$\mathbb{E}(JA(J)) = \mathbb{E}\left(\frac{\partial}{\partial J}A(J)\right), \tag{4.15}$$

valid for a centered unit Gaussian variable J and any smooth function $A(J)$, it is straightforward to see that the following equation holds:

$$\frac{1}{N}\langle H_N\rangle = \frac{1}{N}\mathbb{E}\omega_J(H_N) = -\frac{\beta}{2}(1 - \langle q_{12}^2\rangle). \tag{4.16}$$

An other example is given by its β derivative:

$$\begin{aligned} N^{-1}\partial_\beta\langle H_N\rangle &= -N^{-1}\left(\langle H_N^2\rangle - \langle H_N\rangle^2\right) \\ &= -\frac{1}{2}\left(1 - \langle q_{12}^2\rangle\right) + \frac{N\beta^2}{2}\left(\langle q_{12}^4\rangle - 4\langle q_{12}^2 q_{23}^2\rangle + 3\langle q_{12}^2 q_{34}^2\rangle\right). \end{aligned}$$

4.4 Parisi theory of Replica Symmetry Breaking

In this section, we will briefly focus on the Parisi theory of the Sherrington Kirkpatrick model, introducing some central concepts and results. In particular we will try to explain the meaning of the Replica Symmetry Breaking and of the corresponding functional order parameter $x(q)$. We refer to [31] for a complete review of this beautiful theory.

4.4.1 Replica method and symmetry breaking

Let us recall the basic concepts of spontaneous symmetry breaking and phase coexistence in statistical mechanics [53]. Consider a system on a d-dimensional hypercubic lattice, defined by a Hamiltonian $H(\sigma)$, depending on the configurations of all spins σ_i, with $i \in \mathbb{Z}^d$. The system is initially restricted to a finite subset Λ of the lattice with partition function $Z_\Lambda(\beta)$, in order to deal with mathematically well defined objects, and its finite volume free energy per site at the temperature $T = 1/\beta$ is

$$f_\Lambda(\beta) = -\frac{1}{|\Lambda|\beta}\log Z_\Lambda(\beta). \tag{4.17}$$

Then one lets Λ grow to the whole infinite lattice $\mathbb{Z}^d$ in a suitable way, and in doing so impose boundary conditions, *i.e.*, the positions of the boundary spins or their interaction with the external world, with a certain arbitrariness. These conditions, if interactions are short range, do not affect the free energy per site in the limit $\Lambda \to \mathbb{Z}^d$, but the equilibrium thermodynamic state of the system is also determined by all the correlation functions

$$\lim_{\Lambda \to \mathbb{Z}^d} \langle \sigma_{i_1} ... \sigma_{i_n} \rangle_\Lambda, \tag{4.18}$$

for all finite sets indices $i_1, ..., i_n$, where $\langle . \rangle$ is the Boltzmann-Gibbs thermal average at the temperature $1/\beta$. The correlation functions in general depend on the choice of the boundary conditions also in the infinite volume limit. When the equilibrium state is not unique, like for example in a ferromagnet below its critical temperature, one says that a first order phase transition occurs.

Another usual and strictly related way to select different equilibrium states is to break a symmetry *explicitly* in the Hamiltonian, introducing proper auxiliary external fields λ_i, which are removed only after the thermodynamic limit has been performed. More precisely, the thermodynamic limit for the free energy and for the correlation functions are computed with the explicitly broken symmetry Hamiltonian, and the external fields are then put to zero. In the Curie-Weiss model, for instance, one selects one of the two equilibrium states with positive or negative remanent magnetization by introducing a term $-h \sum_i \sigma_i$ in the Hamiltonian, which explicitly breaks the spin-flip symmetry, and taking the limit $h \to 0^{\pm}$ after the thermodynamic limit.

The set of all equilibrium states forms a simplex, and every state can be written in an unique way as a convex linear combination of certain *extremal* states, called *pure states* or *pure phases*. These are characterized by the cluster property, or spatial decay of correlations, that is their connected correlations functions vanish at large distance (or for different points in mean field models):

$$\langle \sigma_{i_1} ... \sigma_{i_n} \sigma_{j_1} ... \sigma_{j_m} \rangle \to \langle \sigma_{i_1} ... \sigma_{i_n} \rangle \langle \sigma_{j_1} ... \sigma_{j_m} \rangle \tag{4.19}$$

for

$$\min_{a,b} |i_a - j_b| \to \infty.$$

Pure states correspond to our intuitive idea of an equilibrium state: in the Boltzmann-Gibbs state for water at zero Celsius the system has probability

1/2 of being all water and 1/2 of being all ice, while in a pure state the whole sample is water or ice.

First order phase transitions are usually associated with the phenomenon of spontaneous symmetry breaking: the Hamiltonian of the model (and the non-clustering Boltzmann-Gibbs state) is invariant under the action of a symmetry group (for instance spin-flip in the Curie-Weiss model, or rotational symmetry in the Heisemberg model), but equilibrium states belong to smaller symmetry groups. It is the symmetry of the model which suggests the choice of the auxiliary external fields (or boundary conditions) that select the pure states, and applying the symmetry group transformation to a particular symmetry-breaking state one obtains another equilibrium state.

Spin-glasses are much more complicated from this point of view, since at low temperature there is an infinite number of pure phases, and it is not clear *a priori* which should be the right external fields (or boundary conditions) to select them, since the broken symmetry in the phase transition is not obvious. Moreover, due to this infinite number of states, the Gibbs' phase rule, which states that $k-1$ thermodynamic parameters have to be fixed in order to have k coexisting pure phases (e. g. temperature and pressure in the triple point of a fluid), does not hold in this case.

As Parisi showed, the spin glass phase transition is associated to a very peculiar spontaneous symmetry breaking. In fact, the symmetry to break is the group of permutations of a set of n identical replicas of the system, in the limit $n \to 0$. To briefly explain this, we have to introduce the *replica trick*, which is a method developed for the calculation of the free energy, based on the fact that the free energy can be expressed as

$$f_N(\beta) = -\frac{1}{\beta N} \lim_{n\to 0} \frac{\mathbb{E}Z^n - 1}{n}. \tag{4.20}$$

The integer moments $\mathbb{E}Z_N^n$ of the partition function in the r.h.s. are simpler to compute than the averaged logarithm $\mathbb{E}\log Z_N$, and the trick consists in considering their analytic continuation to real n, and then the limit $n \to 0$. For integer n the moments are nothing but the average of the partition function of a system of n identical (i.e., with the same disorder) replicas of the original system

$$\mathbb{E}Z_N^n(\beta, h; J) = \mathbb{E}\sum_{\sigma^{(1)}} \ldots \sum_{\sigma^{(n)}} \exp\left(-\beta \sum_{a=1}^{n} H_N(\sigma^{(a)}, h; J)\right). \tag{4.21}$$

The average over disorder can be easily carried out since it involves only

independent Gaussian integrals, and one finds

$$\mathbb{E}Z_N^n(\beta,h;J) = \exp\left(\frac{\beta^2 n(N-n)}{4}\right) \sum_{\sigma^{(1)}\ldots\sigma^{(n)}} \exp\left(\frac{\beta^2}{2N}\sum_{1\le a<b\le n}\left(\sum_i \sigma_i^{(a)}\sigma_i^{(b)}\right)^2 + \beta h\sum_{a=1}^n\sum_i \sigma_i^{(a)}\right), \tag{4.22}$$

which contains the square overlaps between replicas. The sum over configurations of replicated systems can be computed if one linearizes each of these terms by Gaussian integrals, so one introduces a $n\times n$ symmetric matrix Q_{ab}, with zeros on the diagonal, and writes the sum in Eq. (4.22) as

$$\sum_{\sigma^{(1)}\ldots\sigma^{(n)}}\int\prod_{a<b}\left(\sqrt{\frac{\beta^2 N}{2\pi}}dQ_{ab}\right)\exp\left(-\frac{\beta^2 N}{2}\sum_{a<b}Q_{ab}^2 + \beta^2\sum_{a<b}\left(\sum_i \sigma_i^{(a)}\sigma_i^{(b)}\right)Q_{ab} + \beta h\sum_a\sum_i\sigma_i^{(a)}\right). \tag{4.23}$$

As there are no couplings between spins belonging to the same replica, it is possible to define new spin variables $s_a = \pm 1$, with $a = 1,\ldots n$, and observe that

$$\sum_{\sigma^{(1)}\ldots\sigma^{(n)}}\exp\left(\beta^2\sum_{a<b}\left(\sum_i\sigma_i^{(a)}\sigma_i^{(b)}\right)Q_{ab} + \beta h\sum_a\sum_i\sigma_i^{(a)}\right) = \left(\sum_{\{s\}}\exp\left(\beta^2\sum_{a<b}Q_{ab}s_a s_b + \beta h\sum_a s_a\right)\right)^N.$$

Then (4.22) becomes

$$\mathbb{E}Z_N^n(\beta,h;J) = \int\prod_{a<b}\left(\sqrt{\frac{\beta^2 N}{2\pi}}dQ_{ab}\right)\exp\left(-NA[Q]\right) \tag{4.24}$$

$$A[Q] = \frac{\beta^2}{2}\sum_{a<b}Q_{ab}^2 - \log\sum_{\{s\}}\exp\left(\beta^2\sum_{a<b}Q_{ab}s_a s_b + \beta h\sum_a s_a\right) - \frac{\beta^2 n(N-n)}{4N}, \tag{4.25}$$

with the functional $A[Q]$ depending on Q, n, β and h. Since the exponent in the integrand of (4.24) is proportional to N, in the limit of N going to

infinity the n-th moment of Z_N can be evaluate through the saddle point method.

The infinite volume free energy, once the saddle point has been found is then obtained as

$$f(\beta, h) = \lim_{n\to 0} \frac{1}{\beta n} A[Q_{sp}] \tag{4.26}$$

Since Q is a symmetric matrix with zeros on the diagonal, it has $n(n-1)/2$ independent parameters, and for a given choice of Q there are such many saddle-point equations $\partial A/\partial Q_{ab} = 0$, which take the form

$$Q_{ab} = \frac{\sum_{\{s\}} s_a s_b \exp\left(\beta^2 \sum_{a<b} Q_{ab} s_a s_b + \beta h \sum_a s_a\right)}{\sum_{\{s\}} \exp\left(\beta^2 \sum_{a<b} Q_{ab} s_a s_b + \beta h \sum_a s_a\right)} \tag{4.27}$$

In the limit $n \to 0$ it can be shown [32] that the r.h.s. of this equation is equivalent to

$$\mathbb{E}\Omega_J(\sigma_i^{(a)}\sigma_i^{(b)}) \equiv \langle \sigma_i^{(a)}\sigma_i^{(b)} \rangle,$$

whence, since all sites i are equivalent for large N, the saddle point equation (4.27) can be written as

$$\lim_{n\to 0} Q_{ab} = \langle q_{ab} \rangle. \tag{4.28}$$

This relation is valid for a replica symmetric solution. When this symmetry is broken, if a particular choice of Q is a solution of the saddle point equation, any matrix obtained with a permutation of rows or columns of Q is a valid one. So in general one should divide the l.h.s. by $n(n-1)/2$.

In the spin glass phase the average overlap is expected to be different from zero, since it is the average of the positive quantity $\omega_J^2(\sigma_i)$ for different realizations of the disorder (while $\omega_J(\sigma_i)$ can be positive or negative depending on the particular realization of J, and its average vanishes). On the other hand in the high temperature phase the thermal average of magnetization in each site is zero for every sample, so that $\langle \sigma_i^{(a)}\sigma_i^{(b)} \rangle = 0$.

4.4.2 Replica Symmetric solution

Before solving the saddle point equations, one has to choose a form for Q, which should be symmetric with respect to permutation of row or columns, due to equivalence among replicas. The most natural idea seems then to look for a *replica symmetric* (RS) saddle point, corresponding to a matrix Q with all non-diagonal elements equal to the same value q, and the elements on the diagonal being zero. The integral in Eq. (4.24) reduces in this case to

an ordinary integral over the real variable q, so that the free energy is easily computed as

$$-\beta f_{RS}(\beta, h) = \log 2 + \int_{-\infty}^{+\infty} d\mu(z) \log\cosh(\beta\sqrt{q}z + \beta h) + \frac{\beta^2}{4}(1-q)^2, \quad (4.29)$$

where $d\mu(z) = (2\pi)^{-1/2} e^{-z^2/2} dz$ is the Gaussian measure and with q satisfying the saddle point equation

$$q = \int_{-\infty}^{+\infty} d\mu(z) \tanh(\beta\sqrt{q}z + \beta h). \quad (4.30)$$

At zero external field this equation correctly predicts a phase transition at $1/\beta_c = T_c = 1$, since it has solution $q = 0$ for $\beta < \beta_c$ and it admits a solution with $q \neq 0$ for $\beta > \beta_c$. However it is possible to see [31], that the replica symmetric free energy is not physically acceptable for a temperature $T < T_c(h)$, since it violates basic thermodynamic stability conditions, such as, for example, the positivity of entropy [37].

The free energy (4.29) can be developed near the critical point, where the spin glass parameter q is expected to be small. Then the coefficient for the q^2 term, which according to Landau theory of phase transitions vanishes at the critical point [9], is found to be proportional to $\beta^2 - 1$, so that, consistently, $\beta_c = 1$. It is interesting to note that this coefficient is negative if $\beta < \beta_c$, so that the paramagnetic solution $q = 0$ maximizes (instead of minimizing) the free energy, and this is also true for the spin glass solution with $q > 0$ in the low-temperature phase $\beta > \beta_c$. This is a consequence of the fact that the number $n(n-1)/2$ of replica pairs becomes negative in the limit $n \to 0$ [32].

Since the RS solution is not physically valid everywhere, one has to look for a form of the Q which breaks symmetry between replicas, and the correct solution was found by Parisi, in a series of remarkable papers [38, 39, 40], by means of a powerful *Ansatz*.

In the Ising model at low temperature and zero magnetic field there is a symmetry breaking with two pure phases, one with magnetization $+m(\beta)$ and the other with $-m(\beta)$. The overlap (4.4) between two typical configurations belonging to the same phase equals

$$q_{++} = q_{--} = m^2(\beta)$$

while, for two different phases,

$$q_{+-} = -m^2(\beta).$$

Note that symmetry breaking can be present, strictly speaking, only in the thermodynamic limit. In the limit of infinite volume the distribution function of the overlap q_{12} between the configurations of two replicas , picked according to their Boltzmann weights, is given by the sum of two delta functions

$$P(q) = \frac{\delta(q - m^2(\beta)) + \delta(q + m^2(\beta))}{2}. \tag{4.31}$$

Above the critical temperature, on the other hand, there is just one pure phase, with zero magnetization, and in that case

$$P(q) = \delta(q). \tag{4.32}$$

This means that, looking at $P(q)$, one is able to detect the phenomenon of non-uniqueness of the state, without introducing an explicitly symmetry breaking field or proper boundary conditions. Since for spin glasses there is no obvious symmetry to be broken, with associated order parameter and field, the natural way to proceed is to compute

$$P(q) = \lim_{N\to\infty} \mathbb{E} P_J^{(N)}(q)$$

where $P_J^{(N)}(q)$ is the finite volume probability distribution of the overlap, for a given disorder realization J. When $P(q)$ is a single delta distribution the system is said to be replica symmetric. The same holds when $P(q)$, in absence of magnetic field, is the sum of two deltas, with the two corresponding states related by spin-flip symmetry. On the contrary, if $P(q)$ has more than two peaks, or has a continuous part, replica symmetry is said to be broken.

Knowing the distribution $P(q)$ is then equivalent to know the structure of pure states. Given the average overlap

$$\langle q_{12} \rangle = \frac{1}{N} \sum_i \mathbb{E} \Omega_J (\sigma_i^{(1)} \sigma_i^{(2)})$$

one can think of expressing the Boltzmann weights $\Omega_J = \omega^{(1)} \times \omega^{(2)}$ in terms of pure states, and this decomposition is encoded in the $P(q)$:

$$\langle q_{12} \rangle = \int dq P(q) q. \tag{4.33}$$

This equation, combined with 4.28, tells us that in the language of replicas $P(q)$ represents the fraction of elements of the matrix Q assuming the value q [31].

4.4.3 Replica Symmetry Broken *Ansatz*

We have seen that the replica symmetric solution is not adequate, since it violates thermodynamic stability conditions. The simplest way to construct a matrix Q which breaks replica symmetry is to divide the n replicas in n/m groups of m, where m is obviously a submultiple of n. Then one takes $Q_{ab} = q_2$ if a and b belong to the same group (with $a \neq b$), and $Q_{ab} = q_1$ if they belong to different replicas. For example, if $n = 4$ we can have a matrix of the kind:

$$\left(\begin{array}{cc|cc} 0 & q_2 & q_1 & q_1 \\ q_2 & 0 & q_1 & q_1 \\ \hline q_1 & q_1 & 0 & q_2 \\ q_1 & q_1 & q_2 & 0 \end{array}\right).$$

With such an *Ansatz*, the overlap distribution is given by [31]:

$$P(q) = (1-m)\delta(q-q_2) + m\delta(q-q_1), \tag{4.34}$$

which is not negative only if $0 \leq m \leq 1$. The free energy corresponding to this first step of broken replica symmetry (1-RSB) is given by

$$\begin{aligned} -\beta f_{1RSB}(\beta, h) &= \log 2 + \frac{\beta^2}{4}\left[(1-m)q_1^2 + mq_0^2 + 1 - 2q_1\right] \\ &\quad + \frac{1}{m}\int d\mu(u) \log \int d\mu(v) \cosh^m \Theta \qquad (4.35) \\ \Theta &= \beta\left(\sqrt{q_0}u + \sqrt{q_1 - q_0}v + h\right), \qquad (4.36) \end{aligned}$$

where the parameters q_0 and q_1 are the solutions of the self-consistence (saddle point) equations

$$\begin{aligned} q_0 &= \int d\mu(u) \left(\frac{\int d\mu(v) \cosh^m \Theta \tanh \Theta}{\int d\mu(v) \cosh^m \Theta}\right)^2 \qquad (4.37) \\ q_1 &= \int d\mu(u) \frac{\int d\mu(v) \cosh^m \Theta \tanh^2 \Theta}{\int d\mu(v) \cosh^m \Theta}. \qquad (4.38) \end{aligned}$$

We refer to [31] for a detailed treatment of the interpretation and for the physical consequences of the RSB *Ansatz*. This solution turns out to be better than the RS one below the critical temperature, but it is not yet the right one, and one can apply this procedure iteratively. In a second step the off-diagonal blocks are left untouched, while the diagonal blocks are further divided into m_1/m_2 blocks, with the matrix elements assuming the value $Q_{ab} = q_3$ for $a \neq b$ inside the same block and $Q_{ab} = q_2$ otherwise. To find the proper free energy one has to apply this procedure an infinite number of times (full-RSB or ∞-RSB [31], [2]).

4.5 Full RSB solution

Since now we have seen how to compute the free energy and the distribution $P(q)$ in the setting of the replica method. In the following, we try to continue presenting the main results of the theory, but using a slightly different language, referring for instance to [1] for a presentation along these lines. Let us then introduce the convex space $\mathcal{X}$ of the functional order parameters x, as non-decreasing functions of the auxiliary variable q, with both x and q taking values on the real interval $[0,1]$, *i.e.*,

$$\mathcal{X} \ni x : [0,1] \ni q \to x(q) \in [0,1]. \tag{4.39}$$

Notice that we call x the non-decreasing function, and $x(q)$ its values. A metric on $\mathcal{X}$ is introduced through the $L^1([0,1], dq)$ norm, where dq is the Lebesgue measure. We will consider piecewise constant functional order parameter, since every regular function in this interval can be approximated with arbitrary precision in this way. So, given an integer number K of intervals, we have two sequences $q_0, q_1, ..., q_K$ and $m_1, m_2, ..., m_K$ satisfying

$$0 = q_0 \leq q_1 \leq ... \leq q_{K-1} \leq q_K = 1, \tag{4.40}$$

$$0 \leq m_1 \leq m_2 \leq ...m_K \leq 1, \tag{4.41}$$

and such that

$$x(q) = \begin{cases} m_1 & \text{for} \quad 0 = q_0 \leq q < q_1, \\ m_2 & \text{for} \quad 0 = q_1 \leq q < q_2, \\ ... & \\ m_K & \text{for} \quad 0 = q_{K-1} \leq q < q_K. \end{cases} \tag{4.42}$$

as it is shown in Figure 4.3(a). The choice of a piecewise constant functional order parameter corresponds to consider replica symmetry breaking to a finite number of steps in the frame of Parisi theory.

For instance, the replica symmetric case is reconstructed by taking

$$K = 2,\ q_1 = \bar{q},\ m_1 = 0,\ m_2 = 1, \tag{4.43}$$

while for the 1-RSB distribution one has to take $K = 3$, and so on, see Figure 4.3(b).

Let us now introduce the function $f = f(q, y; x, \beta)$, depending on the variables $q \in [0,1]$, $y \in \mathbb{R}$, on the functional order parameter x and on the inverse temperature β. This function should not be confused with the free

energy per site in the thermodynamic limit $f(\beta, h)$, and it is defined as the solution of the nonlinear antiparabolic equation

$$\frac{\partial}{\partial q} f(q,y) + \frac{1}{2}\frac{\partial^2}{\partial y^2} f(q,y) + \frac{1}{2} x(q) \left(\frac{\partial}{\partial y} f(q,y) \right)^2 = 0, \tag{4.44}$$

with final condition

$$f(1,y) = \log\cosh(\beta y). \tag{4.45}$$

For the sake of clearness here we only stressed the dependence of f on q and y. This equation, if we consider q corresponding to the time and y to the position in space, is formally equivalent to a diffusive heat equation when $x(q) \equiv 0$, while it is equivalent to a Hamilton-Jacobi equation with varying mass $(x(q))^{-1}$ if the second derivative in y vanishes identically.

Let us consider the solution is some simple cases.

- $x \equiv 0$

The solution can be easily obtained starting from Eq. (4.45), adding to y a gaussian variable z weighted with the root $\sqrt{1-q}$, which vanishes at the end of the interval, and integrating over z:

$$\begin{aligned} f(q,y) &= \int d\mu(z) \log\cosh\beta\left(y + z\sqrt{1-q}\right), \\ d\mu(z) &\equiv e^{-\frac{z^2}{2}} \frac{dz}{\sqrt{2\pi}}. \end{aligned} \tag{4.46}$$

- $x \equiv 1$

In this case, taking $f(q,y) = \log\cosh\beta y + a(q)$, with $a(1) = 0$, and solving Eq. (4.44) respect to a, one finds

$$f(q,y) = \log\cosh\beta y + \frac{1}{2}\beta^2(1-q) \tag{4.47}$$

- $x \equiv x_{\bar{q}} = \begin{cases} 0 & \text{for} \quad 0 \le q < \bar{q}, \\ 1 & \text{for} \quad \bar{q} \le q \le 1 \end{cases}$

Starting from Eq. (4.47), which is valid in the interval $\bar{q} \le q \le 1$ one gets the final condition for $f(q,y)$ in the previous interval:

$$f(\bar{q},y) = \log\cosh\beta y + \frac{1}{2}\beta^2(1-\bar{q}). \tag{4.48}$$

The solution for $q \in [0, \bar{q}]$ can be found, similarly to the case of $x \equiv 0$, starting from the final condition in $q = \bar{q}$ and then adding to y a properly weighted gaussian variable z, to be integrated,

$$f(q,y) = \int d\mu(z) \log\cosh\beta\left(y + z\sqrt{\bar{q} - q}\right) + \frac{1}{2}\beta^2(1-\bar{q}). \tag{4.49}$$

In general, for a piecewise constant x, with $x(q) = m_a$ for $q_{a-1} \leq q < q_a$ ($m_a > 0$), it is convenient to introduce the auxiliary function $g_a(q,y) = \exp m_a f(q,y)$, which satisfies the equation

$$\frac{\partial}{\partial q} g_a(q,y) + \frac{1}{2}\frac{\partial^2}{\partial y^2} g_a(q,y) = 0. \tag{4.50}$$

The final condition (4.45) for g_K in the last interval is $g_K(q_K, y) = \cosh^{m_K}\beta y$, and, as we have seen for $f(q,y)$ in the case $x \equiv 0$, the solution in the interval $[q_{K-2}, q_{K-1}]$ is obtained from the final condition, adding to y a properly weighted gaussian variable, and then integrating it

$$g_{K-1}(q,y) = \int d\mu(z_K) g_K\left(q_K, y + z_K\sqrt{q_K - q}\right), \tag{4.51}$$

whence one obtains the solution

$$\exp f(q,y) = \left(\int d\mu(z_K) \exp\left(m_K f\left(q_K, y + z_K\sqrt{q_K - q}\right)\right)\right)^{\frac{1}{m_K}}, \tag{4.52}$$

valid for $q \in [q_{K-2}, q_{K-1}]$. The general solution for all previous intervals is then found by iterating this algorithm. Notice that if $m_1 = 0$ the solution in the corresponding interval can be computed, as we have seen for $x = x_{\bar{q}}$, starting from the one valid for $q \in [q_1, q_2]$ and integrating it

$$f(q,y) = \int d\mu(z_1) f(q_1, y + z_K\sqrt{q_K - q_{K-1}} + ... + z_1\sqrt{q_1 - q}), \tag{4.53}$$

which is equivalently obtained from the general formula for a finite m_a, in the limit $m_1 \to 0$.

Since now we considered a piecewise constant x, but any functional order parameter can be approximated in the L^1 norm in this way, and it can be shown that f is pointwise continuous with respect to x, which allows us to deal mostly with piecewise constant order parameters. This important result is stated in the following

Theorem 1. *The function f is monotone in x in the sense that*

$$x(q) \leq \bar{x}(q) \ \ \forall q \in [0,1] \quad \Rightarrow \quad f(q,y;x,\beta) \leq f(q,y;\bar{x},\beta)$$

for any $q \in [0,1]$, $y \in R$. Moreover f is pointwise continuous in the $L^1([0,1],dq)$ norm. In fact, for generic x and $\bar{x}$, we have

$$|f(q,y;x,\beta) - f(q,y;\bar{x},\beta)| \leq \frac{\beta^2}{2} \int_q^1 |x(q') - \bar{x}(q')| dq'.$$

Having introduced f, we are now ready for the following important definitions.

Definition 1. *The trial auxiliary function $\bar{\alpha}$, depending on the functional order parameter x, is defined as*

$$\bar{\alpha}(\beta,h;x) \equiv \log 2 + f(0,h;x,\beta) - \frac{\beta^2}{2} \int_0^1 qx(q)dq. \tag{4.54}$$

Let us observe that in this definition the function f appears evaluated at $q = 0$, and $y = h$, where h is the value of the external magnetic field.

Definition 2. *The Parisi spontaneously broken replica symmetry solution is defined by*

$$\bar{\alpha}(\beta,h) \equiv \inf_x \bar{\alpha}(\beta,h;x), \tag{4.55}$$

where the infimum is taken with respect to all functional order parameters x.

The main prediction of Parisi theory is that, for the Sherrington-Kirkpatrick model, this infimum is related to the free energy in the thermodynamic limit

$$-\beta f(\beta,h) = \lim_{N\to\infty} N^{-1} \mathbb{E} \log Z_N(\beta,h;J) = \bar{\alpha}(\beta,h). \tag{4.56}$$

Moreover, the functional parameter x realizing the infimum in (4.55), was interpreted by Parisi as the accumulated distribution of the overlap distribution $P(q)$:

$$x(q) = \int_0^q P(q')dq'. \tag{4.57}$$

If replica symmetry holds $P(q) = \delta(q - \bar{q})$, and the optimal order parameter is just a step function, as in Figure 4.3(b). The form of $x(q)$ with two steps corresponds to the first level of broken replica symmetry, and so on.

When discussing the replica symmetric solution, we already noticed that the RS free energy is maximized by the proper choice of the parameter

q. Here we stress again that, according to Eq. (4.55), the trial functional $-\beta\bar{\alpha}(\beta, h; x)$ has to be maximized over the space of functional order parameter in order to obtain the infinite volume free energy $f(\beta, h)$. The usual variational principle of statistical mechanics, which follows from the second principle of thermodynamics, states that the free energy can be obtained through minimization of a suitable free energy functional, on all possible trial states. This means that, for any order parameter x different from the optimal one, $-\beta\bar{\alpha}(\beta, h; x)$ cannot be interpreted as the free energy associated to some trial state. However, it has been shown that the the value given in the Parisi *Ansatz* is a lower bound for the quenched average of the free energy, uniformly in the size of the system [1], and in the same paper a sum rule for the difference between the Parisi formula (4.55) and the real free energy was given. Afterwards, this difference has been showed to be vanishing in the thermodynamic limit [2].

4.6 The Almeida-Thouless line and the phase diagram

In this section we briefly consider the phase diagram of the Sherrington-Kirkpatrick model as it emerges from Parisi theory. First of all, let us discuss the high temperature (or high external field) region. The SK order parameter $\bar{q}$ [37], depending on β and h is defined as the solution of the implicit equation

$$\bar{q} = \int \tanh^2(\beta h + \beta z\sqrt{\bar{q}}) d\mu(z). \tag{4.58}$$

The solution for this equation, for any $\beta \geq 0$ and $h \neq 0$, exists and is unique, as proven in [54]. The ergodic high temperature region, corresponding to the replica symmetric part of the phase diagram, is defined by the condition

$$\beta^2 \int \frac{1}{\cosh^4(\beta h + \beta z\sqrt{\bar{q}(\beta, h)}} \leq 1. \tag{4.59}$$

The locus of the points in the (β, h)-plane where the equality holds is known as the Almeida-Thouless (AT) line (see figure 4.3). It is worth noting that initially it was only conjectured that the high temperature region, whose first precise characterization is due to Talagrand [30], coincided with the the region above the AT line, as defined by (4.59). A work by Guerra [45] confirmed that this is indeed the case.

In the high temperature region, the infimum in (4.55) is obtained for an $x(q)$ with the simple step form

$$x = \begin{cases} 0 & \text{for} \quad 0 \leq q < \bar{q}, \\ 1 & \text{for} \quad \bar{q} \leq q \leq 1 \end{cases} \tag{4.60}$$

and the Parisi solution (4.56) for this simple expression for the functional order parameter is given by

$$\alpha_{SK}(\beta, h) = \log 2 + \int \log\cosh(\beta h + \beta z\sqrt{\bar{q}}) d\mu(z) + \frac{\beta^2}{4}(1-\bar{q})^2, \tag{4.61}$$

which is just the so called "replica symmetric solution" originally found in [37]. It is easy to see that the Sherrington-Kirkpatrick order parameter defined by Eq. (4.58) is just the value which minimizes the expression (4.61), considered as a function of a generic $\bar{q}$, in agreement with (4.55). Since the derivative of a step distribution is a delta, according to Eq. (4.57) we find that, in the region where the replica symmetric solution holds, the overlap does not fluctuate and its typical value is just $\bar{q}$:

$$P(q) = \delta(q - \bar{q}). \tag{4.62}$$

As said before, the authors of [37] soon realized that the replica symmetric solution cannot hold for all values of β and h, since entropy computed within this solution would be negative at sufficiently low temperature (and field). Below the AT line, replica symmetry is broken, and at an infinite number of levels. The optimal order parameter $x(q)$ in this region is given by a limit of piecewise constant functional order parameters, in which the number of steps tends to infinity. As a consequence, $P(q)$ has support on a whole interval $[q_m, q_M]$. According to Parisi theory, the corresponding free energy should have infinitely many minima, believed to correspond to the pure states. The arrangement of these valleys has the property of ultrametricity, as we are going to explain in next section (see [31] for a deep analysis of this topic).

4.7 Ultrametricity

In the spin glass phase there exists an infinite number of pure thermodynamic states and, in contrast with usual non disordered systems, these states are not connected one to another by any simple symmetry transformation. The set of all pure states is nonetheless characterized by the very peculiar geometric structure of ultrametricity, which can be explained as follows. For

almost (with respect to Gibbs measure) every choice of the configurations $\sigma^{(a)}, \sigma^{(b)}, ...$ belonging to the different pure phases of the system $a, b, ...$, the overlap

$$q_{ab} = \frac{1}{N} \sum_{i=1}^{N} \sigma_i^{(a)} \sigma_i^{(b)} \tag{4.63}$$

will assume the same value

$$q_{ab} = \frac{1}{N} \sum_{i=1}^{N} m_i^{(a)} m_i^{(b)}, \tag{4.64}$$

where $m_i^{(a)}$ is the thermal average of σ_i in the state a. We can now introduce a very natural notion of distance between two states as

$$d_{ab}^2 \equiv \frac{1}{N} \sum_{i=1}^{N} \left(m_i^{(a)} - m_i^{(b)} \right)^2 . \tag{4.65}$$

Since from Parisi theory [31] it follows that

$$q_{aa} = \frac{1}{N} \sum_{i=1}^{N} \left(m_i^{(a)} \right)^2 = q_{EA}, \tag{4.66}$$

does not depend on the state a, we can write

$$d_{ab}^2 = 2(q_{EA} - q_{ab}). \tag{4.67}$$

Given any choice of three pure states, the property of ultrametricity states that the resulting triangle is either equilateral or isosceles with respect to the metric d_{ab} and, in the latter case, the different side must be the smaller one. This is clearly a stronger property than the usual triangular inequality.

Denoting with P_a the Gibbs-Boltzmann (sample-dependent) weight of pure state a, we can consider the configurational average of the distribution of overlaps between three different states

$$P(q_1, q_2, q_3) = \lim_{N \to \infty} \mathbb{E} \sum_{abc,\, a \neq b \neq c,\, a \neq c} P_a P_b P_c \delta(q_1 - q_{ab}) \delta(q_2 - q_{bc}) \delta(q_3 - q_{ac}). \tag{4.68}$$

This, evaluated in the frame of the replica method (see [31] and references therein) yields to

$$\begin{aligned} P(q_1,q_2,q_3) &= \frac{1}{2}P(q_1)x(q_1)\delta(q_1-q_2)\delta(q_1-q_3) \\ &+\frac{1}{2}\left[P(q_1)P(q_2)\Theta(q_1-q_2)\delta(q_2-q_3)\right. \\ &+P(q_2)P(q_3)\Theta(q_2-q_3)\delta(q_3-q_1) \\ &\left.+P(q_3)P(q_1)\Theta(q_3-q_1)\delta(q_1-q_2)\right], \end{aligned} \tag{4.69}$$

where $x(q)$ is the Parisi order parameter. The first term on the r.h.s. is non vanishing only if the three overlaps are all equal to each other, while the second term requires that the overlaps are the edges of an isosceles triangle ($q_1 > q_2 = q_3$ and the other two possibilities with permuted indices). This result can be interpreted as a tree-like structure of the space of the states [31]. It is important to stress that ultrametricity is assumed from the beginning in Parisi theory, since it follows from the Parisi *ansatz* for the relevant saddle point in (4.23). A deeper understanding of the low temperature spin glass phase came with the proof of some correlation identities for the SK model, *i.e.*, the Ghirlanda-Guerra (GG) identities, which follow from the property of self-averaging of the free energy density. These state that, given the overlaps among s real replicas, the overlap between one of these and an additional $s+1$ replica is either independent of the former overlaps or it is identical to one of them, each of these cases having probability $1/s$ [55]. In a very recent work [56], Panchenko has proven that ultrametricity is just a consequence of the Ghirlanda-Guerra identities, closing the debate about the ultrametric conjecture. What remains a matter of controversy, however, is the supposed low-temperature ultrametric structure of the 3d Edwards-Anderson model [57, 58].

4.8 Derrida's p-spin glass model

Among the many models for spin glasses, let us also consider a generalization of the Sherrington-Kirkpatrick model, *i. e.* the Derrida's p-spin glass [59], [60]. This model has a relatively simpler behavior, as the first step of broken replica symmetry is sufficient to describe their behavior for a wide range of temperatures below the critical temperature; Moreover, the transition in this case is first-order [61]. One of the motivations for the study of this model is its connection with structural glasses [62].

In this case the spins interact in p-tuples, through random independent gaussian couplings $J_{i_1,...i_p}$, so that the hamiltonian is defined as

$$H_N(\sigma, h; J) = -\sqrt{\frac{p!}{2N^{p-1}}} \sum_{i_1<...<i_p}^{1,N} J_{i_1...i_p}\sigma_{i_1}...\sigma_{i_p} - h\sum_{i}^{1,N}\sigma_i, \qquad (4.70)$$

with, possibly, an external field h, as in the SK case. The summation is taken over all the possible choices of indices $1 \leq i_1 < ... < i_p \leq N$, which are, of course,

$$\frac{N!}{p!(N-p)!}.$$

For large N and finite p this number goes as $N^{p-1}/p!$, whence the normalization factor to guarantee that the Hamiltonian is an extensive quantity, while the factor 2 at the denominator allows recovering the SK definition when $p = 2$.

In fact for two configurations $\sigma^{(1)}$ and $\sigma^{(2)}$ we have

$$\begin{aligned} \mathbb{E}\left(H_N(\sigma^{(1)}; J)H_N(\sigma^{(2)}; J)\right) &= \frac{p!}{2N^{p-1}} \sum_{i_1<...<i_p} \sigma^{(1)}_{i_1}\sigma^{(2)}_{i_1}...\sigma^{(1)}_{i_p}\sigma^{(2)}_{i_p} \qquad (4.71) \\ &= \frac{N}{2}q_{12}^p - \frac{1}{2N^{p-1}} \sum_{\text{c. i.}} \sigma^{(1)}_{i_1}\sigma^{(2)}_{i_1}...\sigma^{(1)}_{i_p}\sigma^{(2)}_{i_p}, \end{aligned}$$

where $\sum_{\text{c. i.}}$ denotes the sum over all choices of indices $i_1, ...i_p$ such that at least two of them coincide. This sum has at most a number of terms proportional to N^{p-1}, and can be neglected for large N, so the covariance of the Hamiltonian is given essentially by the overlap to the power p. When $\sigma^{(1)} \neq \pm\sigma^{(2)}$, then, one can observe that by increasing the order of interactions p the correlations become more and more negligible, until in the limit $p \to \infty$ one recovers the simpler uncorrelated Random Energy Model [63]. Note that this is not an immediate result but it has to be proven, since one cannot exchange the limits for p and N [30].

For the sake of simplicity, we will only consider, here and in the following, an even number p of interacting spins. In this case the system has a gauge symmetry when the external field h is set equal to zero, as it is left invariant under the transformation $\sigma_{i_k} \to \sigma_{i_k}\sigma_{i_{p+1}}$, for all $k = 1, 2, ..., p$.

In the case of two spins-couplings, we have seen how a phase transition occurs in crossing the AT line, and one expects it to be of second order [31]. The transition manifests itself in a broadening of the probability distribution $P(q)$ of the overlap, which is a delta function peaked at $q = \bar{q}$ above the AT

line but has a finite (and initially small) width below it. This is in contrast with the case of the p-spin model with $p > 2$, where the transition is *first order* and, as soon as a suitably defined critical line is crossed, $P(q)$ becomes the sum of two delta function located at finite distance from each other [31]. This means that for these systems the 1-RSB solution is exact for a large range of temperatures below the critical AT line.

Using the Jensen's inequality one can bound, as in the Sherrington-Kirkpatrick case, the quenched free energy with the annealed free energy:

$$\lim_{N\to\infty} \frac{1}{N}\mathbb{E}\log Z_N(\beta) \leq \log 2 + \frac{\beta^2}{4} \tag{4.72}$$

Then the critical value β_p of β can be defined as

$$\beta_p = \sup\{\beta : \lim_{N\to\infty} \frac{1}{N}\mathbb{E}\log Z_N(\beta) = \log 2 + \frac{\beta^2}{4}\} \tag{4.73}$$

This β_p converges to the value $2\sqrt{\log 2}$ exponentially fast as p grows, recovering the REM transition temperature [30].

For a detailed analysis of the physical properties of this model see for instance [61].

Figure 4.2: Order parameter functional distributions

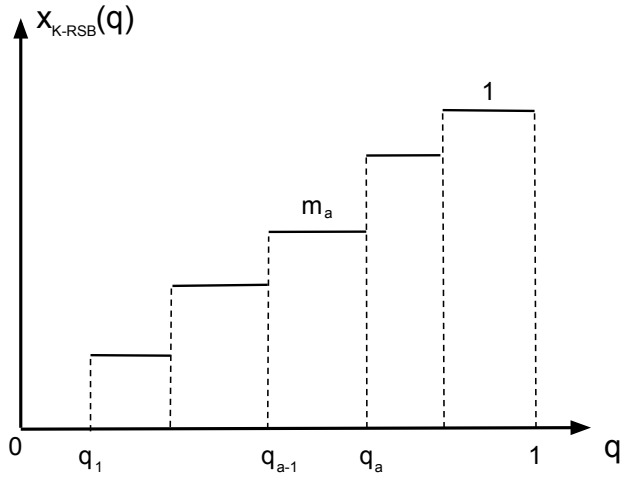

(a) Piecewise constant form of the order parameter functional distribution $x(q)$ in the general case, with $x(q) = m_a$ for $q_{a-1} \leq q \leq q_a$.

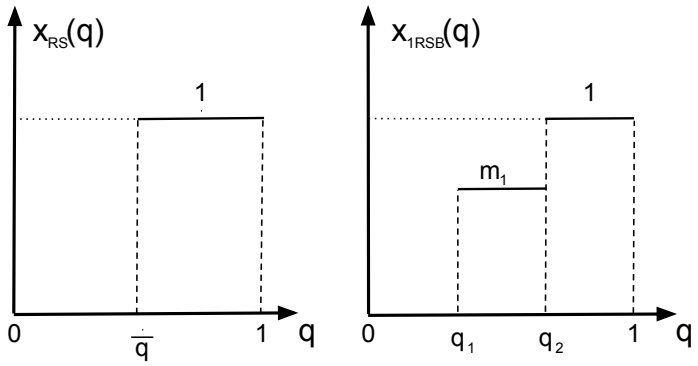

(b) The order parameter functional distribution for the replica symmetric case (left) and for the firs step of replica symmetry breaking (right). In the RS case it has only a single step, passing directly from 0 to 1 for $q = \bar{q}$. In the 1RSB distribution there is an intermediate interval, where $x(q)$ assumes a value $0 < m_1 < 1$.

Figure 4.3: The Almeida-Thouless line, separating the high temperature replica symmetric phase and the low temperature spin glass phase, where the symmetry is broken. Notice that on the horizontal axis is represented the inverse temperature $\beta = 1/T$.

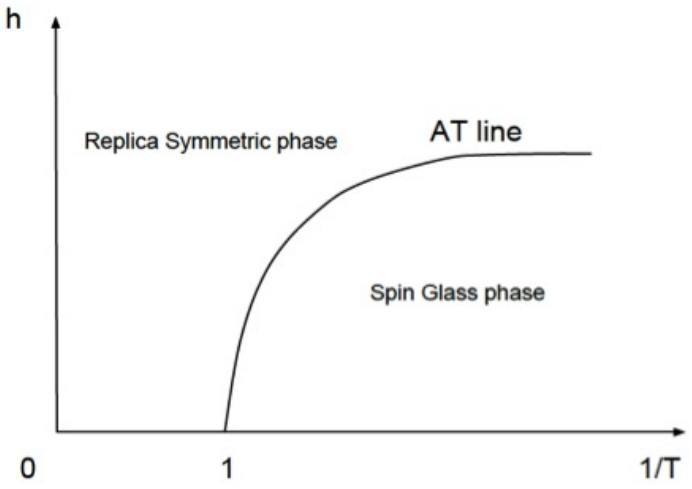

Chapter 5

Interpolation techniques

In the previous chapter we outlined the Parisi replica theory for spin glasses, trying to describe the main features of the Sherrington-Kirkpatrick model, with a short overview on the p-spin glass. Now we would like to show some of the more recent techniques and ideas that led to a deeper insight into the model and that can be used for a wide range of models in statistical physics. To make the presentation of these new methodologies self-contained, the first part of the chapter is still a review of other people's work, while the second part is dedicated to the original contribution of this thesis to the SK and p-spin glass models, as it will be clearly indicated later on.

5.1 The thermodynamic limit

The main object of interest in equilibrium statistical mechanics is the free energy per site. From this quantity one can compute indeed all equilibrium thermal averages, by simply performing derivatives with respect to the suitable thermodynamic parameters, like temperature for the entropy, magnetic field for the magnetization and so on. The first problem one should face is, of course, the uniqueness of the limit of the free energy per site when the size of the system grows to infinity. In principle, in fact, this limit could depend on the particular sequence of system sizes chosen to reach the thermodynamic limit.

For translation invariant systems with short range interactions, as it is well known the uniqueness is proven by dividing the system into large subsystems: the interaction energy among these is a surface effect, negligible with respect to the bulk energy, so that the free energy per site does not change essentially when the size of the system is increased [53]. When the

model is disordered, and finite-dimensional with short range interactions, if the disorder distribution is translation invariant, this approach still works: the subsystems interact weakly, due to the short range character of the potential, and the free energy of the blocks can be approximated as independent identically distributed random variables; the existence of the large N limit of the free energy per site follows then from the strong law of large numbers [64].

For mean field models, surface terms are actually of the same order as the bulk terms, and the approach outlined above does not work. In this case the proof of the existence of the thermodynamic limit is based on a smooth interpolation between a large system, made of N spin sites, and two similar but independent subsystems, made of N_1 and N_2 sites, respectively, with $N_1 + N_2 = N$. For a very large class of mean field spin glass systems, one can prove in this way the existence and uniqueness of the limit, both of the quenched average free energy per site, and of the disorder dependent one, for almost every disorder realization. This result holds not only in the high temperature region, where the limit is easily computed, but for arbitrary values of the temperature and magnetic field. Moreover, the methods we are going to describe for the p-spin glass, easily extend to other cases, such non-Gaussian couplings, non-Ising type spins, the Random Energy Model (REM), and diluted spin-glasses [43, 65, 66, 46].

5.1.1 Self-averaging of the free energy

The problem of proving the existence of the thermodynamic limit of the free energy remained open for more than twenty years, before the work by Guerra and Toninelli [43]. However, it was earlier noticed that the disorder fluctuations of the free energy vanish when taking the infinite volume limit. Obviously, this does not necessarily implies convergence, since the mean value could oscillate as the system size grows. The property of absence of fluctuations for a physical quantity in the thermodynamic limit is called *self-averaging*. This property is usually expected, in ordinary statistical mechanics, for intensive quantities, such as magnetization or free energy per site, with respect to thermal fluctuations, away from phase transition points. In spin-glass system there is a somewhat different scenario [31], and one expects some quantities (like magnetization and internal energy) to be self-averaging, and others, in particular the overlap between the configurations of two replicas, to fluctuate even in the thermodynamic limit, at low temperature. As we have seen in the previous chapter, this is just an indication of the occurrence of Replica Symmetry Breaking.

The free energy of the Sherrington-Kirkpatrick model was first proved to be self-averaging by Pastur and Shcherbina [42], by using martingale techniques. They found that

$$\mathbb{E}\left(\frac{1}{N}\log Z_N(\beta;J)\right)^2 - \left(\mathbb{E}\frac{1}{N}\log Z_N(\beta;J)\right)^2 \leq \frac{C}{N} + O\left(\frac{1}{N^2}\right), \quad (5.1)$$

for some constant C. This result was later improved by Guerra [67], which gave a more precise estimate by showing that

$$C \leq \beta^2 \frac{q_{12}^2}{2}. \quad (5.2)$$

5.1.2 Thermodynamic limit for the Curie-Weiss model

To understand the idea behind the proof of the existence of the thermodynamic limit in the SK model, we start with a simpler model, namely the non-random Curie-Weiss model. Its hamiltonian is given by

$$H_N^{CW}(\sigma,h) = -\frac{J}{N}\sum_{1\leq i<j\leq N}\sigma_i\sigma_j - h\sum_{1\leq i\leq N}\sigma_i, \quad (5.3)$$

where J is the (positive) coupling strength. Given the magnetization associated to a spin configuration σ

$$m(\sigma) = \frac{1}{N}\sum_{1\leq i\leq N}\sigma_i \quad (5.4)$$

the hamiltonian can be written as

$$-N\left(\frac{Jm^2(\sigma)}{2} + hm(\sigma)\right), \quad (5.5)$$

neglecting a trivial additive constant of order unity. The partition function then becomes

$$Z_N(\beta,h) = \sum_\sigma \exp N\beta\left(\frac{Jm^2(\sigma)}{2} + hm(\sigma)\right). \quad (5.6)$$

From now on, let us consider for simplicity the case of zero external field $h = 0$, but it will be obvious from the calculations that the method works perfectly also when a field is present.

Un upper bound on the free energy can be easily found by considering the trivial inequality, valid for all fixed trial magnetizations M,

$$m^2 \geq 2mM - M^2, \tag{5.7}$$

which allows one to write

$$Z_N(\beta) \geq \sum_\sigma \exp\left(N\beta JmM - \frac{1}{2}N\beta JM^2\right). \tag{5.8}$$

The r.h.s., where the magnetization appears linearly, can be immediately computed, since the sum factorizes into sums for each spin, and one finds the uniform upper bound on the free energy

$$\frac{1}{N}\log Z_N(\beta) \geq \sup_M\{\log 2 + \log\cosh(\beta JM) - \frac{1}{2}\beta JM^2\}. \tag{5.9}$$

The result is quite typical, with the first two terms giving the entropy and the third one the internal energy.

Let us now divide the N spin system into two subsystems of N_1 and N_2 spins each, with $N = N_1 + N_2$. Denoting by $m_1(\sigma)$ and $m_2(\sigma)$ the corresponding magnetizations in the two subsytems,

$$m_1(\sigma) = \frac{1}{N_1}\sum_{i=1}^{N_1}\sigma_i \tag{5.10}$$

$$m_2(\sigma) = \frac{1}{N_2}\sum_{i=N_1+1}^{N}\sigma_i, \tag{5.11}$$

one sees that $m(\sigma)$ is a convex linear combination of the two:

$$m(\sigma) = \frac{N_1}{N}m_1(\sigma) + \frac{N_2}{N}m_2(\sigma). \tag{5.12}$$

Since the function $x \to x^2$ is convex, one has

$$Z_N(\beta) \leq \sum_\sigma \exp\beta J\left(N_1m_1^2(\sigma) + N_2m_2^2(\sigma)\right) = Z_{N_1}(\beta)Z_{N_2}(\beta), \tag{5.13}$$

whence

$$Nf_N(\beta) = -\frac{1}{\beta}\log Z_N(\beta) \geq N_1f_{N_1}(\beta) + N_2f_{N_2}(\beta). \tag{5.14}$$

This is the well known property of superadditivity of the free energy in the system size. The existence of the limit then follows from standard methods:

the only other ingredient for the proof, in a nutshell, is that the free energy is bounded from above uniformly in N, which can be easily seen by setting $M = 0$ in Eq. (5.9), to get $f_N(\beta) \leq -\beta^{-1} \log 2$. The property of superadditivity is not only fundamental in proving that the limit exists, but it also implies that, in fact, the limit equals the $\sup_N f_N(\beta)$.

This can be checked directly in the Curie-Weiss model, by finding an opposite bound to (5.9). The magnetization m can take only $N + 1$ distinct values, and we can insert the identity $\sum_M \delta_{mM} = 1$ in the sum on configuration in the partition function as

$$Z_N(\beta) = \sum_\sigma \sum_M \delta_{mM} \exp\left(\frac{1}{2}\beta J N m^2\right). \tag{5.15}$$

Now inside the sum $m = M$, which also implies

$$m^2 = 2mM - M^2. \tag{5.16}$$

Substituting this into $Z_N(\beta)$ and using the fact that $\delta_m M \leq 1$ one finds

$$Z_N(\beta) \leq \sum_M \sum_\sigma \exp\left(\beta J N \left(-\frac{1}{2}M^2 + mM\right)\right). \tag{5.17}$$

The sum over σ can be now carried out and, bounding the remaining sum over M by $2N + 1$ times its largest term, one is led to the following bound for the free energy:

$$\frac{1}{N} \log Z_N(\beta) \leq \frac{1}{N} \log(2N + 1) + \sup_M \{\log 2 + \log \cosh(\beta J M) - \frac{1}{2}\beta J M^2\}. \tag{5.18}$$

The first term on the r.h.s. vanishes in the thermodynamic limit, and comparison with (5.9) shows that the second term is just the limit of the free energy.

Summarizing, we have seen how the existence of the limit for the free energy of the CW model can be proved by exploiting the property of superadditivity, which implies that the free energy converges to its supremum. Moreover one can find the exact limit by finding an upper and a lower bound and showing that they coincide in the thermodynamic limit. In the Sherrington-Kirkpatrick model it is very difficult to find the exact value of the limit in this way. In regard to the existence, the proof is based in this case on *subadditivity* of the free energy, but this property cannot be exploited directly on the Hamiltonian, due to the randomness of couplings. The strategy is, in a

nutshell, to interpolate between the original system of N spins and two non-interacting subsystems with respectively N_1 and N_2 spins, comparing their free energies. For the Curie-Weiss model, for instance, one would introduce an interpolating parameter $t \in [0,1]$ and an auxiliary partition function

$$Z_N(t) = \sum_\sigma \exp\beta \left(NtJm^2(\sigma) + N_1(1-t)Jm_1^2(\sigma) + N_2(1-t)Jm_2^2(\sigma) \right). \tag{5.19}$$

For the boundary values $t = 0, 1$ one has

$$-\frac{1}{N\beta}\log Z_N(1) = f_N(\beta) \tag{5.20}$$

$$-\frac{1}{N\beta}\log Z_N(0) = \frac{N_1}{N} f_{N_1}(\beta) + \frac{N_2}{N} f_{N_2}(\beta) \tag{5.21}$$

and, taking the derivative respect to t,

$$-\frac{d}{dt}\frac{1}{N\beta}\log Z_N(\beta,t) = -J\omega_t\left(m^2(\sigma) - \frac{N_1}{N}m_1^2(\sigma) - \frac{N_2}{N}m_2^2(\sigma) \right) \geq 0, \tag{5.22}$$

where $\omega_t(.)$ denotes the Boltzmann-Gibbs thermal average corresponding to the t-dependent partition function (5.19). Then, integrating over t between 0 and 1 and recalling the boundary conditions (5.20, 5.21), one finds again the superadditivity property (5.14).

5.1.3 Thermodynamic limit: from the Curie-Weiss model to the SK model

For mean field spin glass systems, the interpolation method outlined in the previous section is the only one that works in proving the existence of the thermodynamic limit for the free energy. As for the Curie-Weiss model, we divide the N sites in two blocks N_1, N_2, with $N_1 + N_2 = N$, and define an auxiliary partition function

$$\begin{aligned} Z_N(\beta,t) = \sum_\sigma \exp\beta \Bigg(& \sqrt{\frac{t}{N}} \sum_{1\leq i<j\leq N} J_{ij}\sigma_i\sigma_j + \sqrt{\frac{1-t}{N_1}} \sum_{1\leq i<j\leq N_1} J'_{ij}\sigma_i\sigma_j \\ & + \sqrt{\frac{1-t}{N_2}} \sum_{N_1\leq i<j\leq N} J''_{ij}\sigma_i\sigma_j \Bigg), \end{aligned} \tag{5.23}$$

depending on the parameter $t \in [0,1]$. The external disorder is represented by the independent families of unit Gaussian random variables J, J' and

J''. Let us stress that the two subsystem are subject to an external disorder which is independent with respect to the original system, but the probability distributions are the same. As in the previous case, the boundary values of the auxiliary partition function correspond respectively to the original system, at $t = 1$, and to the two independent subsystems at $t = 0$:

$$\begin{aligned} Z_N(\beta, 1) &= Z_N(\beta) && (5.24)\\ Z_N(\beta, 0) &= Z_{N_1}(\beta) Z_{N_2}(\beta). && (5.25) \end{aligned}$$

As a consequence, for the free energies one has

$$\begin{aligned} \mathbb{E} \log Z_N(\beta, 1) &= -N\beta f_N(\beta) && (5.26)\\ \mathbb{E} \log Z_N(\beta, 0) &= -N_1\beta f_{N_1}(\beta) - N_2\beta f_{N_2}(\beta), && (5.27) \end{aligned}$$

while the derivative with respect to t of the auxiliary free energy is given by

$$\begin{aligned} -\frac{d}{dt}\frac{1}{N\beta}\mathbb{E} \log Z_N(\beta, t) = -\frac{1}{2N}\mathbb{E}\left(\frac{1}{\sqrt{tN}} \sum_{1\le i<j\le N} J_{ij}\omega_t(\sigma_i\sigma_j) \right. \qquad (5.28)\\ \left. -\frac{1}{\sqrt{(1-t)N_1}} \sum_{1\le i<j\le N_1} J'_{ij}\omega_t(\sigma_i\sigma_j) - \frac{1}{\sqrt{(1-t)N_2}} \sum_{N_1\le i<j\le N} J''_{ij}\omega_t(\sigma_i\sigma_j) \right) \end{aligned}$$

where $\omega_t(.)$ denotes the Gibbs state corresponding to the auxiliary partition function (5.23). For a generic smooth function $A(J)$ of a normal gaussian variable J, integration by part gives

$$\mathbb{E}\left(JA(J)\right) = \mathbb{E}\left(\partial_J A(J)\right), \qquad (5.29)$$

which, applied to the previous expression, gives

$$\begin{aligned} -\frac{d}{dt}\frac{1}{N\beta}\mathbb{E} \log Z_N(\beta, t) &= -\frac{\beta}{4N^2} \sum_{1\le i<j\le N} \mathbb{E}\left(1 - \omega_t^2(\sigma_i\sigma_j)\right) && (5.30)\\ &\quad + \frac{\beta}{4NN_1} \sum_{1\le i<j\le N_1} \mathbb{E}\left(1 - \omega_t^2(\sigma_i\sigma_j)\right)\\ &\quad + \frac{\beta}{4NN_2} \sum_{N_1\le i<j\le N} \mathbb{E}\left(1 - \omega_t^2(\sigma_i\sigma_j)\right)\\ &= \frac{\beta}{4}\langle q_{12}^2 - \frac{N_1}{N}(q_{12}^{(1)})^2 - \frac{N_2}{N}(q_{12}^{(2)})^2\rangle_t, \end{aligned}$$

where we have written $\langle . \rangle_t = \mathbb{E}\omega_t(.)$ and defined the partial two-replica overlaps

$$N_1 q_{12}^{(1)} = \sum_{1 \le i \le N_1} \sigma_i^1 \sigma_i^2 \tag{5.31}$$

$$N_2 q_{12}^{(2)} = \sum_{N_1 \le i \le N} \sigma_i^1 \sigma_i^2, \tag{5.32}$$

corresponding to the two subsystems. The overlap plays here a role similar to the magnetization in the non-disordered case, in fact q_{12} is a convex linear combination of $q_{12}^{(1)}$ and $q_{12}^{(2)}$ of the form

$$q_{12} = \frac{N_1}{N} q_{12}^{(1)} + \frac{N_2}{N} q_{12}^{(2)} \tag{5.33}$$

and due to convexity of the function $x \to x^2$ we have the inequality

$$\langle q_{12}^2 - \frac{N_1}{N} (q_{12}^{(1)})^2 - \frac{N_2}{N} (q_{12}^{(2)})^2 \rangle_t \le 0. \tag{5.34}$$

Therefore, we can state as a preliminary result:

Lemma 1. *The quenched average of the logarithm of the interpolating partition function, defined by (5.23), is increasing in t, i. e.,*

$$-\frac{d}{dt} \frac{1}{N\beta} \mathbb{E} \log Z_N(\beta, t) \le 0. \tag{5.35}$$

By integrating over t and recalling the boundary conditions (5.26, 5.27), we get the first main result.

Theorem 2. *The free energy for the SK model is subadditive:*

$$N f_N(\beta) \le N_1 f_{N_1}(\beta) + N_2 f_{N_2}(\beta). \tag{5.36}$$

It is interesting to compare this result with the corresponding (5.14) for the Curie-Weiss model, whose free energy is superadditive. Of course for the SK model it is the pressure $\alpha_N(\beta) = -\beta f_N(\beta)$ which is superadditive, due to the minus sign. Together with an N-independent upper bound on the pressure, which is easy to obtain, one deduces again the existence of the thermodynamic limit [43] (for both the pressure and the free energy density as they are trivially related):

Theorem 3. *The infinite volume limit for $f_N(\beta)$ exists and equals its infimum:*

$$f(\beta) \equiv \lim_{N\to\infty} f_N(\beta) = \inf_N f_N(\beta). \tag{5.37}$$

Note that this result is easily extended to the p-spin glass, since the overlaps to the square in (5.30) and (5.34) in this case are replaced by the overlap to the power p, and the (5.35) still holds.

5.2 Mechanical analogy

In the previous section we have seen how, with some interpolation techniques, it is possible to determine fundamental properties for the SK and other spin-glass models, such as the existence of the thermodynamic limit for the free energy density. Among the results obtained with this approach, it is worth mentioning the Guerra's sum rule [1], which gives the difference between the Parisi formula and the free energy of the SK model in terms of some overlap fluctuations. This paved the way for Talagrand's proof of the correctness of the Parisi formula [2].

In this chapter we are going to use an approach very similar to the interpolation scheme used in [1], merging it with an other interpolation method, based on the formal analogy with a mechanical system, obeying a Hamilton-Jacobi equation [54]. The main idea is to introduce an auxiliary partition function, containing a number of random external fields, tuned by suitable parameters, that mimic the effect of the random interaction to the chosen level of broken symmetry, and are easier to analyze, being one-body terms. The related free energy can be put in a formal correspondence with the action for an Hamilton-Jacobi: studying the dynamics of this mechanical system in absence of external potential, we obtain more and more refined approximations of the free energy of the original system by adding new interpolation parameters. This correspond to our original modest contribution [49] [50]. A simpler application of this method to the Curie-Weiss model can be found in [68].

Let us introduce then the *Boltzmannfaktor*

$$\exp\left(\sqrt{\frac{t}{N}}\sum_{i<j}^{1,N} J_{ij}\sigma_i\sigma_j + \sum_{a=1}^{K}\sqrt{x_a}\sum_{i=1}^{N} J_i^a\sigma_i\right), \tag{5.38}$$

where t and the x_a's are non-negative parameters, the former tuning the interaction between couples of spins, and the latter tuning the interaction

of the single spins with the K external random fields J_i^a, which are independent and distributed as the J_{ij}. The Sherrington-Kirkpatrick model is immediately recovered by taking $t = \beta^2$ and $x_a = 0$ for all $a = 1, ..., K$, The number K of parameters x_a and random fields is related, as we will see, to the numbers of steps of broken replica symmetry. In fact in sec. 4.5 we have introduced non-decreasing piecewise constant functional $x(q)$, assuming the sequence of values

$$0 \leq m_1 \leq m_2 \leq ... \leq m_K \leq 1$$

respectively in the intervals bounded by the values

$$0 \equiv q_0 \leq q_1 \leq ... \leq q_{K-1} \leq q_K \equiv 1$$

and we have seen how the replica symmetric case is obtained by taking a trial order parameter with two intervals (K=2), the first step of replica symmetry breaking with a $x(q)$ with three intervals (K=3), and so on. It is also convenient to define $m_0 \equiv 0$ and $m_{K+1} \equiv 1$.

We will call $\tilde{\omega}$ the Boltzmann state associated to the factor above, and $\tilde{\Omega}$ its replicated, both of them depending on the t and x_a. The averages on the disordered random fields are denoted with $\mathbb{E}_a$, while $\mathbb{E}_0$ is the average on the couplings J_{ij}. Through the (5.38) we define the corresponding auxiliary "partition function" $\tilde{Z}_N(t; x_1, ..., x_K)$, and, recursively, the random variables

$$\begin{aligned} Z_K &\equiv \tilde{Z}_N, && (5.39)\\ Z_{K-1}^{m_K} &\equiv \mathbb{E}_K Z_K^{m_K}, && (5.40)\\ &\cdots \\ Z_0^{m_1} &\equiv \mathbb{E}_1 Z_1^{m_1}. && (5.41) \end{aligned}$$

Note that each of the Z_a, with $1 \leq a \leq K$, depends only on the J_{ij} and on the J_i^b with $b \leq a$, while Z_0 depends only on the J_{ij}. We are then ready to define the auxiliary function

$$\tilde{\alpha}_N(t; x_1, ..., x_K) \equiv \frac{1}{N}\mathbb{E}_0 \log Z_0, \tag{5.42}$$

where all the disorder has been averaged out. It is easy to see that for $t = 0$ this reproduces the form of the solution $f(q, h; x, \beta)$ of the Parisi equation (4.44), computed for $q = 0$ and $h = 0$:

$$\begin{aligned} &\tilde{\alpha}_N(t = 0; x_1, ..., x_K) = \log 2 + \\ &+ \log \left[\int d\mu(z_1) ... \left[\int d\mu(z_K) \cosh^{m_K} \left(\sum_{a=1}^{K} \sqrt{x_a} z_a \right) \right]^{\frac{1}{m_K}} ... \right]^{\frac{1}{m_1}} \\ &= \log 2 + f(0, 0), \end{aligned} \tag{5.43}$$

where the last equation holds if $x_a = \beta^2(q_a - q_{a-1})$. Note that this is still valid for a non-vanishing external field h, if one introduces the term $h\sum_i \sigma_i$ in the factor (5.38).

To exploit our mechanical analogy we have to compute the derivatives of the auxiliary function $\tilde{\alpha}_N$ with respect to the parameters, and to this aim it is useful to define the random variables

$$f_a \equiv \frac{Z_a^{m_a}}{\mathbb{E}_a Z_a^{m_a}}, \quad a = 1, ..., K \tag{5.44}$$

and the states $\tilde{\omega}_a$ (with their replicated ones $\tilde{\Omega}_a$) as

$$\tilde{\omega}_K(.) \equiv \tilde{\omega}(.), \tag{5.45}$$

$$\tilde{\omega}_a(.) \equiv \mathbb{E}_{a+1}...\mathbb{E}_K(f_{a+1}...f_K\omega(.)), \tag{5.46}$$

for $a = 0, ..., K$. Moreover, an important role is played by the generalized averages defined as follows

$$\langle . \rangle_a \equiv \mathbb{E}\left(f_1...f_a\tilde{\Omega}_a(.)\right) \tag{5.47}$$

where with $\mathbb{E}$ we indicated the average respect to all the random variables (but note that f_a does not depend on the J_i^b with $b > a$).

With all these definitions, we are now able to write down the derivatives of $\tilde{\alpha}_N$ with respect to the parameters t and x_a (which is indicated with ∂_a) in a compact way as

$$\partial_t\tilde{\alpha}_N(t; x_1, ..., x_K) = \frac{1}{4}\left(1 - \sum_{a=0}^{K}(m_{a+1} - m_a)\langle q_{12}^2\rangle_a\right) \tag{5.48}$$

$$\partial_a\tilde{\alpha}_N(t; x_1, ..., x_K) = \frac{1}{2}\left(1 - \sum_{b=a}^{K}(m_{b+1} - m_b)\langle q_{12}\rangle_b\right). \tag{5.49}$$

The calculation is simple but rather cumbersome, so we included it in the appendix B.

5.2.1 Hamilton-Jacobi equation

The parameters t and x_a will play the role, in a formal analogy, of the time and the generalized coordinates for a mechanical system. In fact, having computed the derivatives of the auxiliary function $\tilde{\alpha}_N$, we would like to write a Hamilton-Jacobi equation with a suitable potential (which is related to some fluctuations of the overlap). In a nutshell, the idea is to solve this

equation in the case of a vanishing potential, to get informations on the SK model by taking the solution for $t = \beta^2$ and all the $x_a = 0$.

To this aim, we define the action for the mechanical problem in terms of the function $\tilde{\alpha}_N$, as

$$S(t;\boldsymbol{x}) = 2\left(\alpha(t;x_1,\ldots,x_K) - \frac{1}{2}\sum_{a=1}^{K} x_a - \frac{1}{4}t\right). \tag{5.50}$$

Using the (5.48) and (5.49), the derivatives of this action with respect to t and the x_a's take the following form:

$$\partial_t S(t;\boldsymbol{x}) = -\frac{1}{2}\sum_{a=0}^{K}(m_{a+1}-m_a)\langle q_{12}^2\rangle_a \tag{5.51}$$

$$\partial_a S(t;\boldsymbol{x}) = -\sum_{b=a}^{K}(m_{b+1}-m_b)\langle q_{12}\rangle_b. \tag{5.52}$$

The action (5.50) satisfies a Hamilton-Jacobi equation

$$\partial_t S(t;\boldsymbol{x}) + \frac{1}{2}\sum_{a,b=1}^{K}\partial_a S(t;\boldsymbol{x})\,(M^{-1})_{ab}\,\partial_b S(t;\boldsymbol{x}) + V(t;\boldsymbol{x}) = 0 \tag{5.53}$$

where M^{-1} is the inverse of a $K \times K$ mass matrix that we are going to specify and $V(t;\boldsymbol{x})$ is a suitable potential, which can be written in the form

$$V(t;\boldsymbol{x}) = \frac{1}{2}\sum_{a=0}^{K}(m_{a+1}-m_a)(\langle q_{12}^2\rangle_a - \langle q_{12}\rangle_a^2) + \frac{1}{2}(m_1-m_0)\langle q_{12}\rangle_0^2. \tag{5.54}$$

Let us now show how Eq. (5.53), with the potential (5.54), is satisfied with a proper choice of M. The kinetic term in the Hamilton-Jacobi equation is, using (5.49),

$$\begin{aligned} T(t;\boldsymbol{x}) &\equiv \frac{1}{2}\sum_{a,b=1}^{K}\partial_a S\,(M^{-1})_{ab}\,\partial_b S \\ &= \frac{1}{2}\sum_{a,b=1}^{K}(M^{-1})_{ab}\sum_{c\geq a}^{K}\sum_{d\geq b}^{K}(m_{c+1}-m_c)\langle q_{12}\rangle_c(m_{d+1}-m_d)\langle q_{12}\rangle_d \\ &= \frac{1}{2}\sum_{c,d=1}^{K} D_{cd}\,(m_{c+1}-m_c)\langle q_{12}\rangle_c(m_{d+1}-m_d)\langle q_{12}\rangle_d \end{aligned} \tag{5.55}$$

where we have defined the matrix D as

$$D_{cd} \equiv \sum_{a=1}^{c} \sum_{b=1}^{d} (M^{-1})_{ab}. \tag{5.56}$$

Now we impose the condition

$$D_{cd}(m_{c+1} - m_c) = \delta_{cd} \tag{5.57}$$

and find the following expression for the kinetic term

$$\begin{aligned} T(t;\boldsymbol{x}) &= \frac{1}{2}\sum_{c=1}^{K}(m_{c+1}-m_c)\langle q_{12}\rangle_c^2 & (5.58)\\ &= \frac{1}{2}\sum_{c=0}^{K}(m_{c+1}-m_c)\langle q_{12}\rangle_c^2 - \frac{1}{2}(m_1-m_0)\langle q_{12}\rangle_0^2 & (5.59) \end{aligned}$$

Eq. (5.57) determines the elements of the inverse of the mass matrix M^{-1} and, consequently, of M . The inverse M^{-1} comes out to be symmetric, and the only non-vanishing elements are the diagonal ones, or the ones around the diagonal like $(M^{-1})_{a,a+1}$:

$$\begin{aligned} (M^{-1})_{11} &= \frac{1}{m_2 - m_1} & (5.60)\\ (M^{-1})_{a,a} &= \frac{1}{m_{a+1}-m_a} + \frac{1}{m_a - m_{a-1}} & (5.61)\\ (M^{-1})_{a,a+1} &= (M^{-1})_{a+1,a} = -\frac{1}{m_{a+1}-m_a} & (5.62) \end{aligned}$$

Without losing generality, we can take $m_K < 1$, so that for the last matrix element we can use (5.61), remembering that $m_{K+1} \equiv 1$. For instance, if $K = 3$, M^{-1} takes the form

$$\begin{pmatrix} \frac{1}{m_2-m_1} & -\frac{1}{m_2-m_1} & 0 \\ -\frac{1}{m_2-m_1} & \frac{1}{m_2-m_1}+\frac{1}{m_3-m_2} & -\frac{1}{m_3-m_2} \\ 0 & -\frac{1}{m_3-m_2} & \frac{1}{m_3-m_2}+\frac{1}{1-m_3} \end{pmatrix} \tag{5.63}$$

Computing the inverse one finds M, whose elements are specified by

$$M_{ab} = 1 - m_{(a\wedge b)}, \tag{5.64}$$

where $a \wedge b = \sup(a, b)$, or, more explicitly,

$$M = \begin{pmatrix} 1-m_1 & 1-m_2 & \cdots & 1-m_K \\ 1-m_2 & 1-m_2 & \cdots & 1-m_K \\ \vdots & \vdots & \ddots & \vdots \\ 1-m_K & 1-m_K & \cdots & 1-m_K \end{pmatrix}$$

whence it is evident that choosing $m_K = 1$ cancels a degree of freedom, as we are going to see later. The choice (5.64) for M (following from the condition (5.57), which simplifies the kinetic term) determines the potential (5.54) for which the Hamilton-Jacobi equation (5.53) is satisfied. This potential depends on some generalized variance of the overlap, which we are going to put to zero to study the simple zero source problem. We will see how, solving the HJ equation and taking $t = \beta^2$ and $x_a = 0$ we are able to find the annealed, replica symmetric, and 1RSB free energies for the Sherrington-Kirkpatrick model.

We may also define the velocity field for the mechanical problem. For $a > 1$ we find

$$v_a(t; \boldsymbol{x}) \equiv \sum_{b=1}^{K} \left(M^{-1}\right)_{ab} \partial_b S = \langle q_{12} \rangle_{a-1} - \langle q_{12} \rangle_a, \tag{5.65}$$

while for $a = 1$

$$v_1(t; \boldsymbol{x}) = -\langle q_{12} \rangle_1. \tag{5.66}$$

5.3 Annealed free energy

Let us now consider the simplest case, $K = 1$, with just one parameter $x_1 = x$ corresponding to the generalized coordinate of the mechanical problem, to see how the solution of the mechanical problem will enable us to find the annealed free energy. The corresponding form of $x(q)$ compatible with just one parameter is the simplest possible: $x(q) = m_1 = 1$ in the whole interval $[0, 1]$. Note that the choice $m_1 = m_K = 1$ will make the action independent on the only generalized coordinate x.

Using the definition (5.41) and integrating on the disorder J_i^a we immediately obtain Z_0 as

$$Z_0 \equiv \mathbb{E}_1 Z_1 = \exp\left(\frac{N}{2} x\right) \sum_{\sigma} \exp\left(\sqrt{\frac{t}{N}} \sum_{i<j} J_{ij} \sigma_i \sigma_j\right), \tag{5.67}$$

whence the auxiliary function $\tilde{\alpha}_N$, given by

$$\tilde{\alpha}_N(t,x) = \frac{x}{2} + \frac{1}{N} E_0 \log \sum_\sigma \exp\left(\sqrt{\frac{t}{N}} \sum_{i<j} J_{ij}\sigma_i\sigma_j\right). \tag{5.68}$$

This expression implies, as anticipated, that the action does not depend on x, so that the velocity field vanish identically:

$$\begin{aligned} S(t) &= 2\tilde{\alpha}(t,x) - x - \frac{t}{2} \\ &= \frac{2}{N} E_0 \log \sum_\sigma \exp\left(\sqrt{\frac{t}{N}} \sum_{i<j} J_{ij}\sigma_i\sigma_j\right) - \frac{t}{2} \qquad (5.69) \\ \partial_x S(t) &\equiv v(t,x) = 0 \qquad (5.70) \\ \partial_t S(t) &= -\frac{1}{2}\langle q_{12}^2\rangle_0. \qquad (5.71) \end{aligned}$$

The equation of motion is then, trivially, $x(t) = x_0$, where $x_0 = x(0)$ is the starting point. The potential in this case is simply given by $-\partial_t S(t) = \langle q_{12}^2\rangle_0/2$, since the sum $\partial_t S(t) + V(t)$ must vanish to satisfy the Hamilton-Jacobi equation (5.53).

Let us now consider the case of a vanishing source, $V(t) = 0$: In this hipotesys the Hamilton's principal function $\bar{S}(t)$, solution of the HJ equation, is simply a constant, and can be identified with the action $S(t)$ calculated at the initial time $t_0 = 0$,

$$\bar{S} = S(0) = 2\log 2. \tag{5.72}$$

Despite the triviality of the case we are dealing with, it is worth noticing that the choice $t_0 = 0$ simplify the computation of the solution, since in this case the sum over the spin configurations in (5.68) is particularly easy, due to the absence of couplings.

From the solution of the mechanical problem above, we obtain the auxiliary function $\bar{\alpha}(t,x)$

$$\bar{\alpha}(t,x) = \frac{1}{2}\bar{S}(t) - \frac{x}{2} - \frac{t}{4} = \log 2 + \frac{x}{2} + \frac{t}{4}. \tag{5.73}$$

At this point, choosing $t = \beta^2$ e $x = 0$ we find the corresponding free energy (or, properly speaking, pressure)

$$\alpha_N(\beta) = \log 2 + \frac{\beta^2}{4} \tag{5.74}$$

which corresponds to the annealed value.

The potential that we have neglected is proportional to $\langle q_{12}^2 \rangle_0 = \mathbb{E}_0 \tilde{\Omega}(q_{12}^2)$, corresponding to the average of the square overlap of the SK model, but computed at the inverse temperature $\beta = \sqrt{t}$. This approximation corresponds then to assuming a overlap equal to zero, which is in accord with the annealed solution. This is the solution valid above the critical temperature (for $h = 0$), where the overlap self-averages to zero and it is not surprising that, assuming a vanishing overlap, one is able to find the annealed solution.

5.4 Replica Symmetric solution

Let us skip now to the less trivial case of $K = 2$, which will lead us to the Replica Symmetric solution of the SK model. This case was first studied in [54].

The simplest non trivial form for the functional $x(q)$ for $K = 2$ is given by the expression

$$x(q) = \begin{cases} 0 & \text{if } q \in [0, \bar{q}) \\ 1 & \text{if } q \in [\bar{q}, 1]. \end{cases} \tag{5.75}$$

where the interval bounds and the corresponding constants for the piecewise constant functional are

$$q_1 = \bar{q}, \quad q_2 = q_K \equiv 1 \tag{5.76}$$

$$m_0 = m_1 = 0, \quad m_2 = m_K = 1 = m_3 = m_{K+1}. \tag{5.77}$$

In this case we will have two generalized coordinates (x_1, x_2) but, since $m_2 = 1$, the action will not depend on the coordinate x_2, as we have seen in the annealed case.

However the function $Z_2 = \tilde{Z}_N$ has in this case two external random fields, tuned by x_1 and x_2, *i. e.*,

$$Z_2(t; x_1, x_2) = \sum_\sigma \exp\left(\sqrt{\frac{t}{N}} \sum_{i<j} J_{ij}\sigma_i\sigma_j + \sqrt{x_1} \sum_i J_i^1 \sigma_i + \sqrt{x_2} \sum_i J_i^2 \sigma_i \right), \tag{5.78}$$

while from the definition of Z_1 we have

$$Z_1 = \mathbb{E}_2 Z_2 = \exp\left(N \frac{x_2}{2}\right) \sum_\sigma \exp\left(\sqrt{\frac{t}{N}} \sum_{i<j} J_{ij}\sigma_i\sigma_j + \sqrt{x_1} \sum_i J_i^1 \sigma_i \right). \tag{5.79}$$

Since we have to compute

$$Z_0 = (\mathbb{E}_1 Z_1^{m_1})^{1/m_1}$$

but $m_1 = 0$, we can simply adopt as a definition of Z_0 the limit of the expression above for $m_1 \to 0$, corresponding to

$$Z_0 = \exp E_1 \log Z_1, \tag{5.80}$$

so that the auxiliary function is defined as

$$\begin{aligned} \tilde{\alpha}_N(t; x_1, x_2) &= \frac{x_2}{2} + \frac{1}{N} E_0 E_1 \log \left[\sum_\sigma \exp \left(\sqrt{\frac{t}{N}} \sum_{i<j} J_{ij} \sigma_i \sigma_j \right.\right. \\ &\quad \left.\left. + \sqrt{x_1} \sum_i J_i^1 \sigma_i + \right) \right] \end{aligned} \tag{5.81}$$

At the initial time $t_0 = 0$ the sum over configurations factorizes and this easily gives

$$\tilde{\alpha}(0; x_1^0, x_2^0) = \frac{x_2^0}{2} + \log 2 + \int d\mu(z) \, \log \cosh \left(\sqrt{x_1^0}\, z \right), \tag{5.82}$$

where $x_1^0 = x_1(t = 0)$ and $x_2^0 = x_2(t = 0)$ are the initial values of the generalized coordinates.

Substituting (5.81) into the definition (5.50) it is immediate to see that the action S for the mechanical problem,

$$S(t; x_1) = 2 \left(\tilde{\alpha}_N(t; x_1, x_2) - \frac{x_1}{2} - \frac{x_2}{2} - \frac{t}{4} \right) \tag{5.83}$$

does not depend on x_2, so that we can forget about the mass matrix and consider a one-dimensional mechanical problem. From (5.51) and (5.52), the streaming is given by

$$\partial_t S(t; x_1) = -\frac{1}{2} \langle q_{12}^2 \rangle_1 \tag{5.84}$$

$$\partial_{x_1} S(t; x_1) = -\langle q_{12} \rangle_1 \tag{5.85}$$

$$\partial_{x_2} S(t; x_1) = 0 \tag{5.86}$$

so that the velocity corresponds to the generalized overlap

$$v_1(t; x_1) = -\langle q_{12} \rangle_1 = -\mathbb{E}_0 \mathbb{E}_1 f_1 \frac{1}{N} \sum_i \left(\mathbb{E}_2 f_2 \tilde{\omega}(\sigma_i) \right)^2 \tag{5.87}$$

which can be explicitly verified to be independent on x_2, using the definitions of the variables f_a and of the states $\tilde{\omega}$ for this particular case. The Hamilton-Jacobi equation for $K = 2$ is then

$$\partial_t S(t; x_1) + \frac{1}{2} \left(\partial_{x_1} S(t; x_1)\right)^2 + V(t; x_1) = 0, \tag{5.88}$$

and this has no singularities since $S(t; x_1)$ is given explicitly by (5.83), in the whole quadrant $x_1 \geq 0$, $t \geq 0$. In particular for every point (x_1, t) there exists a unique trajectory $x_1(t')$ whose velocity field is defined above, which passes through the point x_1 at time t [54]:

$$\dot{x}_1(t') = v(x_1(t'), t'), \qquad x_1(t') = x_1. \tag{5.89}$$

The potential

$$V(t; x_1) = \frac{1}{2} \left(\langle q_{12}^2 \rangle_1 - \langle q_{12} \rangle_1^2\right) \tag{5.90}$$

is related to a generalized variance of the overlap, and in fact for $x_1 = 0$ e $t = \beta^2$ we just find the physical variance of the overlap

$$V(\beta^2; 0) = \frac{1}{2} \left(\langle q_{12}^2 \rangle - \langle q_{12} \rangle^2\right). \tag{5.91}$$

As in the previous case, we want now to consider the mechanical problem in the simple case of $V(t; x_1) \equiv 0$. The velocity is then a constant, and it is equal to its initial value

$$\bar{q}(x_1^0) \equiv -v_1(0, x_1^0) = \int d\mu(z) \, \tanh^2 \left(z \sqrt{x_1^0}\right). \tag{5.92}$$

When the parameters take the right values, this equation corresponds to the Sherrington-Kirkpatrick self-consistence equation

$$\bar{q}(\beta) = \int d\mu(z) \, \tanh^2(\beta \sqrt{\bar{q}} z), \tag{5.93}$$

satisfied by the order parameter q in the high temperature and field phase. In fact, for $x_1 = x_1^0 - \bar{q}(x_1^0)t = 0$ and $t = \beta^2$, one finds $x_1^0 = \beta^2 \bar{q}(x_1^0)$, which substituted in (5.92) gives (5.93).

The trajectories of the mechanical system are described by the straight lines

$$x_1(t) = x_1^0 - \bar{q}(x_1^0)t. \tag{5.94}$$

and it can be prooved that the trajectory passing for a generic point (x_1, t) is unique. The proof is based on the fact that the point $t(x_0)$ at which the

free trajectory intersects the t-axis is a monotonous function of the starting point x_0 [54]. Then we can immediately solve the HJ equation by taking the action at the initial point and adding the integral over t of the Lagrangian, which in this case ($V \equiv 0$) is simply given by the kinetic term $v_1^2/2$, that is conserved and can be put out of the integral:

$$\bar{S}(t; x_1) = \bar{S}(0; x_1^0) + \frac{1}{2}\bar{q}^2(x_1^0)t. \tag{5.95}$$

The auxiliary function related to this solution is then

$$\bar{\alpha}(t; x_1, x_2) = \log 2 + \int d\mu(z)\ \log\cosh(\sqrt{x_1^0}z) + \frac{t}{4}(1-\bar{q})^2 + \frac{x_2}{2} \tag{5.96}$$

and it fully corresponds to the replica symmetric solution (4.29) when we take the right parameters $x_1 = x_2 = 0$ and $t = \beta^2$. This makes sense, since we have seen that the potential is directly related to the variance of the overlap, and neglecting the potential is equivalent to assume a non-fluctuating overlap, just as in the replica symmetric approach.

5.5 1RSB solution

In the previous two sections we have seen how the mechanical problems for $K = 1$ and $K = 2$, in the case of free motion, allow us to recover respectively the annealed and the replica symmetric free energies. Now we want to skip to the first step of replica symmetry breaking by following the same approach.

The simplest non trivial form for the piecewise constant functional $x(q)$, for $K = 3$, is obtained by taking (see also Fig. 4.3(b), right side)

$$0 = q_0 < q_1 < q_2 < q_3 = 1 \tag{5.97}$$
$$0 = m_1 < m_2 \equiv m < m_3 = 1, \tag{5.98}$$

and the corresponding value for the free energy density is given by Eq. (4.35), *i. e.*, which is just the 1RSB free energy.

Let us then see how this result can be recovered by using the mechanical approach. The Boltzmann factor 5.38 has now three random fields inside, tuned by the respective parameters, and the generalized partition function is

$$\tilde{Z}_N(t; x_1, x_2, x_3) = \sum_{\sigma} \exp\left[\sqrt{\frac{t}{N}}\sum_{i<j} J_{ij}\sigma_i\sigma_j + \sum_{a=1}^{3}\sqrt{x_a}\sum_i J_i^a\sigma_i\right], \tag{5.99}$$

whence

$$\begin{aligned} Z_3 &= \tilde{Z}_N \qquad (5.100) \\ Z_2 &= \mathbb{E}_3 Z_3 \\ &= e^{\frac{Nx_3}{2}} \sum_\sigma e^{\sqrt{\frac{t}{N}} \sum_{i<j} J_{ij}\sigma_i\sigma_j + \sum_{a=1}^2 \sqrt{x_a} \sum_i J_i^a \sigma_i}. \qquad (5.101) \end{aligned}$$

Since $m_1 = 0$ we adopt the definition (5.80), as we have seen for $K = 2$,

$$Z_0 = \exp(\mathbb{E}_1 \log Z_1) = \exp\left(\frac{1}{m}\mathbb{E}_1 \log \mathbb{E}_2 Z_2^m\right). \qquad (5.102)$$

The explicit expression for the auxiliary function $\tilde{\alpha}_N$ is then

$$\begin{aligned} &\tilde{\alpha}_N(t; x_1, x_2, x_3) = \frac{1}{N}\mathbb{E}_0 \log Z_0 = \qquad (5.103) \\ &= \frac{x_3}{2} + \frac{1}{Nm}\mathbb{E}_0\mathbb{E}_1 \log \mathbb{E}_2 \left(\sum_\sigma e^{\sqrt{\frac{t}{N}} \sum_{i<j} J_{ij}\sigma_i\sigma_j + \sum_{a=1}^2 \sqrt{x_a} \sum_i J_i^a \sigma_i}\right)^m. \end{aligned}$$

We are going to use the same strategy as before, that is solving the HJ equation for a vanishing potential. This solution is found, again, by taking the action at the initial time and propagating the integral of the kinetic energy, which is conserved, over time. So we need the value of $\tilde{\alpha}_N$ at the initial time $t_0 = 0$, particularly easy to find, since for $t = 0$ the coupling term in the the Boltzmann factor disappears and the sum over configurations factorizes:

$$\begin{aligned} \tilde{\alpha}_N(0; x_1^0, x_2^0, x_3^0) &= \frac{x_3}{2} + \log 2 \qquad (5.104) \\ &+ \frac{1}{m}\int d\mu(z_1) \log \int d\mu(z_2) \cosh^m\left(\sqrt{x_1^0} z_1 + \sqrt{x_2^0} z_2)\right), \end{aligned}$$

where, again, we indicated with x_a^0 the initial condition $x_a(t = 0)$, for all a.

Because we have defined $m_3 = 1$, the action will not depend, as before, on the corresponding generalized coordinate x_3, and the mechanical problem will be about a two-dimensional system with action

$$\begin{aligned} S(t; x_1, x_2) &= \frac{2}{Nm}\mathbb{E}_0\mathbb{E}_1 \log \mathbb{E}_2 \left(\sum_\sigma e^{\sqrt{\frac{t}{N}} \sum_{i<j} J_{ij}\sigma_i\sigma_j + \sum_{a=1}^2 \sqrt{x_a} \sum_i J_i^a \sigma_i}\right)^m \\ &\quad - x_1 - x_2 - \frac{t}{2}. \qquad (5.105) \end{aligned}$$

Using Eq.s (5.51) and (5.52) the derivatives are computed as

$$\begin{aligned}
\partial_t S(t;x_1,x_2) &= -\frac{m}{2}\langle q_{12}^2\rangle_1 - \frac{1-m}{2}\langle q_{12}^2\rangle_2 && (5.106)\\
\partial_1 S(t;x_1,x_2) &= -m\langle q_{12}\rangle_1 - (1-m)\langle q_{12}\rangle_2 && (5.107)\\
\partial_2 S(t;x_1,x_2) &= -(1-m)\langle q_{12}\rangle_2. && (5.108)
\end{aligned}$$

and we can also write the kinetic term

$$T(t;x_1,x_2) = \frac{m}{2}\langle q_{12}\rangle_1^2 + \frac{1-m}{2}\langle q_{12}\rangle_2^2. \tag{5.109}$$

and the potential

$$V(t;x_1,x_2) = \frac{1}{2}\left[m\left(\langle q_{12}^2\rangle_1 - \langle q_{12}\rangle_1^2\right) + (1-m)\left(\langle q_{12}^2\rangle_2 - \langle q_{12}\rangle_2^2\right)\right], \tag{5.110}$$

that contains some form of generalized overlap fluctuations. Note that this expression gives, correctly, the RS potential if $m = 0$ or $m = 1$.

The mass matrix (5.64) and its inverse will no more be trivial, since we are dealing with a two-dimensional mechanical system:

$$M^{-1} = \begin{pmatrix} \frac{1}{m} & -\frac{1}{m} \\ -\frac{1}{m} & \frac{1}{m(1-m)} \end{pmatrix}, \quad M = \begin{pmatrix} 1 & 1-m \\ 1-m & 1-m \end{pmatrix} \tag{5.111}$$

and we can write the velocity field using the inverse mass matrix and the the derivatives of the action, or the general formulas (5.65) and (5.66), finding

$$\begin{aligned}
v_1(t;x_1,x_2) &= \sum_{b=1}^{2}(M^{-1})_{1b}\,\partial_b S(t;x_1,x_2) = -\langle q_{12}\rangle_1 && (5.112)\\
v_2(t;x_1,x_2) &= \sum_{b=1}^{2}(M^{-1})_{2b}\,\partial_b S(t;x_1,x_2) = \langle q_{12}\rangle_1 - \langle q_{12}\rangle_2. && (5.113)
\end{aligned}$$

5.5.1 Free motion

We now have all the ingredients to study the dynamics of the mechanical system, whose action (5.105) satisfies the Hamilton-Jacobi equation

$$\partial_t S(t;x_1,x_2) + \frac{1}{2}\sum_{a,b=1}^{2}\partial_a S(t;x_1,x_2)\,(M^{-1})_{ab}\,\partial_b S(t;x_1,x_2) + V(t;x_1,x_2) = 0 \tag{5.114}$$

with the potential (5.110). As before, we are interested in solving this equation in the simple case of free motion ($V \equiv 0$), when the trajectories are given by the straight lines

$$x_1(t) = x_1^0 - \langle q_{12}\rangle_1(0; x_1^0, x_2^0)\, t \tag{5.115}$$
$$x_2(t) = x_2^0 + \left[\langle q_{12}\rangle_1(0; x_1^0, x_2^0) - \langle q_{12}\rangle_1(0; x_1^0, x_2^0)\right]\, t, \tag{5.116}$$

where we stressed the dependence of $\langle q_{12}\rangle_1$ e $\langle q_{12}\rangle_2$ (and consequently, of the velocity field) on the initial condition x_1^0 and x_2^0. For the sake of brevity we can define the quantities

$$\bar{q}_1(x_1^0, x_2^0) \equiv \langle q_{12}\rangle_1(0; x_1^0, x_2^0) \tag{5.117}$$
$$\bar{q}_2(x_1^0, x_2^0) \equiv \langle q_{12}\rangle_2(0; x_1^0, x_2^0) \tag{5.118}$$

and writing explicitly these, using the definitions of section 5.2, we find out, interestingly, that $\bar{q}_1$ and $\bar{q}_2$ satisfy the self-consistence equations

$$\bar{q}_1(x_1^0, x_2^0) = \int d\mu(z) \left[\frac{\int d\mu(y) \cosh^m \Theta \tanh \Theta}{\int d\mu(y) \cosh^m \Theta}\right]^2 \tag{5.119}$$
$$\bar{q}_2(x_1^0, x_2^0) = \int d\mu(z) \left[\frac{\int d\mu(y) \cosh^m \Theta \tanh^2 \Theta}{\int d\mu(y) \cosh^m \Theta}\right] \tag{5.120}$$
$$\Theta \equiv \sqrt{x_1^0} z + \sqrt{x_2^0} y$$

which correspond exactly to the 1RSB equations (4.37,4.38). In fact, taking as usual $x_1 = x_1^0 - \bar{q}_1 t = 0$ e $x_2 = x_2^0 + \bar{q}_1 t - \bar{q}_2 t = 0$ with $t = \beta^2$, one has

$$x_1^0 = \beta^2 \bar{q}_1 \tag{5.121}$$
$$x_2^0 = \beta^2 (\bar{q}_2 - \bar{q}_1). \tag{5.122}$$

We can also observe that the velocities along the two directions are both negative or vanishing, so there will be an instant when at least one of the coordinates $x_1(t)$ e $x_2(t)$ becomes negative, while we are interested in the motion inside the region of non-negative x_1 and x_2. In the simpler mechanical problem of the previous section for the RS solution, it can be shown that the quadrant of the plane (x, t) with $x \leq 0$ and $t > 0$ splits in two regions through a line given by the envelope of all the straight trajectories $x_1(t) = x_1^0 - \bar{q}(x_1^0)t$. Every point on such line can be joint with a unique starting point x_1^0 by a unique trajectory. The region of the quarter below the envelope line contains the points where no trajectory can pass through, while the unicity is lost for the points of the quarter $x \leq 0,\ t > 0$ above that line.

In the case we are dealing now things get more complicated, since we have now two generalized coordinates x_1 and x_2 and we should consider the lines in the three-dimensional space (x_1, x_2, t). However, we expect that something similar happens, *i. e.*, that there exists, in the octants where at least one of the two coordinates is negative, an envelope surface, whose point have a unique trajectory passing through them, delimiting a region where unicity is lost (above) from one whose point cannot be reached by any trajectory (below).

In what follows, we solve the HJ equation in the region where both the coordinates are positive. As before, we can write a solution by taking the action at the initial time and propagating the kinetic energy, which is conserved (so we can simply consider its initial value):

$$\begin{aligned} \bar{S}(t; x_1, x_2) &= S(0; x_1^0, x_2^0) + T(0; x_1^0, x_2^0)t \qquad (5.123) \\ &= \tilde{\alpha}_N(0; x_1^0, x_2^0, x_3^0) - \frac{x_1^0}{2} - \frac{x_2^0}{2} - \frac{x_3^0}{2} - \frac{t}{4} + T(0; x_1^0, x_2^0)\frac{t}{2}. \end{aligned}$$

From this, noting that

$$\begin{aligned} x_1 - x_1^0 &= -\bar{q}_1 t \qquad (5.124) \\ x_2 - x_2^0 &= (\bar{q}_1 - \bar{q}_2)t \qquad (5.125) \end{aligned}$$

we get the corresponding auxiliary function

$$\begin{aligned} \bar{\alpha}_N(t; x_1, x_2, x_3) &= \frac{x_3}{2} + \log 2 - \frac{t}{4}[-1 + 2\bar{q}_2 - m\bar{q}_1^2 - (1-m)\bar{q}_2^2] \qquad (5.126) \\ &\quad + \frac{1}{m}\int d\mu(z_1) \log \int d\mu(z_2) \cosh^m \left(\sqrt{x_1^0} z_1 + \sqrt{x_2^0} z_2 \right). \end{aligned}$$

The 1-RSB free energy, then, is recovered computing the expression above for $t = \beta^2$, $x_1 = x_2 = x_3 = 0$, whence $x_1^0 = \bar{q}_1\beta^2$ and $x_2^0 = (\bar{q}_1 - \bar{q}_2)\beta^2$, in fact for this choice we find

$$\begin{aligned} \bar{\alpha}(\beta^2; 0, 0, 0) &= \log 2 - \frac{1}{4}\beta^2 \left((m-1)\bar{q}_2^2 - 1 - m\bar{q}_1^2 + 2\bar{q}_2 \right) + \qquad (5.127) \\ &+ \frac{1}{m}\int d\mu(z_1) \log \int d\mu(z_2) \cosh^m \left(\beta\sqrt{\bar{q}_1} z_1 + \beta\sqrt{\bar{q}_2 - \bar{q}_1} z_2 \right), \end{aligned}$$

which is the same as the (4.35). We have found again the 1-RSB free energy, together with the self-consistence equations satisfied by the order parameters.

The neglected potential (5.110) corresponds to the variance of the overlap according to the averages $\langle . \rangle_1$ and $\langle . \rangle_2$, weighted with m and $1 - m$. This

term is nothing more than the difference between the real free energy for the SK model and the Parisi formula, as can be found in [1], and neglecting this potential corresponds to neglect the overlap fluctuations around q_1 e q_2. In particular, when taking $x_1 = x_2 = x_3 = 0$ and $t = \beta^2$ one simply found the variance

$$V(\beta^2; 0, 0) = \frac{1}{2}\left[\langle q_{12}^2\rangle - \langle q_{12}\rangle^2\right]. \tag{5.128}$$

5.5.2 Unicity for small values of the overlap

The proof of unicity for the solution found above is much more difficult to find than in the RS case. In particular, we should proof that, given a generic (x_1, x_2, t), with $x_1 > 0$, $x_2 > 0$, $t > 0$, there exists a unique trajectory for the point (x_1, x_2) at time t, or, equivalently, that the initial condition (x_1^0, x_2^0) and the velocities, which depend on these values, are univocally determined by x_1 , x_2 and t through the equations

$$\begin{aligned} x_1(t) &= x_1^0 - \bar{q}_1(x_1^0, x_2^0)\, t & (5.129)\\ x_2(t) &= x_2^0 + \left[\bar{q}_1(x_1^0, x_2^0) - \bar{q}_2(x_1^0, x_2^0)\right]\, t, & (5.130) \end{aligned}$$

where $\bar{q}_1$ and $\bar{q}_2$ satisfy Eq.s (5.119, 5.120).

We want now to show that unicity holds if we choose the initial points around the origin, since for $x_1 = x_2 = 0$ and $t = \beta^2$ the equations of motion give

$$\begin{aligned} x_1^0 &= \beta^2 \bar{q}_1 & (5.131)\\ x_2^0 &= \beta^2(\bar{q}_2 - \bar{q}_1), & (5.132) \end{aligned}$$

and taking small initial points corresponds to develop around the replica symmetric solution with small overlaps.

Consider then the following functions:

$$\begin{aligned} F(x_1, t; x_1^0, x_2^0) &\equiv x_1 - x_1^0 + \bar{q}_1(x_1^0, x_2^0)t & (5.133)\\ G(x_2, t; x_1^0, x_2^0) &\equiv x_2 - x_2^0 + \bar{q}_2(x_1^0, x_2^0)t - \bar{q}_1(x_1^0, x_2^0)t. & (5.134) \end{aligned}$$

These vanish in correspondence of the solutions of the equations of motion, in particular for all the $A_t \equiv (x_1 = 0, x_2 = 0, t > 0; x_1^0 = 0, x_2^0 = 0)$. Indicating with ∂_1 and ∂_2 the derivatives respect to the initial points x_1^0 and x_2^0, the Dini prescription about implicit functions ensures us that if the determinant

$$\frac{\partial(F, G)}{\partial(x_1^0, x_2^0)} = 1 + (\partial_2\bar{q}_1 - \partial_1\bar{q}_1 - \partial_2\bar{q}_2)t + (\partial_1\bar{q}_1\partial_2\bar{q}_2 - \partial_2\bar{q}_1\partial_1\bar{q}_2)t^2$$

is different from zero around A_t, then we can explicit x_1^0 and x_2^0 in terms of x_1, x_2 and t around A_t, which means unicity, at least in that region. Developing $\bar{q}_1$ and $\bar{q}_2$ to the first order in the initial points it comes out [49]:

$$\frac{\partial(F,G)}{\partial(x_1^0,x_2^0)} \approx (1-t)^2. \tag{5.135}$$

This tells us that we can have unicity around $x_1 = x_2 = 0$, but we should have $t = \beta^2 \neq 1$, which means that unicity is lost for sure when we are exactly at the critical temperature.

5.6 Mechanical analogy for the p-spin

We have seen how the Sherrington-Kirkpatrick model can be studied by means of a mechanical analogy, and we want to use the same approach for the p-spin glass model, with $p > 2$ and even.

We will consider here the general case, suitable for the construction of the free energy to an arbitrary number of steps in the breaking of replica symmetry, skipping afterwards to the concrete cases of replica symmetry and then to the 1-RSB solution, which is known to be the valid one below a critical temperature β_p, for these systems. The generalized "partition function", depending on the non-negative parameters t and x_a, with $a = 1, ..., K$ is defined in this case as follows

$$\tilde{Z}_N(t; x_1, ..., x_K) = \sum_{\sigma} \exp\left(\sqrt{\frac{tp!}{2N^{p-1}}} \sum_{1 \leq i_1 < ... < i_p \leq N} J_{i_1,...i_p} \sigma_{i_1} ... \sigma_{i_p} + \sum_{a=1}^{K} \sqrt{x_a} \left(\frac{p}{2} Q_a^{p-2} \right)^{1/4} \sum_{i=1}^{N} J_i^a \sigma_i \right).$$

As before, the J_i^a's are independent external random fields whose averages are denoted with $\mathbb{E}_a$, with the same distribution as the $J_{i_1...i_p}$, but note that in this case we have some new quantities multiplying the random fields, *i. e.* the $Q_a(\beta)$, that can be thought as regular functions of β with the property

$$0 \equiv Q_0(\beta) < Q_1(\beta) < ... < Q_K(\beta) < 1. \tag{5.136}$$

and which we will later identify with accumulation values for the replica overlaps.

We can use the same definitions (5.39 - 5.47) previously introduced for the recursive functions Z_a, and the generalized states ω_a and averages $\langle . \rangle_a$. Here we just rewrite the auxiliary function $\tilde{\alpha}_N(t; x_1, ..., x_K)$

$$\tilde{\alpha}(t; x_1, ..., x_K) \equiv \frac{1}{N}\mathbb{E}_0 \log Z_0 = \frac{1}{N}\mathbb{E}_0\mathbb{E}_1 \log Z_1. \tag{5.137}$$

This will be the starting point for the introduction of the action for the mechanical analogy. To this aim, we need the derivatives of this function with respect to the interpolating parameters,

$$\begin{aligned}
\partial_t \tilde{\alpha}_N(t; x_1, ..., x_K) &= \frac{1}{4}\left[1 - \sum_{a=1}^{K}(m_{a+1} - m_a)\langle q_{12}^p \rangle_a\right], \qquad (5.138)\\
\partial_a \tilde{\alpha}_N(t; x_1, ..., x_K) &= \frac{1}{2}\left(\frac{p}{2}Q_a^{p-2}(\beta)\right)^{1/2}\left[1 - \sum_{b=a}^{K}(m_{b+1} - m_b)\langle q_{12}\rangle_b\right],
\end{aligned}$$

whose computation is analogous to the one for the $p = 2$ case, described in the appendix B. Note that the derivative respect to t depends on the averages $\langle q_{12}^p \rangle_a$ instead of $\langle q_{12}^2 \rangle_a$, while the derivatives respect to the x_a's are the same as before, apart from the Q_a-dependent multiplying factors appearing in $\tilde{Z}_N$, equal to one for $p = 2$.

The action for the mechanical problem is then defined as

$$\begin{aligned}
S(t; x_1, ..., x_K) &= 2\tilde{\alpha}(t; x_1, ..., x_K) - \sum_{a=1}^{K} x_a \left(\frac{p}{2}Q_a^{p-2}(\beta)\right)^{1/2} \qquad (5.139)\\
&\quad -\frac{t}{2}\left[1 + \left(\frac{p}{2} - 1\right)\sum_{a=1}^{K}(m_{a+1} - m_a)Q_a^p(\beta)\right],
\end{aligned}$$

whose derivatives with respect to the parameters are

$$\begin{aligned}
\partial_t S(t; x_1, ..., x_K) = &-\frac{1}{2}\sum_{a=1}^{K}(m_{a+1} - m_a)\langle q_{12}^p \rangle_a\\
&-\left(\frac{p}{4} - \frac{1}{2}\right)\sum_{a=1}^{K}(m_{a+1} - m_a)Q_a^p(\beta), \qquad (5.140)\\
\partial_a S(t; x_1, ..., x_K) = &-\left(\frac{p}{2}Q_a^{p-2}(\beta)\right)^{1/2}\sum_{b=a}^{K}(m_{b+1} - m_b)\langle q_{12}\rangle_b,
\end{aligned}$$

so that it is now possible to write down, again, the Hamilton-Jacobi equation which implicitly defines the potential $V(t; x_1, ..., x_K)$, to whom our auxiliary

mechanical system is subject:

$$\partial_t S(t;\boldsymbol{x}) + \frac{1}{2}\sum_{a,b=1}^{K} \partial_a S(t;\boldsymbol{x}) \times M^{-1}_{ab} \times \partial_b S(t;\boldsymbol{x}) + V(t;\boldsymbol{x}) = 0. \tag{5.141}$$

As we are going to see, in this case the mass matrix has matrix elements depending on the Q_a. The kinetic energy is the second term in the equation above:

$$T(t;\boldsymbol{x}) = \frac{1}{2}\sum_{a,b=1}^{K} \partial_a S(t;\boldsymbol{x}) \times M^{-1}_{ab} \times \partial_b S(t;\boldsymbol{x}), \tag{5.142}$$

or, using (5.140),

$$T(t;\boldsymbol{x}) = \frac{p}{4}\sum_{c,d=1}^{K} D_{cd}(m_{c+1}-m_c)\langle q_{12}\rangle_c (m_{d+1}-m_d)\langle q_{12}\rangle_d. \tag{5.143}$$

Here we introduced for convenience the matrix D, whose elements are

$$D_{cd} \equiv \sum_{a=1}^{c}\sum_{b=1}^{d} (M^{-1})_{ab} Q_a^{(p-2)/2}(\beta) Q_b^{(p-2)/2}(\beta) \tag{5.144}$$

and, as done in the case $p = 2$, to decouple the overlaps $\langle q_{12}\rangle_c$ and $\langle q_{12}\rangle_d$ we now pose

$$D_{cd}(m_{c+1}-m_c) = \delta_{cd} Q_c^{(p-2)/2}(\beta) Q_d^{(p-2)/2}(\beta), \tag{5.145}$$

where δ_{cd} is the Kronecker delta, so that

$$T(t;\boldsymbol{x}) = \frac{p}{4}\sum_{a=1}^{K} (m_{a+1}-m_a)\langle q_{12}\rangle_a^2 Q_a^{p-2}(\beta). \tag{5.146}$$

The condition (5.145), which decouples the generalized overlap averages, determines the elements of M^{-1}. This has the same structure as in the $p = 2$ case, with all its elements vanishing except that on the diagonal and the terms whose indexes differ only by one, which are symmetric:

$$\begin{aligned}
(M^{-1})_{aa} &= \frac{1}{m_{a+1}-m_a} + \frac{1}{m_a - m_{a-1}}\left(\frac{Q_a(\beta)}{Q_{a+1}(\beta)}\right)^{p-2} \qquad a \geq 2, \\
(M^{-1})_{a,a+1} &= (M^{-1})_{a,a+1} = -\frac{1}{m_{a+1}-m_a}\left(\frac{Q_a(\beta)}{Q_{a+1}(\beta)}\right)^{(p-2)/2} \qquad a \geq 2,
\end{aligned} \tag{5.147}$$

and with

$$(M^{-1})_{11} = \frac{1}{m_2}. \tag{5.148}$$

However, note that in this case the matrix elements can depend also on the Q_a. In this case, in fact, the system energy is no longer a quadratic form in the overlap averages, and this has deep physical consequences; in particular, the phase transition is first order for $p > 2$, meaning that the order parameter changes discontinuously at the critical temperature. The matrix M^{-1} clearly admits an inverse, its determinant being non-null:

$$\det M^{-1} = \prod_{a=2}^{K+1} (m_a - m_{a-1}) \neq 0. \tag{5.149}$$

Notice that the elements of M^{-1} and consequently M depend on the overlaps q_a, differently from the case $p = 2$ [49].

The potential $V(t; \boldsymbol{x})$ is, again, directly related to the fluctuations of the overlaps:

$$V(t; \boldsymbol{x}) = \frac{1}{2} \sum_{a=1}^{K} (m_{a+1} - m_a) \left(\langle q_{12}^p \rangle_a - Q_a^p(\beta) + \frac{p}{2} \left[Q_a^p(\beta) - \langle q_{12} \rangle_a^2 Q_a^{p-2}(\beta) \right] \right). \tag{5.150}$$

5.6.1 Replica symmetric solution

Having introduced the general structure of the functions for the mechanical analogy, we can now consider the concrete cases, starting from the replica symmetric one. Instead of using $K = 2$ with $m_K = m_2 = 1$, which, as we have seen, cancels one degree of freedom of the mechanical problem, we can equivalently take a generalized coordinate less ($K = 1$), defining the auxiliary function for the replica symmetric case as

$$\tilde{\alpha}_N(t, x) = \frac{1}{N} \mathbb{E}_0 \mathbb{E}_0 \mathbb{E}_1 \log \tilde{Z}_N(t, x), \tag{5.151}$$

where $\tilde{Z}_N(t, x)$ contains only one external random field J_i^1, tuned by the parameter $x_1 \equiv x$. The p-spin free energy will be recovered, again, by taking $t = \beta^2$ and $x = 0$.

The bridge with the mechanical description is given by the action

$$S(t, x) \equiv 2\alpha(t, x) - x \left[\frac{p}{2} Q^{p-2}(\beta) \right]^{1/2} - \frac{t}{2} \left[1 + \left(\frac{p}{2} - 1 \right) Q^p(\beta) \right]. \tag{5.152}$$

whose derivatives respect to the parameters are immediately deduced by (5.140):

$$\partial_t S(t,x) = -\frac{1}{2}\langle q_{12}^p\rangle_1 - \left(\frac{p}{4}-\frac{1}{2}\right)Q^p(\beta), \tag{5.153}$$

$$\partial_x S(t,x) = -\left(\frac{p}{2}Q^{p-2}(\beta)\right)^{1/2}\langle q_{12}\rangle_1. \tag{5.154}$$

Lastly, we introduce the proper potential

$$V(t,x) \equiv \frac{1}{2}\left(\langle q_{12}^p\rangle_1 - Q^p(\beta)\right) + \frac{p}{4}\left(Q^p(\beta) - Q^{p-2}(\beta)\langle q_{12}\rangle_1^2\right). \tag{5.155}$$

With these definitions we are now able to formulate our suitable mechanical problem to solve the thermodynamics of the p-spin model. The Hamilton principal function $S(t,x)$, together with the potential $V(t,x)$ satisfies the Hamilton-Jacobi equation:

$$\partial_t S(t,x) + \frac{1}{2}(\partial_x S(t,x))^2 + V(t,x) = 0. \tag{5.156}$$

This problem can be easily solved if we neglect the potential, assuming that the variance of the generalized overlap vanishes

$$\langle q_{12}^2\rangle_1 = \langle q_{12}\rangle_1^2 \tag{5.157}$$

and we will later make the identification

$$\langle q_{12}\rangle_1 = Q(\beta). \tag{5.158}$$

These assumptions are very important as they imply, in statistical mechanics, the self-averaging property for the order parameter. Under these hypotheses, within the mechanical analogy we are developing, motion is free and the corresponding solution $\bar{S}(t,x)$ is related to the replica symmetric free energy, which is the approximation of the free energy density $f_N(\beta)$ obtained by neglecting overlap fluctuations. This phenomenology, as it is based on free-field propagation, gives straight lines as equations of motion:

$$x(t) = x_0 - \left(\frac{p}{2}Q^p(\beta)\right)^{\frac{1}{2}}t, \tag{5.159}$$

where x_0 is the starting point. When $x=0$ and $t=\beta^2$ (namely, in the point recovering the standard statistical mechanics framework) we get

$$x_0 = \beta^2\left(\frac{p}{2}Q^p(\beta)\right)^{1/2}. \tag{5.160}$$

The uniqueness of the solution can be proved as in the corresponding SK case.

The Hamilton-Jacobi equation admits both an Hamiltonian $H(t,x)$ and a Lagrangian $L(t,x)$ description, being respectively

$$H(t,x) = \frac{1}{2}\left(\frac{dS(t,x)}{dx}\right)^2 + V(t,x), \tag{5.161}$$

$$L(t,x) = \frac{1}{2}\left(\frac{dS(t,x)}{dx}\right)^2 - V(t,x). \tag{5.162}$$

As we are working in the assumption of zero potential, they both correspond to the kinetic energy only, that is given by

$$T(t,x) \equiv \frac{1}{2}\left(\partial_x S(t,x)\right)^2 = \frac{p}{4}Q^p(\beta). \tag{5.163}$$

The solution $\bar{S}(t,x)$ of the Hamilton-Jacobi problem (5.156) for $V(t,x)=0$ is obtained, as usual, by taking the function $S(t,x)$ in one point (e.g. at time $t=0$ and space $x=x_0$) and adding the Lagrangian times t (strictly speaking it should be times $(t-t_0)$ but we choose $t_0=0$).

$$\bar{S}(t,x) = S(0,x_0) + L(t,x)t = S(0,x_0) + T(t,x)t. \tag{5.164}$$

We stress again that the freedom in the assignation of the Cauchy problem plays an important role as, by choosing $t_0=0$, we are left with a one-body problem in the calculation of the starting point and all the technical difficulties are left in the propagator which, at the replica symmetric level (e.g. $V(t,x)=0$), simply reduces to the kinetic energy times time.

From (5.164) and (5.152), we obtain the corresponding expression for the auxiliary function $\bar{\alpha}(t,x)$ in the replica symmetric approximation:

$$\begin{aligned}\bar{\alpha}(t,x) =& \alpha(0,x_0) - \frac{1}{2}x_0\left(\frac{p}{2}Q^{p-2}(\beta)\right)^{1/2} + \frac{p}{8}Q^p(\beta)t + \frac{1}{2}x\,Q^{\frac{p-2}{2}}(\beta) \\ &+ \frac{t}{4}\left[1 + \left(\frac{p}{2}-1\right)Q^p(\beta)\right].\end{aligned} \tag{5.165}$$

Since the free energy for $t=0$ does not contain the interaction it may be computed straightforwardly as

$$\alpha(0,x_0) = \log 2 + \int d\mu(z)\log\cosh\left[\left(\frac{p}{2}Q^{p-2}(\beta)\right)^{\frac{1}{4}}\sqrt{x_0}z,\right] \tag{5.166}$$

and, using (5.160), we finally find the expression for the physical (RS) free energy of the p-spin model [61], obtained under the assumption of zero potential $V(t,x)$ in the mechanical analogy, encoded in the following formula (which must be extremized over the order-parameter):

$$\begin{aligned}\bar{\alpha}(\beta) = \log 2 + \int d\mu(z) \log\cosh \beta z \left(\frac{p}{2} Q^{p-1}(\beta)\right)^{\frac{1}{2}} \\ + \frac{\beta^2}{4}\left(1 + (p-1)Q^p(\beta) - pQ^{p-1}(\beta)\right).\end{aligned} \tag{5.167}$$

This represents the RS free energy, which corresponds to the true free energy only for sufficiently small values of β [31]. In fact, assuming a vanishing potential corresponds to neglect overlap fluctuations, and the overlap may be identified with a single value (RS approximation) only for high temperatures.

As for the overlap, which is related to the initial velocity of the mechanical system, we obtain the following viscous Burger equation which encodes the standard self-consistency procedure of the statistical mechanics counterpart

$$\langle q_{12}\rangle_{0,x_0} = Q(\beta) = \int d\mu(z) \tanh^2 \beta z \left(\frac{p}{2} Q^{p-1}(\beta)\right)^{1/2} \tag{5.168}$$

and corresponds to the minimum condition on the RS free energy. Note that the correct SK Replica Symmetric free energy and self-consistence equation are recovered for $p = 2$.

5.6.2 The first step of broken replica symmetry

We now extend the technique presented before to the case of one step of broken replica symmetry, which is known to broaden the correctness of the solution to values of β higher than those required by the previous approximation [61]. Following the usual mechanical approach we have learned that in order to account for breaking of this symmetry in our mechanical analogy, we have to add one degree of freedom, with its related random field, in the generalized partition function. Using results from the previous section, here we find out the expression of the free-energy corresponding to the first step of broken replica symmetry (1-RSB).

For the generalized partition function we take the (5.136) and the auxiliary function is defined as

$$\tilde{\alpha}_N(t; x_1, x_2) = \frac{1}{Nm} \mathbb{E}_0 \mathbb{E}_1 \log \mathbb{E}_2 Z_2^m, \tag{5.169}$$

where we took $m_2 \equiv m$ and we assumed

$$\begin{aligned} &Z_2 \equiv \tilde{Z}_N, \\ &0 = Q_0(\beta) < Q_1(\beta) < Q_2(\beta) < 1, \\ &0 = m_1 < m_2 < 1 = m_3. \end{aligned} \tag{5.170}$$

The action for the Hamilton-Jacobi problem $S(t, x_1, x_2)$ can be introduced as

$$\begin{aligned} S(t,x_1,x_2) =& 2\tilde{\alpha}(t,x_1,x_2) - \left(\frac{p}{2}Q_1^{p-2}(\beta)\right)^{1/2} x_1 - \left(\frac{p}{2}Q_2^{p-2}(\beta)\right)^{1/2} x_2 \\ &- \frac{t}{2}\left[1 + \left(\frac{p}{2} - 1\right)(mQ_1^p(\beta) + (1-m)Q_2^p(\beta))\right]. \end{aligned} \tag{5.171}$$

and its derivatives are

$$\begin{aligned} \partial_t S(t,x_1,x_2) =& -\frac{1}{2}m\langle q_{12}^p\rangle_1 - \frac{1}{2}(1-m)\langle q_{12}^p\rangle_2 \\ &- \left(\frac{p}{4} - \frac{1}{2}\right)(mQ_1^p(\beta) + (1-m)Q_2^p(\beta)), \\ \partial_1 S(t,x_1,x_2) =& -m\left(\frac{p}{2}Q_1^{p-2}(\beta)\right)^{1/2}\langle q_{12}\rangle_1 - (1-m)\left(\frac{p}{2}Q_2^{p-2}(\beta)\right)^{1/2}\langle q_{12}\rangle_2, \\ \partial_2 S(t,x_1,x_2) =& -(1-m)\left(\frac{p}{2}Q_2^{p-2}(\beta)\right)^{1/2}\langle q_{12}\rangle_2. \end{aligned} \tag{5.172}$$

Note that recovering the 1-RSB solution requires a mechanical problem with two generalized coordinates and we also need to introduce the mass matrix M. Choosing the inverse M^{-1} with the condition (5.145))

$$M^{-1} = \begin{bmatrix} \frac{1}{m} & -\frac{1}{m}(\frac{Q_1}{Q_2})^{(p-2)/2} \\ -\frac{1}{m}(\frac{Q_1}{Q_2})^{(p-2)/2} & \frac{1}{1-m} + \frac{1}{m}(\frac{Q_1}{Q_2})^{p-2} \end{bmatrix}$$

and so the mass matrix itself

$$M = \begin{bmatrix} m + (1-m)(\frac{Q_1}{Q_2})^{p-2} & (1-m)(\frac{Q_1}{Q_2})^{(p-2)/2} \\ (1-m)(\frac{Q_1}{Q_2})^{(p-2)/2} & 1-m \end{bmatrix},$$

we can write down explicitly the kinetic term $T(t; x_1, x_2)$ and the potential

$V(t; x_1, x_2)$ of the equivalent mechanical system:

$$\begin{aligned} T(t; x_1, x_2) &= \frac{p}{4} m \langle q_{12} \rangle_1^2 Q_1^{p-2}(\beta) + \frac{p}{4}(1-m)\langle q_{12}\rangle_2^2 Q_2^{p-2}(\beta), \\ V(t; x_1, x_2) &= \frac{1}{2} m \left[\langle q_{12}^p \rangle_1 - Q_1^p(\beta) + \frac{p}{2}(Q_1^p(\beta) - \langle q_{12}\rangle_1^2 Q_1^{p-2}(\beta)) \right] \\ &\quad + \frac{1}{2}(1-m)\left[\langle q_{12}^p \rangle_2 - Q_2^p(\beta) + \frac{p}{2}(Q_2^p(\beta) - \langle q_{12}\rangle_2^2 Q_2^{p-2}(\beta)) \right]. \end{aligned} \tag{5.173}$$

We want to exploit the mechanical analogy between the 1-RSB statistical mechanics of the p-spin-glass and the equivalent mechanical system whose generalized coordinates satisfy the equations of motion

$$\begin{aligned} x_1(t) &= x_1^0 + v_1(t; x_1, x_2)\, t, \\ x_2(t) &= x_2^0 + v_2(t; x_1, x_2)\, t. \end{aligned} \tag{5.174}$$

The corresponding velocities are defined as

$$\begin{aligned} v_1(t; x_1, x_2) &\equiv \sum_{a=1}^{2} (M^{-1})_{1a} \partial_a S(t; x_1, x_2) = -\left(\frac{p}{2} Q_1^{p-2}(\beta) \right)^{1/2} \langle q_{12} \rangle_1 \\ v_2(t; x_1, x_2) &\equiv \sum_{a=1}^{2} (M^{-1})_{2a} \partial_a S(t; x_1, x_2) \\ &= \left(\frac{p}{2} \right)^{1/2} \frac{Q_1^{p-2}(\beta)}{Q_2^{(p-2)/2}(\beta)} \langle q_{12} \rangle_1 - \left(\frac{p}{2} \right)^{1/2} Q_2^{(p-2)/2}(\beta) \langle q_{12} \rangle_2. \end{aligned} \tag{5.175}$$

As discussed before, we are interested in studying the free motion, i.e. the motion in absence of potential, and deduce the physical free-energy from the solution of the Hamilton-Jacobi equation

$$\partial_t S(t; x_1, x_2) + \frac{1}{2} \sum_{a,b=1}^{K} \partial_a S(t; x_1, x_2) \times M_{ab}^{-1} \times \partial_b S(t; x_1, x_2). \tag{5.176}$$

We stress that here the potential is related to a more complex kind of fluctuations of the overlap as we are requiring much more than the simple self-averaging: Physically we can think at each step of RSB as a refinement, a zoom, in the analysis of the free energy landscape, that allows to see rugged valleys otherwise averaged out and we are asking for adiabatic thermalization within each of these (sub)-valleys ("sub" w.r.t. the macro-ones already

encoded in the RS-approximation). Coherently, a sufficient condition for a vanishing 1-RSB potential is an overlap variance inside the bracket denoted with $\langle . \rangle_a$ equal to zero and the identification of the averages of the overlap with the functions $Q_a(\beta)$:

$$\langle q_{12}^2 \rangle_a = \langle q_{12} \rangle_a^2 = Q_a^2(\beta), \ a = 1, 2. \tag{5.177}$$

In the absence of a potential, the velocities (and so the kinetic energy) are conserved quantities and we can then consider their values at the initial instant $t = 0$, in perfect analogy with the RS case:

$$\begin{aligned} \bar{q_1} \equiv \langle q_{12} \rangle_1 (0; x_1^0, x_2^0) &= \int d\mu(z_1) \left[\frac{\int d\mu(z_2) \cosh^m \theta(z_1, z_2) \tanh \theta(z_1, z_2)}{\int d\mu(z_2) \cosh^m \Theta(z_1, z_2)} \right]^2, \\ \bar{q_2} \equiv \langle q_{12} \rangle_2 (0; x_1^0, x_2^0) &= \int d\mu(z_1) \frac{\int d\mu(z_2) \cosh^m \theta(z_1, z_2) \tanh^2 \theta(z_1, z_2)}{\int d\mu(z_2) \cosh^m \Theta(z_1, z_2)}, \\ \Theta(z_1, z_2) &= \sqrt{x_1^0} \left(\frac{p}{2} Q_1^{p-2} \right)^{1/4} z_1 + \sqrt{x_2^0} \left(\frac{p}{2} Q_2^{p-2} \right)^{1/4} z_2. \end{aligned} \tag{5.178}$$

When considering the statistical-physics point $t = \beta^2, x_1 = x_2 = 0$, the equations of motion (5.174) give This computation, as in the SK case, essentially leads us to the 1-RSB self-consistence equations for the overlaps, In fact, for this values of time and coordinates, and with the condition (5.177)

$$\begin{aligned} x_1^0 &= \beta^2 \left(\frac{p}{2} Q_1^p(\beta) \right)^{1/2}, \\ x_2^0 &= \beta^2 \left(\frac{p}{2} \right)^{1/2} Q_2^{\frac{p}{2}}(\beta) - \beta^2 \left(\frac{p}{2} \right)^{1/2} \frac{Q_1^{p-1}(\beta)}{Q_2^{\frac{p-2}{2}}(\beta)}, \end{aligned} \tag{5.179}$$

and in the self-consistence equation appears the quantity

$$\Theta(z_1, z_2) = \beta \left(\frac{p}{2} \right)^{1/2} z_1 Q_1^{\frac{p-1}{2}}(\beta) + \beta \left(\frac{p}{2} \right)^{1/2} z_2 \sqrt{Q_2^{p-1}(\beta) - Q_1^{p-1}(\beta)}. \tag{5.180}$$

In the second term of the r.h.s. of equation (5.180) the two overlaps are decoupled, and in the limit $p \to 2$ we get the correct 1-RSB self-consistence equation for the SK model too. To compute the free-energy we use the usual recipe: as we assume that the mechanical potential is zero, we write (easily) the solution for the Hamilton-Jacobi problem and then we evaluate it in the point $t = \beta^2, x_a = 0$. First of all, we need the free-energy at the initial instant, which is straightforward to obtain, since the spins are decoupled

$$\tilde{\alpha}(0; x_1^0, x_2^0) = \log 2 + \frac{1}{m} \int d\mu(z_1) \log \int d\mu(z_2) \cosh^m \Theta(z_1, z_2), \tag{5.181}$$

with $\Theta(z_1, z_2)$ given by (5.180). The Hamilton function which is solution of (5.176) for a vanishing potential $V \equiv 0$ is simply given by the function at the initial instant plus the integral of the Lagrangian, (which corresponds to the kinetic energy only), over time

$$S(t; x_1, x_2) = S(0; x_1^0, x_2^0) + \int_0^t dsT(s; x_1, x_2) = S(0; x_1^0, x_2^0) + T(0; x_1^0, x_2^0)t, \tag{5.182}$$

using the fact that the kinetic energy is a conserved quantity. In this way we find

$$\begin{aligned} S(t; x_1, x_2) =& 2\tilde{\alpha}(0; x_1^0, x_2^0) - \left(\frac{p}{2}Q_1^{p-2}(\beta)\right)^{1/2} x_1^0 - \left(\frac{p}{2}Q_2^{p-2}(\beta)\right)^{1/4} x_2^0 \\ &+ \frac{tp}{4}Q_1^p(\beta) + \frac{tp}{4}(1-m)Q_2^p(\beta), \end{aligned} \tag{5.183}$$

and from this, the auxiliary function $\tilde{\alpha}(t; x_1, x_2)$

$$\begin{aligned} \tilde{\alpha}(t; x_1, x_2) =& \frac{1}{2}S(t; x_1, x_2) + \frac{1}{2}\left(\frac{p}{2}Q_1^{p-2}(\beta)\right)^{1/2} x_1 + \frac{1}{2}\left(\frac{p}{2}Q_2^{p-2}(\beta)\right)^{1/2} x_2) \\ &+ \frac{t}{4}\left[1 + \left(\frac{p}{2} - 1\right)\left(mQ_1^p(\beta) + (1-m)Q_2^p(\beta)\right)\right]. \end{aligned} \tag{5.184}$$

Lastly, the physical free-energy free energy for the p-spin glass model corresponding to the 1-RSB is easily computed by taking $t = \beta^2, x_1 = x_2 = 0$:

$$\begin{aligned} \alpha(\beta) =& \log 2 \\ &+ \frac{1}{m}\int d\mu(z_1) \log \int d\mu(z_2) \cosh^m\left(\beta z_1 Q_1^{(p-1)/2}(\beta) + \beta z_2 \sqrt{Q_2^{p-1}(\beta) - Q_1^{p-1}(\beta)}\right) \\ &+ \frac{\beta^2}{4}\left[1 + (p-1)mQ_1^p(\beta) + (p-1)(1-m)Q_2^p(\beta) - pQ_1^{p-1}(\beta) - pQ_2^{p-1}(\beta)\right]. \end{aligned} \tag{5.185}$$

We skip here any digression on the physics behind these formulas as these are in perfect agreement with the original investigation by Gardner [61] and by Gross and Mezard [60], so to highlight only the technique based on the mechanical analogy.

5.6.3 Conservation laws: Polynomial identities

We conclude this section with an analysis of the conserved quantities deriving from the internal symmetries of the theory. We will approach them as Nöther

integrals within the Hamilton-Jacobi formalism. Let us restate the Hamilton-Jacobi equation

$$\partial_t S(t,\boldsymbol{x}) + H(\nabla_{\boldsymbol{x}} S(t,\boldsymbol{x}), t, \boldsymbol{x}) = 0$$

where the Hamiltonian function reads off as

$$H(\nabla_{\boldsymbol{x}} S(t,\boldsymbol{x}), t, \boldsymbol{x}) = T(t,\boldsymbol{x}) + V(t,\boldsymbol{x}). \tag{5.186}$$

Hamilton equations are nothing but characteristics given by:

$$\left\{ \begin{array}{rcl} \dot{\boldsymbol{x}} & = & v(t,\boldsymbol{x}) \\ \dot{t} & = & 1 \\ \dot{P} & = & -v(t,\boldsymbol{x})\nabla_{\boldsymbol{x}} v(t,\boldsymbol{x}) - \nabla_{\boldsymbol{x}} V(t,\boldsymbol{x}) \\ \dot{E} & = & -v(t,\boldsymbol{x})\nabla_{\boldsymbol{x}} \left(\partial_t S(t,\boldsymbol{x})\right) - \partial_t V(t,\boldsymbol{x}), \end{array} \right. \tag{5.187}$$

where we named P our velocity, *i.e.* the velocity field coincides with the generalized time dependent momentum. The latter two equations display space-time translational invariance and express the conservation laws for momentum and energy for our system, further, these can be written in form of streaming equations as

$$\left\{ \begin{array}{rcl} DP(t,\boldsymbol{x}) & = & -\nabla_{\boldsymbol{x}} V(t,\boldsymbol{x}) \\ D\partial_t S(t,\boldsymbol{x}) & = & -\partial_t V(t,\boldsymbol{x}). \end{array} \right.$$

Since we are interested in evaluating the free motion, bearing in mind that $v(\boldsymbol{x},t) = -\langle q_{12}^{p/2}\rangle$ and $\partial_t S(\boldsymbol{x},t) = -\frac{1}{2}\langle q_{12}^{p}\rangle$, so $D = \partial_t - \langle q^{p/2}\rangle\nabla_x$, we conclude

$$\left\{ \begin{array}{rcl} D\langle q^{p/2}\rangle & = & 0, \\ D\langle q^{p}\rangle & = & 0, \end{array} \right. \tag{5.188}$$

i.e.

$$\left\{ \begin{array}{rcl} \langle q_{12}^{p}\rangle - 4\langle q_{12}^{p/2} q_{13}^{p/2}\rangle + 3\langle q_{12}^{p/2} q_{34}^{p/2}\rangle & = & 0, \\ \langle q_{12}^{2p}\rangle - 4\langle q_{12}^{p} q_{23}^{p}\rangle + 3\langle q_{12}^{p} q_{34}^{p}\rangle & = & 0. \end{array} \right. \tag{5.189}$$

The orbits of the Nöther groups of the theory, thus, coincide with the streaming lines of the Hamilton-Jacobi Hamiltonian, and conservation laws along these lines give well known identities in the statistical mechanics of the model often known as Ghirlanda-Guerra relations and Aizenman-Contucci identities [55, 69].

5.7 Conclusions

In this part of the work we analyzed some of the recent techniques introduced for the study of spin glasses without resorting to the replica method, which however remains essential in this field. Alternative methods, nonetheless, have been proved to be essential to give a more firm ground to the previous results and to give new insights and fruitful ideas for an analysis of complex systems.

We have showed how mean-field spin glass related issues can be attacked by coupling the original system with a suitable auxiliary system, where a series of external random fields are introduced to mimic the random two-body interactions among spins, and the partition function has the typical nested structure of the solution of the Parisi equation. The number of external fields introduced is directly related to the number of steps of broken replica symmetry for the free energy that one chooses to take in account. The partition function for this auxiliary system contains some parameters, tuning the intensity of the two-body interactions and of the external random fields, and evaluating the parameters in suitable points one gets the free energy of the original system. As for the auxiliary free energy, we have seen that it can be computed by resorting to a mechanical analogy, where it plays the role of the action in a Hamilton-Jacobi equation. The potential in this mechanical problem is related to some fluctuations of the average overlap, neglecting which one easily finds the solution of the HJ equation, and thus the auxiliary free energy. Enlarging the degrees of freedom, that is, the number of external random fields, allows one to get more and more refined approximations of the free energy in the spin glass model. As for the p-spin glass, we have seen that in this generalized case the random external field mimicking the two body interaction need to be modulated by proper functions which depend on the overlap, but also in this case one is able to reproduce the expected free energy.

Similar methods bases on interpolation, as we have seen for the existence of the thermodynamic limit, have proven to be essential in the recent developments of the study of spin glasses, and can be extended more in general to approach a larger class of complex system models (see for instance [70] [71]).

Appendix A

Fraction saturation for anti-cooperative systems

In this appendix we outline in details the calculations required to obtain explicit expressions for $\langle m_A \rangle$ and $\langle m_B \rangle$, which return the total fraction saturation as a function of the ligand concentration as $\langle \theta \rangle = 1/2 + \langle m_A + m_B \rangle / 4$, namely the binding isotherm. The energy function which defines the corresponding magnetic model is the sum of the energies due to the interaction among spins and with the external field:

$$H(\sigma; \xi, h) = \frac{J_0}{NP} \sum_{i \in A,\, j \in B} \sum_{\mu=1}^{P} (\xi_i^\mu \xi_j^\mu + \bar{\xi}_i^\mu \bar{\xi}_j^\mu) \sigma_i \sigma_j - h \sum_{i=1}^{N} \sigma_i. \tag{A.1}$$

Let us introduce the pattern overlap $q_\mu^A(\sigma^A)$ and the magnetization $m_A(\sigma^A)$ for the subsystem A as

$$q_\mu^A(\sigma^A) = \frac{1}{N_A} \sum_{i \in A} \xi_i^\mu \sigma_i, \quad m_A(\sigma^A) = \frac{1}{N_A} \sum_{i \in A} \sigma_i, \tag{A.2}$$

which respectively measure the resemblance between a microscopic state σ^A and one particular pattern $\xi^\mu_{i=1\ldots N}$ and the net number of active elements. Note that the quantity $q_\mu^A(\sigma^A)$ can be also interpreted as the magnetization of a subgraph of the subsystem A specified by the non-null bits of the string ξ_i^μ, that is a sort of diluted magnetization We similarly define the quantities $q_\mu^B(\sigma^B)$ and $m_B(\sigma^B)$ for the subsystem B. Then we may rewrite the energy

function in terms of these quantities as

$$
\begin{aligned}
H(\xi;\sigma,h) = J_0\frac{N_A N_B}{N}\Bigg[&\frac{2}{P}\sum_{\mu=1}^{P} q_\mu^A(\sigma^A)q_\mu^B(\sigma^B) + m_A(\sigma^A)m_B(\sigma^B) \\
&-\frac{1}{P}\sum_{\mu=1}^{P} q_\mu^A(\sigma^A)m_B(\sigma^B) - \frac{1}{P}\sum_{\mu=1}^{P} q_\mu^B(\sigma^B)m_A(\sigma^A)\Bigg] \\
&- h\left(N_A m_A(\sigma^A) + N_B m_B(\sigma^B)\right).
\end{aligned}
\tag{A.3}
$$

The first term, in square brackets, is clearly large when the magnetizations (and pattern overlaps) of the two systems have the same sign, while the interaction with the external field tends to align all the spins with the sign of h. Due to this competition, we expect that the system goes trough different phases by varying the ratio J/h (the temperature in this corresponding spin model is kept fixed and equal to one), where with J we mean the coupling average value $J = J_0(1+a^2)/4$ (the temperature in this corresponding spin model is kept fixed and equal to one): For small external field (or strong coupling), the leading contribution to the free energy comes from the coupling term J and the system behaves anti-ferromagnetically, hence with different values for the magnetizations of the two subsystems; on the other hand, for strong external field (or small enough couplings), we expect the these magnetizations to be equal and the system behaves as a paramagnet (in a field).

To describe the whole system it is convenient to introduce the global pattern overlap q_μ and the global magnetization m:

$$
q_\mu(\sigma) = \frac{N_A}{N}q_\mu^A(\sigma^A) + \frac{N_B}{N}q_\mu^B(\sigma^B), \tag{A.4}
$$

$$
m(\sigma) = \frac{N_A}{N}m_A(\sigma^A) + \frac{N_B}{N}m_B(\sigma^B). \tag{A.5}
$$

Moreover, we need observables able to describe an antiferromagnetic phase: To this task we introduce the staggered overlap p_μ and staggered magnetization n:

$$
p_\mu(\sigma) = \frac{N_A}{N}q_\mu^A(\sigma^A) - \frac{N_B}{N}q_\mu^B(\sigma^B), \tag{A.6}
$$

$$
n(\sigma) = \frac{N_A}{N}m_A(\sigma^A) - \frac{N_B}{N}m_B(\sigma^B). \tag{A.7}
$$

In terms of these quantities, the energy is

$$H(\sigma;\xi,h) = NJ_0[\frac{1}{2P}\sum_{\mu=1}^{P}\left(q_\mu^2(\sigma)-p_\mu^2(\sigma)\right)+\frac{1}{4}(m^2(\sigma)-n^2(\sigma))$$
$$-\frac{1}{2P}\sum_{\mu=1}^{P}q_\mu(\sigma)m(\sigma)-\frac{1}{2P}\sum_{\mu=1}^{P}p_\mu(\sigma)n(\sigma)]-Nhm(\sigma). \tag{A.8}$$

The quenched free energy $F(J_0,h)$ and the partition function $Z(\xi;J_0,h)$ are introduced as follows:

$$F(J_0,h) = -\lim_{N\to\infty}\frac{1}{N}\mathbb{E}\log Z(\xi;J_0,h) = -\lim_{N\to\infty}\frac{1}{N}\mathbb{E}\log\sum_{\sigma}e^{-H(\sigma;\xi,h)}. \tag{A.9}$$

Since the energy depends on σ only through the quantities (A.4,39,A.6,41) we can choose these as order parameters and define the so-called constrained (with respect to the particular values of q,p,m,n, see also [72]) partition function $Z(\mathbf{q},\mathbf{p},m,n)$ as

$$\begin{aligned} Z &= \int d\mathbf{q}\int d\mathbf{p}\int dm\int dn\; Z(\mathbf{q},\mathbf{p},m,n) \\ &= \int d\mathbf{q}\int d\mathbf{p}\int dm\int dn\; D(\mathbf{q},\mathbf{p},m,n)\exp\left[-N\mathcal{E}(\boldsymbol{q},\boldsymbol{p},m,n)\right] \end{aligned} \tag{A.10}$$

where

$$\begin{aligned} \mathcal{E}(\boldsymbol{q},\boldsymbol{p},m,n) =& J_0\left[\frac{1}{2P}\sum_{\mu=1}^{P}\left(q_\mu^2-p_\mu^2\right)+\frac{1}{4}(m^2-n^2)\right. \\ &\left.-\frac{1}{2P}\sum_{\mu=1}^{P}q_\mu m-\frac{1}{2P}\sum_{\mu=1}^{P}p_\mu n\right]-hm. \end{aligned} \tag{A.11}$$

and $D(\boldsymbol{q},\boldsymbol{p},m,n)$ is the density of states:

$$D(\boldsymbol{q},\boldsymbol{p},m,n) = \sum_{\sigma}\delta(m-m(\sigma))\delta(n-n(\sigma))\prod_{\mu,\nu=1}^{P}\delta(q_\mu-q_\mu(\sigma))\delta(p_\nu-p_\nu(\sigma)). \tag{A.12}$$

Using the integral representation for the δ and summing over σ this can be written as

$$\begin{aligned} D(\boldsymbol{q},\boldsymbol{p},m,n) = &\left(\frac{N}{2\pi}\right)^{2(P+1)}\int_{-\infty}^{+\infty}d\boldsymbol{x}\int_{-\infty}^{+\infty}d\boldsymbol{y}\int_{-\infty}^{+\infty}dz\int_{-\infty}^{+\infty}dw \\ &\times\exp[Ns(\boldsymbol{q},\boldsymbol{p},m,n,\boldsymbol{x},\boldsymbol{y},z,w)] \end{aligned} \tag{A.13}$$

where s, the constrained entropy, reads as

$$s(\boldsymbol{q},\boldsymbol{p},m,n;\boldsymbol{x},\boldsymbol{y},z,w) = i\left[\boldsymbol{x}\cdot\boldsymbol{q}+\boldsymbol{y}\cdot\boldsymbol{p}+zm+wn \right. \\ \left. +\frac{1}{N}\sum_{i=1}^{N}\log 2\cos\left(\sum_{\mu=1}^{P}\xi_i^\mu\left(x_\mu+\epsilon_i y_\mu+z+\epsilon_i w\right)\right)\right]. \tag{A.14}$$

Here ϵ_i is a function of the site which takes the value $+1$ if $i \in A$ and -1 for $i \in B$. The constrained entropy $s(\boldsymbol{q},\boldsymbol{p},m,n)$ in eq.(A.13), namely the log-density of states, is multiplied by a linearly diverging term (N), hence it can be evaluated by saddle point integration, taking the extremum with respect to the $2(P+1)$ parameters $\boldsymbol{x},\boldsymbol{y},z,w$, just as we have seen in Sec. 2.2.2. Then, finding the minimum of the constrained free energy with respect to the order parameters $\boldsymbol{q},\boldsymbol{p},m,n$ is the last missing point:

$$f(\boldsymbol{q},\boldsymbol{p},m,n) = \mathcal{E}(\boldsymbol{q},\boldsymbol{p},m,n) - s(\boldsymbol{q},\boldsymbol{p},m,n). \tag{A.15}$$

This expression accounts for the free energy per spin of the system, in the thermodynamic limit and its extremization with respect to $\boldsymbol{q},\boldsymbol{p},m,n$ has the following system of self-consistence equations as outcome:

$$q_\mu = \frac{1}{N}\sum_i \xi_i^\mu \tanh\theta(\boldsymbol{q},\boldsymbol{p},m,n), \tag{A.16}$$

$$p_\mu = \frac{1}{N}\sum_i \epsilon_i\xi_i^\mu \tanh\theta(\boldsymbol{q},\boldsymbol{p},m,n), \tag{A.17}$$

$$m = \frac{1}{N}\sum_i \tanh\theta(\boldsymbol{q},\boldsymbol{p},m,n), \tag{A.18}$$

$$n = \frac{1}{N}\sum_i \epsilon_i \tanh\theta(\boldsymbol{q},\boldsymbol{p},m,n), \tag{A.19}$$

with

$$\theta(\boldsymbol{q},\boldsymbol{p},m,n) = -J_0\frac{m-\epsilon_i n}{2}\left(1-\frac{1}{P}\sum_{\nu=1}^{P}\xi_i^\nu\right)+\frac{J_0}{P}\sum_{\nu=1}^{P}\frac{q_\nu-\epsilon_i p_\nu}{2}\left(1-2\xi_i^\nu\right)+h. \tag{A.20}$$

From these equations, obtaining the self-consistencies inside each subsystem

is then straightforward and gives

$$q_\mu^A = \frac{1}{N_A}\sum_{i\in A}\xi_i^\mu \tanh\left(-J_0\frac{N_B}{N}m_B\frac{\sum_\nu \bar{\xi}_i^\nu}{P} + J_0\frac{N_B}{N}\frac{\sum_\nu q_\nu^B\,(1-2\xi_i^\nu)}{P} + h\right), \quad \text{(A.21)}$$

$$m_A = \frac{1}{N_A}\sum_{i\in A}\tanh\left(-J_0\frac{N_B}{N}m_B\frac{\sum_\nu \bar{\xi}_i^\nu}{P} + J_0\frac{N_B}{N}\frac{\sum_\nu q_\nu^B\,(1-2\xi_i^\nu)}{P} + h\right), \quad \text{(A.22)}$$

with the corresponding equations for $\boldsymbol{q}^B$ and m_B which are easily obtained by exchanging A and B. Looking at equation (A.22), we notice that the magnetization is a sum of terms which may be interpreted as the (thermal) average of the local magnetizations $\omega(\sigma_i)$, so that

$$\omega(\sigma_i) = \tanh\left(-J_0\frac{N_B}{N}m_B\frac{\sum_\nu \bar{\xi}_i^\nu}{P} + J_0\frac{N_B}{N}\frac{\sum_\nu q_\nu^B\,(1-2\xi_i^\nu)}{P} + h\right) \quad \text{(A.23)}$$

for $i \in A$. The effective field acting on the spin, corresponding to the arguments of the hyperbolic tangent, contain two terms, besides the external field. The first contribution is given by the opposite magnetization of the other subsytem, weighted by a proper factor which is proportional to the fraction of zero bits in the string associated with the spin i, and the second term contains the correlations between the string ξ_i and the strings of the interacting spins, encoded in q_ν.

In the particular cases $a = 1$ and $a = -1$, the interaction is the same (maximum) for all the couples of spins, and there is no randomness. The only difference is that in the first case the pattern overlaps correspond all to the magnetization, while in the second they all vanish. Clearly we have now the mean-field equations for a bipartite anti-ferromagnetic system:

$$m_A = \tanh\left(-J_0\frac{N_B}{N}m_B + h\right), \quad \text{(A.24)}$$

$$m_B = \tanh\left(-J_0\frac{N_A}{N}m_A + h\right). \quad \text{(A.25)}$$

To obtain the average pattern overlap $\langle q_\mu^A\rangle$ and average magnetization $\langle m_A\rangle$, we first observe that, as all the bits are equivalent, the average pattern overlaps are all equivalent and we may drop the index μ, so that $\langle q_\mu^A\rangle = \langle q^A\rangle$.

Then, looking at the arguments of equations (A.21, A.22) - if we approximate q_μ^B and m_B with the averages over the disorder of these quantities- it is clear that they only depend on the bits through the number k of non-zero entries in each string, hence are evaluated over the following binomial distribution:

$$\begin{aligned}\langle q^A\rangle &= \frac{1+a}{2}\sum_{k=0}^{P-1}\binom{P-1}{k}\left(\frac{1+a}{2}\right)^k\left(\frac{1-a}{2}\right)^{P-1-k} \\ &\quad \tanh\left(-J_0\frac{N_B}{N}\frac{P-1-k}{P}\langle m_B\rangle + J_0\frac{N_B}{N}\frac{P-2(k+1)}{P}\langle q^B\rangle + h\right) \qquad \text{(A.26)}\\ \langle m_A\rangle &= \sum_{k=0}^{P-1}\binom{P}{k}\left(\frac{1+a}{2}\right)^k\left(\frac{1-a}{2}\right)^{P-k} \\ &\quad \tanh\left(-J_0\frac{N_B}{N}\frac{P-k}{P}\langle m_B\rangle + J_0\frac{N_B}{N}\frac{P-2k}{P}\langle q^B\rangle + h\right). \qquad \text{(A.27)}\end{aligned}$$

For P (and $P(1+a)/2$) large enough, k behaves as a Gaussian random variable, and we can get explicitly

$$\begin{aligned}\langle q^A\rangle &= \frac{1+a}{2}\langle m_A\rangle \qquad \text{(A.28)}\\ \langle m_A\rangle &= \int_{-\infty}^{+\infty}\frac{dx}{\sqrt{2\pi\sigma^2}}e^{-\frac{(x-x_0)^2}{2\sigma^2}}\tanh\left(-J_0\frac{N_B}{N}\left(\frac{1-a}{2}+az\right)\langle m_B\rangle + h\right)\end{aligned}$$

with

$$z_0 = \frac{1+a}{2}, \qquad \sigma^2 = \frac{1-a^2}{2P}. \qquad \text{(A.29)}$$

Convergence by central limit theorem is quite fast and we can approximate z with its mean value to obtain finally

$$\langle m_A\rangle = \tanh\left(-J_0\frac{N_B}{N}\frac{1+a^2}{2}\langle m_B\rangle + h\right), \qquad \text{(A.30)}$$

and equivalently for $\langle m_B\rangle$. These two observables can then be averaged to get $\theta(\alpha; J)$, which is the binding isotherm.

Appendix B

Derivatives of $\tilde{\alpha}_N$ with respect to t and x_a

We show here the derivation of expressions (5.138, 5.139). The corresponding formulas for the Sherrington-Kirkpatrick model can be computed in the same way. Let's start with the first one:

$$\partial_t \tilde{\alpha}_N = \frac{1}{N} \mathbb{E}_0 Z_0^{-1} \partial_t Z_0 \tag{B.1}$$

It's easy to see that

$$Z_a^{-1} \partial_t Z_a = \mathbb{E}_{a+1} f_{a+1} Z_{a+1}^{-1} \partial_t Z_{a+1} \tag{B.2}$$

so that

$$\mathbb{E}_0 Z_0^{-1} \partial_t Z_0 = \mathbb{E}_0 \mathbb{E}_1 ... \mathbb{E}_K f_1 ... f_K Z_K^{-1} \partial_t Z_K \equiv \mathbb{E} f_1 ... f_K Z_K^{-1} \partial_t Z_K \tag{B.3}$$

and, remembering that $Z_K \equiv \tilde{Z}_N$,

$$\mathbb{E}_0 Z_0^{-1} \partial_t Z_0 = \frac{1}{2\sqrt{t}} \sqrt{\frac{tp!}{2N}} \sum_{1 \le i_1 < ... < i_p \le N} \mathbb{E}(f_1 ... f_K J_{i_1 ... i_p} \tilde{\omega}(\sigma_{i_1} ... \sigma_{i_p})). \tag{B.4}$$

Integrating by parts the $J_{i_1 ... i_p}$ inside the expectation becomes a derivative:

$$\frac{1}{2\sqrt{t}} \sqrt{\frac{tp!}{2N}} \sum_{1 \le i_1 < ... < i_p \le N} \left[\sum_{a=2}^{K} \mathbb{E}(f_1 ... \partial_{J_{i_1 ... i_p}} f_a ... f_K \tilde{\omega}(\sigma_{i_1} ... \sigma_{i_p})) \right.$$
$$\left. + \mathbb{E}(f_1 ... f_K \partial_{J_{i_1 ... i_p}} \tilde{\omega}(\sigma_{i_1} ... \sigma_{i_p})) \right].$$

We now proceed by computing separately the two addends in the square brackets. for the second term we easily find

$$\partial_{J_{i_1\dots i_p}}\tilde{\omega}(\sigma_{i_1}...\sigma_{i_p})) = \sqrt{\frac{tp!}{2N^{p-1}}}(1-\tilde{\omega}^2(\sigma_{i_1}...\sigma_{i_p})) \tag{B.5}$$

while for the first term we have

$$\partial J_{i_1\dots i_p} f_a = m_a f_a Z_a^{-1}\partial J_{i_1\dots i_p} Z_a - m_a f_a E_a(f_a Z_a^{-1}\partial J_{i_1\dots i_p} Z_a). \tag{B.6}$$

Now, using the analogous of (B.2), one has

$$\begin{aligned} Z_a^{-1}\partial J_{i_1\dots i_p} Z_a &= \mathbb{E}_{a+1}...\mathbb{E}_K(f_{a+1}...f_K Z_K^{-1}\partial J_{i_1\dots i_p} Z_K) &\text{(B.7)}\\ &= \sqrt{\frac{tp!}{2N^{p-1}}}\omega_a(\sigma_{i_1}...\sigma_{i_p}) &\text{(B.8)}\end{aligned}$$

and then for $a \geq 2$ (remind that $f_1 = 1$ so its derivative is zero)

$$\partial J_{i_1\dots i_p} f_a = \sqrt{\frac{tp!}{2N^{p-1}}} m_a f_a(\omega_a(\sigma_{i_1}...\sigma_{i_p}) - \omega_{a-1}(\sigma_{i_1}...\sigma_{i_p})). \tag{B.9}$$

Putting together the terms computed we find

$$\begin{aligned}&\mathbb{E}_0 Z_0^{-1}\partial_t Z_0 = \\ &= \frac{1}{4}\frac{p!}{N^{p-1}}\sum_{1\leq i_1<\dots<i_p\leq N}\Bigg[\sum_{a=2}^{K}\mathbb{E}_0...\mathbb{E}_a(f_1...f_a\omega_a(\sigma_{i_1}...\sigma_{i_p})f_{a+1}...f_K\tilde{\omega}(\sigma_{i_1}...\sigma_{i_p}) \\ &\qquad -\sum_{a=2}^{K}\mathbb{E}_0...\mathbb{E}_a(f_1...f_a\omega_a(\sigma_{i_1}...\sigma_{i_p})f_{a+1}...f_K\tilde{\omega}(\sigma_{i_1}...\sigma_{i_p}) \\ &\qquad\qquad + 1 - \mathbb{E}_0...\mathbb{E}_K(f_1...f_K\tilde{\omega}^2(\sigma_{i_1}...\sigma_{i_p}))\Bigg]\end{aligned} \tag{B.10}$$

and noting that in the thermodynamic limit $p!\sum_{i_1<\dots<i_p} \sim \sum_{i_1,\dots,i_p}$ we have

$$\partial_t\tilde{\alpha}_N = \frac{1}{4}\Bigg[\sum_{a=1}^{K} m_a(\langle q^p_{\sigma\sigma'}\rangle_a - \langle q^p_{\sigma\sigma'}\rangle_{a-1}) + 1 - \langle q^p_{\sigma\sigma'}\rangle_K\Bigg] \tag{B.11}$$

from which the derivation of (5.138) is straightforward.

Let's now compute the derivatives of the free energy respect to the "spatial" parameters:

$$\begin{aligned}\partial_a\tilde{\alpha}_N &= \frac{1}{N}\mathbb{E}_0 Z_0^{-1}\partial_a Z_0 \\ &= \frac{1}{N}\mathbb{E}(f_1...f_K Z_K^{-1}\partial_a Z_K) \\ &= \frac{1}{N}\frac{1}{2\sqrt{x_a}}q^{\frac{p-2}{4}}\mathbb{E}(f_1...f_K\sum_{i=1}^{N}J_i^a\tilde{\omega}(\sigma_i))\end{aligned} \tag{B.12}$$

where we used the analogous of (B.3). Integrating by parts this becomes

$$\begin{aligned}\partial_a\tilde{\alpha}_N =&\frac{1}{N}\mathbb{E}_0\sum_i\Bigg[\mathbb{E}_1...\mathbb{E}_K(\sum_{b=2}^{K}f_1...\partial_{J_i^a}f_b...f_K\tilde{\omega}(\sigma_i)) \\ &+\mathbb{E}_1...\mathbb{E}_K(f_1...f_K\partial_{J_i^a}\tilde{\omega}(\sigma_i))\Bigg].\end{aligned} \tag{B.13}$$

The derivatives of the state and of f_b respect to the random fields are respectively given by

$$\begin{aligned}\partial_{J_i^a}\tilde{\omega}(\sigma_i) &= \sqrt{x_a}q_a^{\frac{p-2}{4}}(1-\tilde{\omega}^2(\sigma_i)) \\ \partial_{J_i^a}f_b &= \begin{cases} m_b f_b(Z_b^{-1}\partial_{J_i^a}Z_b - E_b f_b Z_b^{-1}\partial_{J_i^a}Z_b) & \text{if } a<b \\ m_b f_b Z_b^{-1}\partial_{J_i^a}Z_b & \text{if } a=b \\ 0 & \text{if } a>b. \end{cases}\end{aligned} \tag{B.14}$$

Using again the iterative derivation formula we have

$$\begin{aligned}Z_b^{-1}\partial_{J_i^a}Z_b &= E_{b+1}(f_{b+1}Z_{b+1}^{-1}\partial_{J_i^a}Z_{b+1}) \\ &= E_{b+1}...E_K(f_{b+1}...f_K Z_K^{-1}\partial_{J_i^a}Z_K) \\ &= \sqrt{x_a}q_a^{\frac{p-2}{4}}E_{b+1}...E_K(f_{b+1}...f_K\tilde{\omega}(\sigma_i)) \\ &= \sqrt{x_a}q_a^{\frac{p-2}{4}}\omega_b(\sigma_i)\end{aligned} \tag{B.15}$$

so that

$$\partial_{J_i^a}f_b = \begin{cases}\sqrt{x_a}q_a^{\frac{p-2}{4}}m_b f_b(\omega_b(\sigma_i)-\omega_{b-1}(\sigma_i)) & \text{if } a<b \\ \sqrt{x_a}q_a^{\frac{p-2}{4}}m_b f_b\omega_b(\sigma_i) & \text{if } a=b \\ 0 & \text{if } a>b.\end{cases} \tag{B.16}$$

Substituting these in the (B.13), the first term inside the square brackets becomes

$$\begin{aligned}\mathbb{E}_1...\mathbb{E}_K(\sum_{b=2}^{K} f_1...\partial_{J_i^a} f_b...f_K\tilde{\omega}(\sigma_i)) =&\sqrt{x_a}q_a^{\frac{p-2}{4}}\big[m_a\mathbb{E}_1...\mathbb{E}_a(f_1...f_a\omega_a^2(\sigma_i))\\ &+\sum_{b=a+1}^{K} m_b\mathbb{E}_1...\mathbb{E}_b(f_1...f_b\omega_b^2(\sigma_i))\\ &-\sum_{b=a+1}^{K} m_b\mathbb{E}_1...\mathbb{E}_{b-1}(f_1...f_{b-1}\omega_b^2(\sigma_i))\big]\end{aligned} \tag{B.17}$$

and we find

$$\partial_a\tilde{\alpha}_N = \frac{1}{2}q_a^{\frac{p-2}{2}}\big[m_a\langle q_{\sigma\sigma'}\rangle_a+\sum_{b>a} m_b(\langle q_{\sigma\sigma'}\rangle_b-\langle q_{\sigma\sigma'}\rangle_{b-1})+1-\langle q_{\sigma\sigma'}\rangle_K\big] \tag{B.18}$$

from which, after some manipulations, one can easily obtain the (5.49).

Bibliography

[1] F. Guerra, "Broken replica symmetry bounds in the mean field spin glass model," *Commun. Math. Phys.*, vol. 233, no. 1, pp. 1–12, 2003.

[2] M. Talagrand, "The parisi formula," *Annals of Mathematics*, vol. 163, no. 1, pp. 221–263, 2006.

[3] K. E. Van Holde, W. Johnson, and P. Shing Ho, *Principles of Physical Biochemistry*. Pearson Prentice Hall, 2006.

[4] T. L. Hill, *Cooperativity theory in biochemistry*. Springer series in molecular biology, 1985.

[5] J. Monod, J. Wyman, and J. P. Changeux, "On the nature of allosteric transition: A plausible model," *J. Mol. Bio.*, vol. 12, pp. 88–118, 1965.

[6] D. E. Koshland, G. Nemethy, and D. Filmer., "Comparison of experimental binding data and theoretical models in proteins containing subunits," *Biochemistry*, vol. 5, pp. 365–385, 1966.

[7] G. K. Ackers, M. L. Doyle, D. Myers, and M. A. Daugherty, "Molecular code for cooperativity in hemoglobin," *Science*, vol. 255, pp. 54–63, 1992.

[8] G. K. Ackers, J. M. Holt, E. S. Burgie, and C. S. Yarian, "Analyzing intermediate state cooperativity in hemoglobin," *Methods in Enzymology*, vol. 379, pp. 3–28, 2004.

[9] K. Huang, *Statistical Mechanics*. John Wiley, 1963.

[10] C. J. Thompson, *Mathematical statistical mechanics*. Princeton University Press, 1979.

[11] A. Di Biasio, E. Agliari, A. Barra, and R. Burioni, "Mean-field cooperativity in chemical kinetics," *Theor. Chem. Acc.*, vol. 131, no. 3, pp. 1–14, 2012.

[12] E. Agliari, A. Barra, R. Burioni, A. Di Biasio, and G. Uguzzoni, "Toward biochemical cybernetics: Collective behavior in chemical kinetics from a statistical mechanics perspective," *Submitted*, 2012.

[13] Y. Murase, T. Onda, K. Tsujii, and T. Tanaka, "Discontinuous binding of surfactants to a polymer gel resulting from a volume phase transition," *Macromolecules*, vol. 32, pp. 8589–8594, 1999.

[14] L. H. Chao, P. Pellicena, S. Deindl, L. A. Barclay, H. Schulman, and J. Kuriyan, "Intersubunit capture of regulatory segments is a component of cooperative camkii activation," *Nature Struct. and Mol. Bio.*, vol. 17, pp. 264–272, March 2010.

[15] M. Mandal, M. Lee, J. E. Barrick, Z. Weinberg, G. M. Emilsson, W. L. Ruzzo, and R. R. Breaker, "A glycine-dependent riboswitch that uses cooperative binding to control gene expression," *Science*, vol. 306, pp. 275–279, October 2004.

[16] A. Barra, "The mean field ising model trough interpolating techniques," *J. Stat. Phys.*, vol. 132, pp. 787–809, 2008.

[17] J. M. Cases and F. Villieras, "Analyzing intermediate state cooperativity in hemoglobin," *Langmuir*, vol. 8, pp. 1251–1254, 1992.

[18] A. Pagnani, G. Parisi, and F. Ricci-Tersenghi, "Glassy transition in a disordered model for the rna secondary structure," *Phys. Rev. Lett.*, vol. 84, pp. 2026–2029, 2000.

[19] E. Agliari, A. Barra, and F. Camboni, "Criticality in diluted ferromagnet," *J. Stat. Mech.*, p. P10003, 2008.

[20] E. Agliari and A. Barra, "A hebbian approach to complex-network generation," *Europhys. Lett.*, vol. 94, no. 1, p. 10002, 2011.

[21] S. S. Solomatin, M. Greenfeld, and D. Herschlag, "Implications of molecular heterogeneity for the cooperativity of biological macromolecules," *Nature Struct. & Mol. Bio.*, vol. 18, pp. 732–734, 2011.

[22] J. L. Macdonald and L. J. Pike, "Heterogeneity in EFG-binding affinities arises from negative cooperativity in an aggregating system," *Proc. Natl. Acad. Sci.*, vol. 105, pp. 112–117, 2008.

[23] R. Germain, "The art of the probable: system control in the adaptive immune system," *Science*, vol. 293, pp. 240–246, 2001.

[24] D. A. Lavis and G. M. Bell, *Statistical Mechanics of Lattice Systems: Volume 2: Exact, Series and Renormalization Group Methods*, vol. 2. Springer, 1999.

[25] D. E. Koshland Jr, "The structural basis of negative cooperativity: receptors and enzymes," *Curr. Opin. Struct. Bio.*, vol. 6, pp. 757–761, 1996.

[26] C. Khosla and J. E. Bailey, "Heterologous expression of a bacterial hemoglobin improves the growth properties of recombinant *Escherichia coli*," *Nature*, vol. 331, pp. 633–635, 1988.

[27] M. Bolognesi, A. Boffi, M. Coletta, A. Mozzarelli, A. Pesce, C. Tarricone, and P. Ascenzi, "Anticooperative ligand binding properties of recombinant ferric *Vitreoscilla* homodimeric hemoglobin: A thermodynamic, kinetic and x-ray crystallographic study," *J. Mol. Bio.*, vol. 291, no. 3, pp. 637–650, 1999.

[28] T. Cedervall, I. Lynch, S. Lindman, T. Berggard, E. Thulin, H. Nilsson, K. A. Dawson, and S. Linse, "Understanding the nanoparticle-protein corona using methods to quantify exchange rates and affinities of proteins for nanoparticles," *Proc. Natl Acad. Sci.*, vol. 104, pp. 2050–2055, 2007.

[29] C. Röcker, M. Pötzl, F. Zhang, W. J. Parak, and G. U. Nienhaus, "A quantitative fluorescence study of protein monolayer formation on colloidal nanoparticles," *Nature nanotech.*, vol. 4, no. 9, pp. 577–580, 2009.

[30] M. Talagrand, *Spin Glasses: A Challenge for Mathematicians*, vol. 46 of *A Series of Modern Surveys in Mathematics*. Springer-Verlag, 2003.

[31] M. Mézard, G. Parisi, and M. A. Virasoro, *Spin Glass Theory and Beyond*, vol. 9 of *Lecture Notes in Physics*. World Scientific, 1986.

[32] H. Nishimori, *Statistical Physics of Spin Glasses and Information Processing: An Introduction*. Oxford University Press, 2001.

[33] R. Monasson, "Optimization problems and replica symmetry breaking in finite connectivity spin glasses," *J. Phys. A*, vol. 31, no. 2, 1998.

[34] J. D. Amit, *Modeling Brain Functions: The World of Attractor Neural Networks*. Cambridge University Press, 1992.

[35] S. Galluccio, J. P. Bouchaud, and M. Potters, "Rational decisions, random matrices and spin glasses," *Physica A*, vol. 259, pp. 449–456, October 1998.

[36] F. S. Edwards and P. W. Anderson, "Theory of spin glasses," *J. Phys. F*, vol. 5, no. 5, p. 965, 1975.

[37] D. Sherrington and S. Kirkpatrick, "Solvable model of a spin glass," *Phys. Rev. Lett.*, vol. 35, no. 26, pp. 1792–1795, 1975.

[38] G. Parisi, "Toward a mean field theory for spin glasses," *Phys. Lett. A*, vol. 73, no. 3, pp. 203–205, 1979.

[39] G. Parisi, "Infinite number of order parameters for spin-glasses," *Phys. Rev. Lett.*, vol. 43, no. 23, pp. 1754–1756, 1979.

[40] G. Parisi, "A sequence of approximated solutions to the s-k model for spin glasses," *J. Phys. A*, vol. 13, no. 4, pp. 115–121, 1980.

[41] M. Aizenmann, J. Lebowitz, and D. Ruelle, "Absence of self-averaging of the order parameter in the sherrington-kirkpatrick model," *J. Stat. Phys.*, vol. 62, no. 1/2, 1991.

[42] L. Pastur and M. Shcherbina, "Some rigorous results on the sherrington-kirkpatrick spin glass model," *Commun. Math. Phys.*, vol. 112, pp. 3–20, 1987.

[43] F. Guerra and F. L. Toninelli, "The thermodynamic limit in mean field spin glass models," *Commun. Math. Phys.*, vol. 230, no. 1, pp. 71–79, 2002.

[44] L. de Almeida and J. D. Thouless, "Stability of the sherrington-kirkpatrick solution of a spin glass model," *J. Phys. A*, vol. 45, pp. 79–82, 1980.

[45] F. Guerra, "The replica symmetric region in the sherrington-kirkpatrick mean field spin glass model. the almeida-thouless line," *arXiv:cond-mat/0604674*, 2006.

[46] S. Franz and M. Leone, "Replica bounds for optimization problems and diluted spin systems," *J. Stat. Phys.*, vol. 111, no. 3-4, pp. 535–564, 2003.

[47] S. Franz and F. L. Toninelli, "Kac limit for finite-range spin glasses," *Phys. Rev. Lett.*, vol. 92, no. 3, p. 030602, 2004.

[48] A. Barra, G. Genovese, and F. Guerra, "The replica symmetric approximation of the analogical neural network," *J. Stat. Phys.*, vol. 140, no. 4, pp. 784–796, 2010.

[49] A. Barra, A. Di Biasio, and F. Guerra, "Replica symmetry breaking in mean-field spin glasses through the hamilton-jacobi technique," *J. Stat. Phys.*, p. 09006, 2010.

[50] E. Agliari, A. Barra, R. Burioni, and A. D. Biasio, "Notes on the p-spin glass studied via hamilton-jacobi and smooth cavity techniques," *J. Math. Phys.*, vol. 53, p. 063304, 2012.

[51] J. A. Mydosh, *Spin glasses: an experimental introduction.* Taylor and Francis, 1993.

[52] S. Kirkpatrick and D. Sherrington, "Infinite-ranged models of spin-glasses," *Phys. Rev. B*, vol. 17, no. 11, pp. 4384–4403, 1978.

[53] D. Ruelle, *Statistical Mechanics: Rigorous Results.* World Scientific, 1999.

[54] F. Guerra, "Sum rules for the free energy in the mean field spin glass model," *Fields Inst. Commun.*, vol. 30, pp. 1–12, 2001.

[55] S. Ghirlanda and F. Guerra, "General porperties of overlap probability distributions in disordered spin systems.towards parisi ultrametricity," *J. Phys. A*, vol. 31, pp. 9149–9155, 1998.

[56] D. Panchenko, "The parisi ultrametricity conjecture," *Annals of Mathematics*, vol. 177, no. 1, pp. 383–393, 2013.

[57] P. Contucci, C. Giardinà, C. Giberti, G. Parisi, and C. Vernia, "Ultrametricity in the edwards-anderson model," *Phys. Rev. Lett.*, vol. 99, no. 5, p. 057206, 2007.

[58] J. Thomas and F. Krząkała, "Comment on "ultrametricity in the edwards-anderson model"," *Phys. Rev. Lett.*, vol. 100, p. 159701, 2008.

[59] B. Derrida, "Random energy model: An exactly solvable model of disordered systems," *Phys. Rev. B*, vol. 24, p. 2613, 1981.

[60] D. J. Gross and M. Mézard, "The simplest spin glass," *Nucl. Phys. B*, vol. 240, p. 431, 1984.

[61] E. Gardner, "Spin glasses with p-spin interactions," *Nucl. Phys. B*, vol. 257, pp. 747–765, 1985.

[62] T. R. Kirkpatrick and D. Thirumalai, "p-spin-interaction spin-glass models: Connections with the structural glass problem," *Phys. Rev. B*, vol. 36, pp. 5388–5397, 1987.

[63] B. Derrida, "Random energy model: limit of a family of disordered models," *Phys. Rev. Lett.*, vol. 11, no. 5, pp. 983–990, 1978.

[64] P. A. Vuillermot, "Thermodynamics of quenched random spin systems, and application to the problem of phase transitions in magnetic (spin) glasses," *J. Phys. A*, vol. 10, no. 8, p. 1319, 1977.

[65] F. Guerra and F. L. Toninelli, "The infinite volume limit in generalized mean field disordered models," *Markov Proc. and Rel. Fields*, vol. 9, no. 2, pp. 195–207, 2003.

[66] P. Contucci, M. Degli Esposti, C. Giardinà, and S. Graffi, "Thermodynamical limit for correlated gaussian random energy models," *Commun. Math. Phys.*, vol. 236, no. 1, pp. 55–63, 2003.

[67] F. Guerra, "About the overlap distribution in mean field spin glass models," *Int. J. Phys. B*, vol. 10, pp. 1675–1684, 1997.

[68] A. Barra, "The mean field ising model through interpolating techniques," *J. Stat. Phys.*, vol. 132, 2008.

[69] M. Aizenman and P. Contucci, "On the stability of the quenched state in mean field spin glass models," *J. Stat. Phys.*, vol. 92, pp. 765–783, 1998.

[70] E. Agliari, A. Barra, A. Galluzzi, F. Guerra, and F. Moauro, "Parallel processing in immune networks," *to be published on Phys. Rev. E*, 2013.

[71] E. Agliari and A. Barra, "A statistical mechanics approach to granovetter theory," *arXiv:1012.1272*, 2010.

[72] A. C. C. Coolen, R. Kuhn, and P. Sollich, *Theory of neural information processing systems*. Oxford University Press, USA, 2005.